UNIVERSIDAD EUROPEA DE MADRID

ESCUELA DE INGENIERÍA Y DEL ARQUITECTURA

MÁSTER UNIVERSITARIO EN INGENIERÍA AERONÁUTICA

TRABAJO FIN DE MÁSTER

DEVELOPMENT OF ABAQUS MODELS FOR PARAMETRIC STUDY OF JOINT BEHAVIOR IN 2D

Author: Mairena BAQUERO BARBOSA
Tutor: Alan DOMÍNGUEZ MONTERO

April 2025

To obtain the degree of Master of Science in Aerospace Engineering

at the Universidad Europea de Madrid

to be defended publicly on Saturday April 26, 2025 at 10:00 AM.

Master Thesis committee:	Prof. A. Dominguez Montero,	UE, supervisor
	Ir. A. ,	UE professor
	Ir. A. ,	UE professor
	Ir. A. ,	UE professor

"El destino no es una casualidad, sino una consecuencia."
Carlos Ruiz Zafón

I would like to express my gratitude to my supervisor, Alan Domínguez,
for his guidance and assistance throughout these months.

The deepest thanks to my family, who are my unconditional support
and my greatest fortune.

Abstract

This paper presents the development of a finite element model on which several studies are carried out to analyze the performance of the joints. The model is implemented in the commercial software Abaqus using a parametric Python script that generates different configurations of two-plate assemblies connected by fasteners. The plates are meshed with S4R shell elements, while the fasteners are modeled using *fastener elements. Contact is considered through Signorini conditions, without including large displacements or plastic material behavior.

Initially, several models are examined where parameters such as plate thickness, plate length, number of joints or mesh size are varied to determine what effect they have separately on the behavior of the model. In this study is found that the forces in the joints decrease with more number of fasteners, that the axial force grows with plate length as the moment increases, that with a finer mesh more accurate results are obtained or that the deformation is greater when the thicknesses of the plates are different.

In the next analysis, two different methods are used to model the joints in Abaqus: BEAM and CARTESIAN connectors. BEAM provides a rigid beam connection between two nodes, kinematically constraining all components of relative motion. CARTESIAN connector represents a constitutive mechanical behavior between two or three nodes. The constitutive behavior is predicted using a semi-empirical flexibility equation, in this case the Huth equation. With this second approach it can be noted that the axial force decreases significantly due to its inability to transmit moments.

Finally, the presence of clearance in the joints is simulated to determine the effect it has. To introduce this effect into the model, variation of the shear stiffness in the direction perpendicular to the applied force is performed. Clearance leads to a contact region at the bolt-hole interface that varies the stress state around the hole.

The results obtained contribute to a better understanding of load distribution in bolted connections. The methodology developed in this study offers a computationally efficient approach for evaluating fastener performance in structural joints, which can be applied in aerospace and mechanical engineering applications.

Resumen

Este trabajo presenta el desarrollo de un modelo de elementos finitos para analizar en el cual se realizan varios estudios para analizar el rendimiento de las uniones. El modelo se implementa en el software comercial Abaqus mediante un script paramétrico en Python que genera diferentes configuraciones de un ensamblaje de dos placas unidas por remaches. Las placas se mallan con elementos de shell S4R, mientras que los remaches se modelan mediante *fastener elements. El contacto se considera a través de las condiciones de Signorini, sin incluir grandes desplazamientos ni comportamiento plástico del material.

Inicialmente, se examinan varios modelos donde se varían parámetros como el espesor de la placa, la longitud de la misma, el número de uniones o el tamaño de la malla para determinar qué efecto tienen por separado en el comportamiento del modelo. Con este estudio se observa que las fuerzas en las uniones disminuyen a medida que aumenta el número de remaches, que la fuerza axial crece con la longitud de la placa ya que aumenta el momento, que con una malla más fina se obtienen resultados más precisos o que la deformación es mayor cuando los espesores de las placas son diferentes.

En el siguiente análisis, se utilizan dos métodos diferentes para modelar las uniones en Abaqus: conectores BEAM y CARTESIAN. BEAM es un conector tipo viga entre dos nodos, que restringe cinemáticamente todas las componentes del desplazamiento relativo. El conector CARTESIAN representa un comportamiento mecánico constitutivo entre dos o tres nodos. El comportamiento constitutivo se predice utilizando una ecuación de flexibilidad semi-empírica, en este caso la ecuación de Huth. Con este segundo enfoque se puede notar que la fuerza axial disminuye significativamente debido a su incapacidad para transmitir momentos.

Finalmente, se simula la presencia de holgura en las uniones para determinar el efecto que tiene. Para introducir este efecto en el modelo, se realiza una variación de la rigidez a cortadura en las uniones en la dirección perperdicular a la fuerza aplicada. La holgura conduce a una región de contacto en la interfaz del perno-agujero que varía el estado de tensión alrededor del agujero.

Para investigar el efecto de la tolerancia en los remaches, se realiza una variación paramétrica de la rigidez a cortadura de los mismos. El estudio se centra en analizar cómo cambian los caminos de carga en función de la rigidez de los remaches.

Los resultados obtenidos contribuyen a una mejor comprensión de la distribución de carga en conexiones atornilladas. La metodología desarrollada en este estudio ofrece un enfoque computacionalmente eficiente para evaluar el rendimiento de los remaches en uniones estructurales.

Contents

List of Figures

1

Introduction

1.1. Motivation

In the realm of structural engineering, the integrity and performance of joints play a pivotal role in the overall reliability of mechanical systems. Among the various types of joints, riveted joints have been a cornerstone of construction and manufacturing for centuries, providing robust connections in a multitude of applications. This thesis delves into the intricate dynamics of riveted joints, with a particular focus on the influence of clearances in low-loaded scenarios.

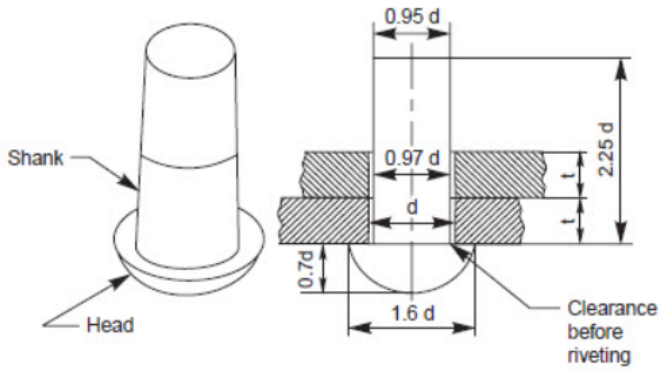

Figure 1.1: Schematic diagram of a rivet

The motivation from this work arises from the growing need to optimize joint performance under minimal load conditions, where traditional design methods may not adequately account for the effects of clearance. Low-loaded joints are ubiquitous in many industries, including aerospace, automotive, and civil engineering, where they are often subjected to varying environmental conditions and operational demands. Understanding how clearances affect the behavior of riveted joints in these contexts is not only critical for ensuring structural integrity but also for enhancing the longevity and safety of engineered systems.

Moreover, as industries strive for greater efficiency and sustainability, there is an increasing emphasis on innovative design solutions that can accommodate variations in manufacturing tolerances and operational conditions. Investigating the interplay between riveted joints and clearances offers valuable insights into optimizing joint design to meet these evolving challenges.

Figure 1.2: Aircraft skin with riveted joints

Riveted joints offer several key benefits for low-loaded applications:

- Flexibility and load distribution
  Riveted joints allow for slight flexibility and better load distribution across the connection. This characteristic is particularly advantageous in low-loaded applications where vibrations may occur, stress needs to be distributed evenly or some degree of joint flexibility is desirable. The ability of riveted joints to accommodate slight movements makes them well-suited for structures that experience dynamic but low-intensity loads.

- Ease of inspection and maintenance
  One of the significant advantages of riveted joints is the ease of inspection and maintenance. Visual inspections can be performed quickly and efficiently, Potential issues can be identified early before they lead to failure and maintenance and repairs are generally less time-consuming compared to welded structures. This simplicity in maintenance is particularly valuable in industries where downtime must be minimized.

- Weight considerations
  For low-loaded applications where weight is a critical factor, riveting can achieve a lighter structure compared to welding. The overlap required for riveted joints is typically smaller than for welded joints, and no additional material (like weld metal) is needed, further reducing overall weight. This weight advantage makes riveted joints particularly suitable for industries such as aerospace and automotive, where every gram matters even in low-load scenarios.

Figure 1.3: Rivets

- Cost-Effectiveness
  Rivets are generally low in cost per unit. The installation process requires less specialized equipment compared to welding. Energy costs are lower since riveting doesn't require electricity for joining, unlike

welding. These factors contribute to overall cost savings, especially in large-scale or mass-production scenarios.

- Versatility in material joining
  Riveted joints excel in joining dissimilar materials, which can be particularly useful when different materials need to be combined for specific properties or thermal or chemical incompatibility prevents the use of welding. This versatility allows to select the most appropriate materials for each component without being constrained by joining limitations.

Figure 1.4: Riveted joints

In summary, this thesis aims to navigate through the complexities of riveted joints with clearances in low-load applications, highlighting their importance in contemporary engineering challenges and paving the way for stronger and more efficient structural solutions.

1.2. State of art

Currently, the increased use of riveted joints has led to numerous studies on this type of assembly. These investigations focus on optimizing joint design, extending their lifespan, and enhancing their performance. All structural assemblies must be joined in one way or another, whether through bolts, rivets, welding, adhesives, or other means. The increasing use of riveted joints as structural elements has created the need for numerous studies on them, either to optimize their design or to prevent failures.

The numerical method is a straightforward and efficient tool for studying the effects of various influencing factors, including geometric dimensions, bolt tightening force, aperture size, and clearance. Among these factors, clearance refers to the intentional or unintentional gap between mating components, such as the space between a bolt and a hole or the clearance in mechanical assemblies to allow for thermal expansion, ease of assembly, or controlled movement. Clearance plays a critical role in the overall performance and reliability of mechanical systems, as excessive clearance can lead to misalignment, vibration, and wear, while insufficient clearance can cause interference, overheating, or material failure. Numerical simulations help in analyzing these parameters under different conditions, providing insights for optimizing the design and functionality of mechanical systems.

1.2.1. Stress analysis method for clearance-fit joints with bearing-bypass loads

The article [9] *"Stress Analysis Method for Clearance-Fit Joints with Bearing-Bypass Loads"* by R. A. Naik and J. H. Crews, Jr., investigates the complex stress behaviors that arise in joints with clearance subjected to combined bearing and bypass loads. These conditions are common in aerospace structures, particularly those utilizing composite materials, where lightweight and high-strength connections are paramount. The study presents an innovative numerical approach for analyzing such systems, offering significant advancements in understanding and optimizing joint performance.

The proposed method employs an inverse formulation coupled with linear elastic finite element analysis. This approach is particularly noteworthy because it circumvents the computational challenges associated with nonlinear contact problems, such as iterative-incremental methods. Instead of requiring time-consuming node tracking along the bolt-hole interface, the inverse formulation defines the boundary conditions using multi-point constraint equations. These equations model the contact between the bolt and the hole, capturing the nonlinear behavior introduced by clearance without the need for specialized algorithms.

One of the critical contributions of the study is its focus on the effects of clearance. Clearance fundamentally alters the contact mechanics of the joint. For tension-dominated bearing-bypass loads, clearance causes the contact angle between the bolt and hole to expand as the load increases. Conversely, under compression-dominated loading, the contact angle diminishes, and in some cases, dual contact occurs when the hole closes onto the bolt. Dual contact significantly reduces stress concentrations, which is a beneficial outcome, particularly under high compressive loading conditions.

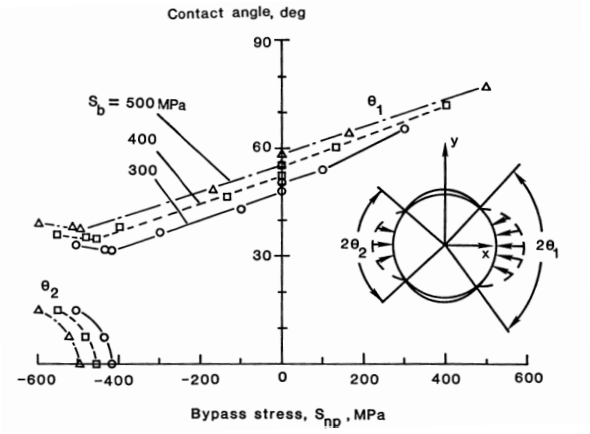

Figure 1.5: Variation of contact angle with bypass stress

The research highlights the importance of the bearing-bypass load ratio (β) in influencing the joint's stress state. This ratio governs the proportion of the load distributed between the bearing and bypass effects. For instance, under tensile bearing-bypass loading, tangential stresses around the bolt-hole interface increase linearly with the bypass load. However, under compressive loading, both tangential and radial stresses show complex variations, influenced heavily by the onset of dual contact. The study provides detailed stress distribution profiles, demonstrating that peak stresses shift location based on the loading conditions, an observation critical for predicting failure modes in composite joints.

Another significant insight is the role of dual contact in enhancing joint strength. When dual contact occurs, load transfer across the fastener increases, reducing the stress concentration around the hole. This phenomenon suggests that optimizing clearance dimensions can improve joint performance. Smaller clearances encourage dual contact at lower loads, leading to a more uniform stress distribution and increased resistance to mechanical failure. This insight is particularly valuable for applications involving high compressive loads, where stress concentrations can lead to premature failure of the joint.

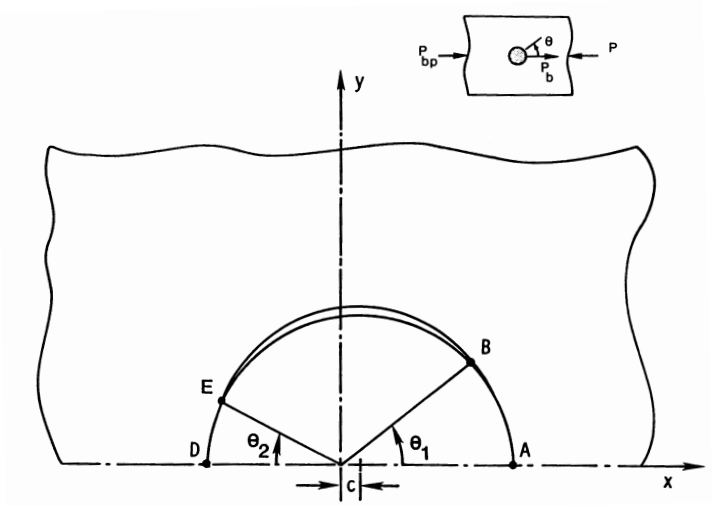

Figure 1.6: Contact angle notation for dual contact

The authors validate their approach using quasi-isotropic graphite/epoxy laminates, materials commonly used in aerospace applications due to their lightweight and high-strength characteristics. By incorporating realistic material properties and applying their method to practical configurations, the study establishes a robust framework for analyzing and designing clearance-fit joints in advanced structural assemblies.

The study underscores the practical applicability of the method. The simplicity of the inverse formulation allows for implementation using standard finite element tools such as MSC/NASTRAN, making it accessible to engineers and designers without requiring extensive customization. This computational efficiency, combined with the method's ability to capture nonlinear contact behaviors accurately, positions it as a powerful tool for the optimization of riveted and bolted joints, particularly in applications where safety and performance are critical.

This work provides a comprehensive framework for understanding and analyzing the behavior of clearance-fit joints under combined bearing and bypass loading. The insights gained are directly applicable to the design and optimization of structural joints, particularly in composite materials, offering a valuable contribution to the field of mechanical and aerospace engineering.

1.2.2. Contact stresses in pin-loaded orthotropic plates

The article [6] *"Contact Stresses in Pin-Loaded Orthotropic Plates"* by M.W. Hyer and E.C. Klang explores the complex interaction of contact stresses in pin-loaded joints within orthotropic materials, such as fiber-reinforced composites. This research provides a significant advancement by integrating the effects of pin elasticity, friction, and clearance — three critical factors often studied in isolation — into a cohesive numerical analysis framework. Its contributions offer valuable insights into optimizing joint design and understanding failure mechanisms in advanced structural assemblies.

This study adopts a two-dimensional contact elasticity model based on complex variable theory, explicitly accounting for the elasticity of both the pin and the plate. Unlike prior studies that simplified the interaction by assuming a rigid pin or a known radial load distribution (e.g., a cosine function), this work models the full coupling between the elastic bodies in contact. The analysis divides the boundary into regions of contact, slip, and no-slip, and iteratively determines these zones under loading conditions. By enforcing boundary conditions at discrete points using a collocation procedure, the study achieves high numerical accuracy, capturing the nuanced behavior of pin-plate interactions.

A central theme of this research is the role of clearance between the pin and the hole in determining stress distributions and contact mechanics. Clearance introduces significant nonlinearity, affecting the size and shape of the contact region, as well as the location and magnitude of peak stresses. When clearance is present, the pin contacts the plate over an arc that evolves nonlinearly with the applied load. This variation creates zones of tensile radial stresses in areas of no contact, which the analysis successfully captures. Smaller clearances generally reduce stress concentrations by encouraging more uniform load transfer across the interface, while larger clearances exacerbate stress localization and misalignment risks.

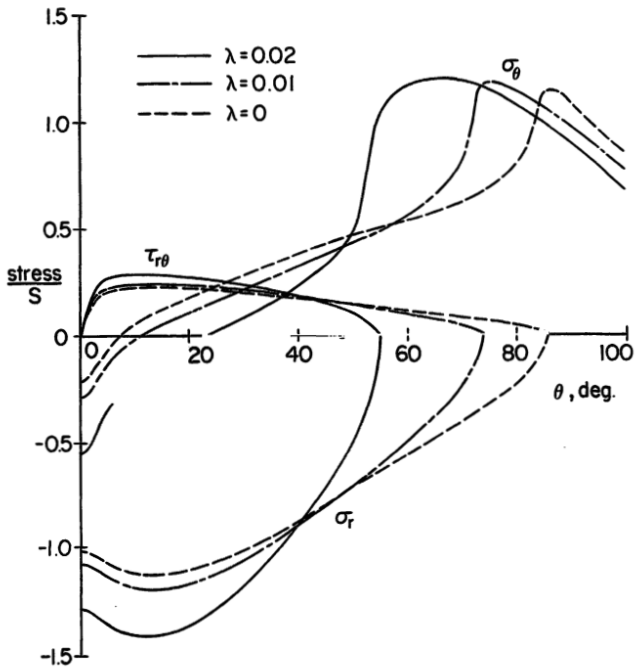

Figure 1.7: Effect of clearance on stresses

The study also incorporates the effect of friction within the contact region, modeled using Coulomb's law. Friction influences the stress state by defining slip and no-slip zones along the contact arc. Higher coefficients of friction increase shear stress while altering the peak locations and magnitudes of radial and circumferential stresses. The interplay of friction and clearance highlights their combined role in defining joint performance. Friction, for instance, significantly affects the contact region's extent and redistributes stresses,

improving joint strength under certain conditions.

One of the most important findings relates to the influence of orthotropic material properties on stress distributions. Plates with different fiber orientations exhibit varying stress profiles around the hole. For example, plates with fibers aligned along the loading direction experience higher stress concentrations, whereas quasi-isotropic laminates exhibit more evenly distributed stresses. Highly orthotropic materials, such as those with fibers exclusively aligned in the load direction, demonstrate stress concentration factors significantly higher than quasi-isotropic configurations, underscoring the importance of material selection in joint design.

Figure 1.8: Fiber reinforced composite

The analysis further evaluates the elasticity of the pin and its relative significance. While the plate's elastic properties dominate the stress behavior, the study reveals that pin flexibility has a secondary yet noticeable effect. Simulations with rigid, steel, and aluminum pins show minor variations in stress distributions, with more flexible pins slightly reducing peak stress magnitudes due to increased deformation and load redistribution. However, the influence of pin elasticity is generally less critical compared to the effects of clearance and friction.

The numerical methodology developed in this study demonstrates the power of iterative approaches for solving complex contact problems. The collocation method enforces boundary conditions precisely, while the iterative process adjusts contact and slip regions until convergence. This computational framework ensures that critical physical conditions such as traction-free zones and the Coulomb friction limit—are satisfied, leading to reliable predictions of stress distributions and contact angles.

The study concludes with practical implications for joint design in fiber-reinforced composites. By integrating clearance, friction, and orthotropic properties into a single analysis, this research offers a comprehensive framework for optimizing joint performance in advanced materials. The results emphasize that assumptions like rigid pins or simple radial load distributions fail to capture the true stress states, especially in cases involving significant orthotropy or clearance. This underscores the importance of realistic modeling in preventing failures and improving the reliability of pin-loaded joints in critical applications, such as aerospace and automotive structures.

This work significantly enriches the state of the art by demonstrating that clearance, friction, and orthotropic properties interact in complex but predictable ways to shape stress distributions. It provides a detailed numerical approach for understanding and optimizing these factors, paving the way for more efficient and robust joint designs in composite materials.

1.2.3. Load distribution of multi-fastener laminated composite joints

The article [4] *"Load Distribution of Multi-Fastener Laminated Composite Joints"* by Wei-Xun Fan and Chijn-Tu Qiu explores the influence of clearance, also referred to as fitting tolerance, on the load distribution in multi-bolt joints. The study applies a robust analytical approach that combines Faber series expansion and complex potential methods to model the stress and load transfer mechanisms in laminated composite materials. Using a configuration with four fasteners, the research provides valuable insights into how clearances impact joint performance under various loading conditions.

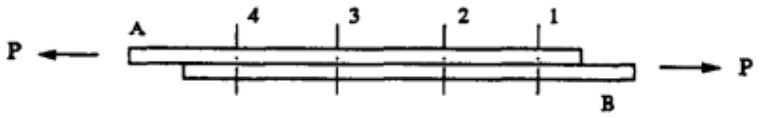

Figure 1.9: Laminated composite joint having four hole/pin connections

A significant finding of the study is the impact of clearance on load distribution. In joints with positive clearance, load sharing among fasteners is inherently uneven, especially at lower load levels. Initially, only the fasteners with the smallest clearances engage in load transfer, leaving the remaining fasteners inactive. As the load increases, more fasteners come into contact, and the load is redistributed more evenly across the joint. This transition highlights the critical role of clearance in determining load-sharing behavior in multi-fastener configurations.

The study identifies two distinct stages of load distribution when clearances are present. In the first stage, referred to as Stage I, only the first and last fasteners in the joint are in contact due to their smaller clearances. These fasteners equally share the external load up to a certain threshold value. In the second stage, or Stage II, all fasteners come into contact as the load exceeds the threshold. In this stage, the load distribution is influenced by the joint's geometric and material properties, transitioning toward a more uniform load-sharing state.

The numerical modeling in the study assumes that the joint's plates are orthotropic, thin, and homogeneous, ensuring symmetry in the stress fields and boundary conditions. By representing contact stresses as cosine functions and expanding them using Faber series, the researchers develop a precise computational model that accurately captures the nonlinearities introduced by clearance. The model effectively simulates the interaction between fasteners and plates, allowing for the prediction of stress concentrations and load distribution patterns.

Clearance magnitude is shown to have a profound effect on joint behavior. Larger clearances result in more pronounced load unevenness, as the fasteners with smaller clearances must bear the majority of the load before others engage. For instance, doubling the clearance not only delays the engagement of additional fasteners but also doubles the threshold load required to transition to a fully engaged state. This finding underscores the need to carefully control clearances during joint design to avoid excessive stress concentrations and potential failures.

The study also examines the influence of friction within the contact regions of the joint. Friction, modeled using a coefficient of friction, plays a stabilizing role by reducing stress concentrations and slightly evening out the load distribution among fasteners. Although the effect of friction is less pronounced than that of clearance or plate stiffness, it still contributes to improved joint performance, particularly under moderate loading conditions.

Material stiffness and laminate properties are additional factors that strongly affect load-sharing behavior. As the axial stiffness of the joint plates increases, the load distribution becomes more uniform, with relative displacements between fasteners diminishing. In the limiting case of infinitely stiff plates, all fasten-

ers carry an equal share of the load, regardless of clearance. Furthermore, orthotropic laminates with fibers aligned along the load direction exhibit more consistent load distribution than cross-ply laminates, where stresses tend to concentrate unevenly.

The numerical results highlight the combined effects of clearance, material stiffness, and friction on load distribution. For example, joints with larger clearances initially exhibit significant load concentration on fewer fasteners, increasing the likelihood of local failure. However, as external loads increase, load-sharing becomes more balanced, even for joints with considerable clearances. Similarly, friction reduces peak stresses near the contact edges and enhances the joint's ability to distribute loads evenly.

This study underscores the practical implications of clearance management in the design of multi-fastener joints. By understanding the interplay of clearance, material properties, and friction, engineers can optimize joint configurations to improve load-sharing efficiency, minimize stress concentrations, and enhance the reliability of composite structures. These findings are particularly relevant for high-performance applications, such as aerospace engineering, where joint integrity is critical.

The article provides a comprehensive analytical framework for studying the effects of clearance in multi-fastener joints. It highlights the critical role of clearance in influencing load distribution, stress concentration, and joint reliability, offering valuable insights for optimizing the design and performance of composite joints.

2

Fundamentals of Numerical Methods in Computational Mechanics

2.1. Linear implicit solver

Linear implicit solvers are a kind of algorithms used in numerical simulations to solve systems of differential equations in the context of structural, dynamic or thermal analysis. In linear problems, the global equation would be:

$$[K]\{u\} = \{F\}, \tag{2.1}$$

where K is a the stiffness matrix, u is the vector of unknown displacement and F is the vector of external nodal forces.

The global stiffness matrix is obtained assembling the individual element stiffness matrices. Since the global matrix has to be inverted to obtain the displacements, it is required to be a square matrix. If the model presents rigid body motion (mechanism) that structure is unstable and the matrix will be singular.

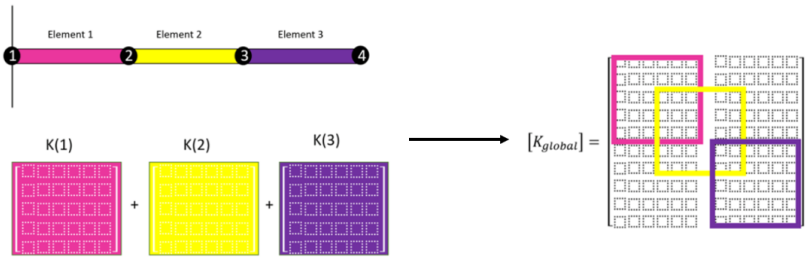

Figure 2.1: Example of global striffness matrix

In 2D elements, displacement variable has two components (u,v), and therefore 2 degrees of freedom (dof) per node. The displacements at any other point of the elements will be expressed as a function of the displacements calculated at the nodes and the shape functions.

$$\begin{aligned} u &= N_1 q_1 + N_2 q_3 + N_3 q_5 \\ v &= N_1 q_2 + N_2 q_4 + N_3 q_6 \end{aligned} \tag{2.2}$$

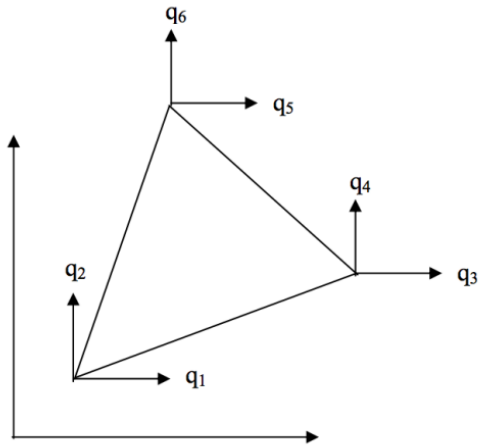

$$q = \{q_1 \quad q_2 \quad q_3 \quad q_4 \quad q_5 \quad q_6\}^T$$

Figure 2.2: Degrees of freedom per node in 2D element

The shape function is an interpolator that represents the displacement relationships between the different nodes. The shape function for node i represents how much node i is displaced with respect to other nodes of the element.

$$N_i = \frac{1}{2a}\left[a_1 + b_1 \cdot x + c_1 \cdot y\right] \tag{2.3}$$

Once the shape functions are obtained, they are derived to determine [B] (matrix of derivatives of the shape functions). With the following relation we can calculate the structure deformation field.

$$\begin{bmatrix} \varepsilon_x \\ \varepsilon_y \\ \gamma_{xy} \end{bmatrix} = \begin{bmatrix} \frac{\partial N_1}{\partial x} & 0 & \frac{\partial N_2}{\partial x} & 0 & \frac{\partial N_3}{\partial x} & 0 \\ 0 & \frac{\partial N_1}{\partial y} & 0 & \frac{\partial N_2}{\partial y} & 0 & \frac{\partial N_3}{\partial y} \\ \frac{\partial N_1}{\partial y} & \frac{\partial N_1}{\partial x} & \frac{\partial N_2}{\partial y} & \frac{\partial N_2}{\partial x} & \frac{\partial N_3}{\partial y} & \frac{\partial N_3}{\partial x} \end{bmatrix} \begin{bmatrix} u_1 \\ v_1 \\ u_2 \\ v_2 \\ u_3 \\ v_3 \end{bmatrix} = B\mathbf{u} \tag{2.4}$$

On the other hand, it is necessary to define the Elastic Tensor [D] depending on whether we are working in plane stress or plane strain.

$$[D] = \frac{E}{(1-\nu)} \begin{bmatrix} 1 & \nu & 0 \\ \nu & 1 & 0 \\ 0 & 0 & \frac{1-\nu}{2} \end{bmatrix} \quad \text{Plane Stress} \tag{2.5}$$

$$[D] = \frac{E}{(1+\nu)(1-2\nu)} \begin{bmatrix} 1-\nu & \nu & 0 \\ \nu & 1-\nu & 0 \\ 0 & 0 & \frac{1-2\nu}{2} \end{bmatrix} \quad \text{Plane Strain} \tag{2.6}$$

Combining with the elastic tensor [D] with the matrix of derivatives of the shape functions, we obtain the stiffness of the element. In this way the elemental stiffness matrix can be calculated without using the displacement method.

$$k_{\text{elemento}} = \int [B]^T \cdot [C] \cdot [B]\, dv \tag{2.7}$$

Thus, we move from a differential equation format to a system of linear equations that is easier to solve.

2.2. Linear vs Nonlinear

A system or model is linear if it satisfies two main properties:

- **Superposition:** If the inputs x_1 and x_2 produce responses y_1 and y_2, then the response to a linear combination of the inputs, such as $ax_1 + bx_2$, will be the same linear combination of the responses: $ay_1 + by_2$.

  Mathematically:
  $$f(ax_1 + bx_2) = af(x_1) + bf(x_2)$$

- **Proportionality:** The system's response is directly proportional to the magnitude of the input. For example, if a load is doubled, the deformations, stresses, or displacements are also doubled.

In structural linear analysis, the following assumptions are made:

1. **Material obeys Hooke's Law:**
   The relationship between stress (σ) and strain (ε) is linear, as defined by Hooke's law:
   $$\sigma = E \cdot \varepsilon$$
   where E is the modulus of elasticity. This assumes the material remains within the elastic region and does not exhibit plastic behavior.

2. **External forces are conservative:**
   The forces applied to the structure are path-independent and do not depend on the history of deformation. Conservative forces mean that the work done by these forces is recoverable, making the potential energy approach valid.

3. **Unchanged supports during loading:**
   Boundary conditions (e.g., fixed, pinned, or roller supports) remain constant throughout the analysis. There are no displacements, rotations, or alterations in the constraints caused by the applied loads.

4. **Infinitesimal deformations:**
   Displacements, rotations, and strains are so small that the geometry of the structure remains effectively unchanged. This allows the use of the small strain approximation:
   $$\varepsilon \approx \frac{\partial u}{\partial x}$$
   The strain is assumed to be less than 0.2%, ensuring that geometric nonlinearity (e.g., buckling or large deformations) does not occur.

A system or model is nonlinear if it does not satisfy the properties of superposition and proportionality. In these cases, the relationship between variables is neither direct nor constant, which can result in complex responses.

2.2.1. Types of nonlinearity

1. **Geometric nonlinearity:** Appears when deformations are large, and the geometry of the system changes significantly under load. It is usually solved using the Newton Raphson scheme solution.

   #### Newton Raphson method

   The Newton-Raphson method is a powerful iterative approach to solve nonlinear equations. In nonlinear systems, the equilibrium equation $R(u) = 0$ does not have a direct analytical solution due to the complexity of the function.

   $$\mathbf{R}(\mathbf{u}) = \mathbf{F}_{\text{int}}(\mathbf{u}) - \mathbf{F}_{\text{ext}} = 0$$

Where:

- $\mathbf{F}_{\text{int}}(\mathbf{u})$: Internal forces, which depend on the deformation state.
- $\mathbf{F}_{\text{ext}}$: External applied forces.

The Newton-Raphson method uses a tangent-based linear approximation to iteratively converge to the solution.

Starting from an initial guess u_0, the function $R(u)$ is approximated using a Taylor expansion:

$$\mathbf{R}(\mathbf{u}_{n+1}) \approx \mathbf{R}(\mathbf{u}_n) + \mathbf{K}_T \Delta \mathbf{u}$$

Where:

$$\Delta \mathbf{u} = \mathbf{u}_{n+1} - \mathbf{u}_n \quad \text{(incremental displacement)},$$

$$\mathbf{K}_T = \frac{\partial \mathbf{R}}{\partial \mathbf{u}} \quad \text{(tangent stiffness matrix, Jacobian)}$$

The next displacement is updated as:

$$\Delta \mathbf{u} = -\mathbf{K}_T^{-1} \mathbf{R}(\mathbf{u}_n)$$

$$\mathbf{u}_{n+1} = \mathbf{u}_n + \Delta \mathbf{u}.$$

This iterative formula updates the solution until convergence is achieved.

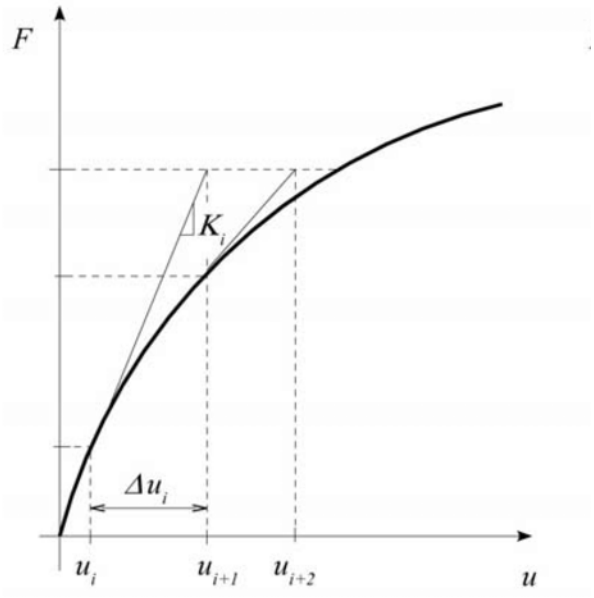

Figure 2.3: Newton Raphson method

2. **Material nonlinearity:** Occurs when the relationship between stress (σ) and strain (ε) deviates from linear behavior. Unlike in linear elasticity, where stress and strain are directly proportional ($\sigma = E \cdot \varepsilon$), material nonlinearity reflects complex phenomena such as plasticity, damage, or viscoelasticity.

   → Plasticity: Irreversible deformation beyond the yield point.

   → Viscoelasticity: Time-dependent deformation

   → Damage or fracture: material degradation leading to crack formation or failure.

   In nonlinear materials, the stress-strain curve is not a straight line. The material behavior varies depending on the load, and properties like stiffness may change during deformation. Common stress-strain curve regions include:

- **Elastic region:** Linear relationship; deformation is fully recoverable.
- **Plastic region:** Permanent deformation begins; stress and strain are no longer proportional.
- **Hardening/Softening:** The material may exhibit strain hardening (increased resistance) or softening (decreased resistance).

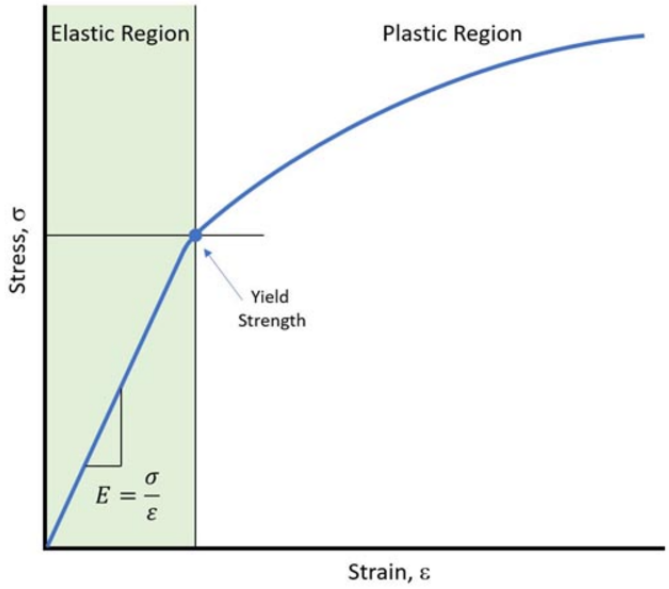

Figure 2.4: Stress-strain curve (nonlinear materials

In addition to material nonlinearities, the relationship between kinematic quantities (displacement, rotation, and strain) can also exhibit nonlinearity. For instance:

(a) **Small strain approximation** (linear strain):

$$\varepsilon(x) = \frac{du}{dx}$$

(b) **Nonlinear strain** (for large deformations):

$$\varepsilon(x) = \frac{du}{dx} + \frac{1}{2}\left(\frac{du}{dx}\right)^2$$

Where:

- $\varepsilon(x)$: Strain in the small deformation regime.
- $E(x)$: Strain in the large deformation regime.
- u: Displacement.
- $\frac{du}{dx}$: Gradient of displacement with respect to position x.

The additional quadratic term in the nonlinear strain expression accounts for large deformation effects, making it crucial in capturing geometric nonlinearity in material models.

3. **Boundary nonlinearity:** Boundary nonlinearity arises in structural systems when the conditions at the boundaries or interfaces are not constant and change due to the applied loads, deformation, or contact. Unlike fixed boundary conditions in linear systems, the response at boundaries in nonlinear systems evolves dynamically, making the problem more complex to analyze and solve.

Contact nonlinearity: Signorini conditions

Contact nonlinearity appears when two or more bodies interact at their surfaces, creating a nonlinear relationship due to changes in the contact area, forces, and relative motion.

When modeling contact nonlinearity, Signorini conditions are used to mathematically describe the interaction between two surfaces. These conditions govern the relationship between the gap, the normal force, and the contact state (contact or separation).

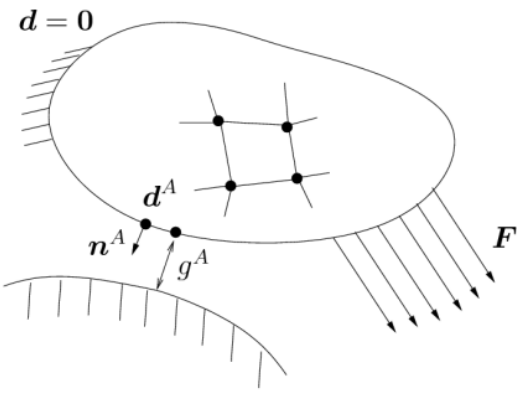

The Signorini conditions ensure that:

(a) **No penetration** occurs between surfaces (unilateral contact).

$$g_n(\mathbf{u}) \geq 0$$

(b) **Contact forces are compressive only** (no tensile forces in the contact zone).

$$F_n \geq 0$$

(c) **Complementarity:** Either contact occurs or separation exists, but not both simultaneously.

$$g_n(\mathbf{u}) \cdot F_n = 0$$

This condition ensures that:

- $g_n(\mathbf{u}) = 0$: Contact occurs, and $F_n > 0$.
- $g_n(\mathbf{u}) > 0$: Separation occurs, and $F_n = 0$.

2.3. Implicit vs Explicit

In implicit methods, the equations of the system cannot be solved directly in a sequential manner, as in explicit methods. At each time step, the system of algebraic equations is solved, which implies the need to solve large matrices, which implies a higher computational cost.

Implicit solvers are known to be more stable, especially in problems involving large changes in time or space, such as in simulations of structural dynamics or fluid flows. This is because they do not depend on a small time step, which allows them to handle large transient or nonlinear changes more efficiently. The time step in explicit analysis must be less than the Courant time step (time it takes a sound wave to travel across an element).

$$C = \frac{u\Delta t}{\Delta x}, \tag{2.8}$$

In contrast, implicit transient analysis has no inherent limit on the size of the time step. As such, implicit time steps are typically several orders of magnitude larger than explicit time steps.

Implicit analysis requires a numerical solver to invert the stiffness matrix once or even several times over the course of a load/time step. This matrix inversion is an expensive operation, especially for large models. Explicit does not require this step.

Implicit solvers usually require a number of iterative steps to converge to the solution, especially when the system is nonlinear or has multiple coupled variables. In explicit dynamic analysis, nodal accelerations are solved directly (not iteratively) as the inverse of the diagonal mass matrix times the net nodal force vector where net nodal force includes contributions from exterior sources (body forces, applied pressure, contact, etc.), element stress, damping, bulk viscosity, and hourglass control. Once accelerations are known at time n, velocities arecalculated at time n+1/2, and displacements at time n+1. From displacements comes strain. From strain comes stress. And the cycle is repeated.

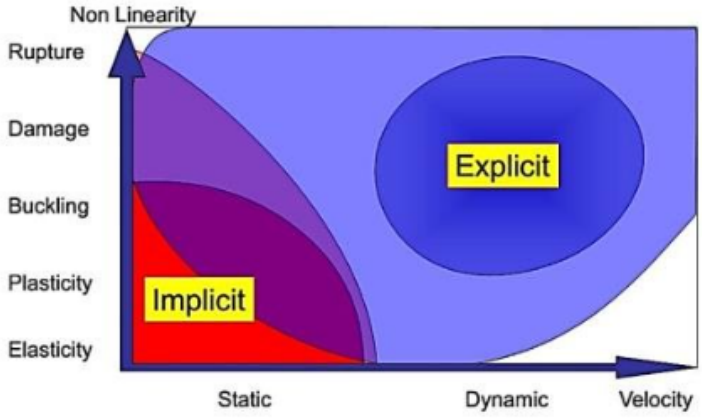

Solver	Implicit	Explicit
Method	Solves a global system of equations.	Calculates nodal acceleration directly
Stability	Inherently stable, admits large time steps	Conditioned by Courant time step
Iteration	Needs iteration to find equilibrium at each step	No iterations required
Computational cost	High due to the inversion of the stiffness matrix	Low because inversion of the stiffness matrix not required
Velocity	Suitable for quasi-static or slow dynamic analysis	Suitable for fast dynamic analysis (impacts)
Non-linearity	More complex to implement for nonlinear problems	Easily handles contact and rupture problems
Time step	Relatively large	Very small, limited by the stability criterion

Table 2.1: Comparation between implicit and explicit solver

3

Modelization

3.1. FE model

The basic model on which we rely for the parametrization is a single shear joint model. It consists of two plates joined by a fastener and subjected to a shear force. See Appendix A for detailed model construction in Abaqus CAE.

One of the plates has one of its sides fixed ($U_x = U_y = U_z = 0, R_x = R_y = R_z = 0$) and the other is subjected to a shear force, as shown in Figure 3.1

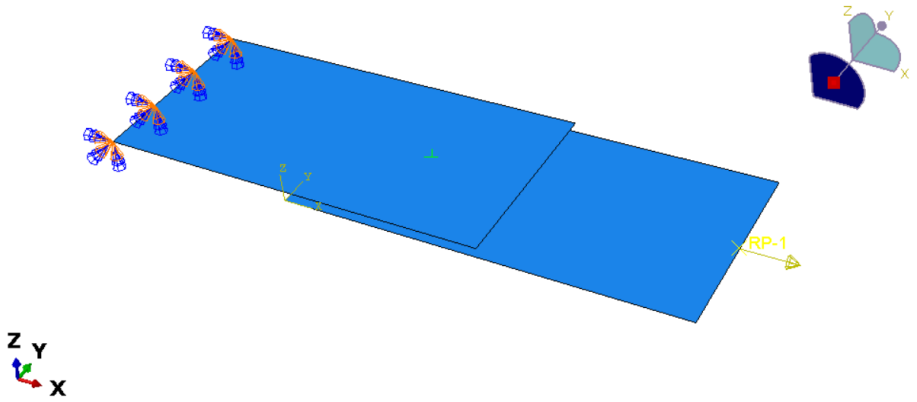

Figure 3.1: Boundary conditions and load applied

For the modeling plate elements are used since there is no triaxiality and fastener elements for the rivets. No large displacements or plastic material are considered in the model, but contact is applied to describe the interaction between the surfaces.

3.1.1. Plate theory

Plates are structural elements characterized by its flat, broad shape, where the thickness is significantly smaller in comparison to its other two dimensions, such as its length and width. This disparity in dimensions allows plates to be categorized as thin structural elements.

The measurement of the plate's thickness is always taken normal to the middle surface of the plate. The middle surface is an imaginary plane that lies exactly halfway between the two broad faces of the plate. This middle surface serves as a reference point for analyzing the plate's mechanical behavior, such as when evaluating bending, shear stresses, or deflections under load.

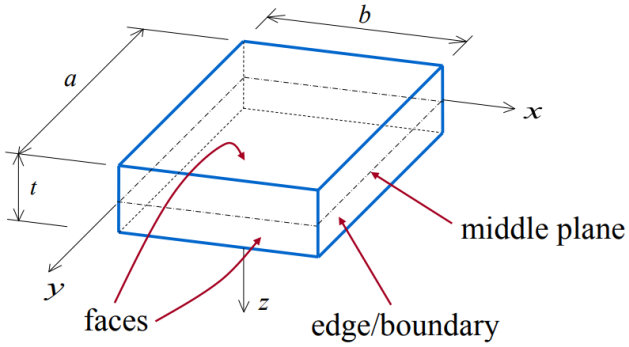

Figure 3.2: Plate

Plate theory is an approximate theory; assumptions are made and the general three dimensional equations of elasticity are reduced. It turns out to be an accurate theory provided the plate is relatively thin but also that the deflections are small relative to the thickness.

Kirchhoff-Love Plate Theory

The Kirchhoff–Love theory is an extension of Euler–Bernoulli beam theory to thin plates. It is assumed that a mid-surface plane can be used to represent the three-dimensional plate in two-dimensional form.

Let the plate mid-surface lie in the x-y plane and the z axis be along the thickness direction, forming a right handed set.

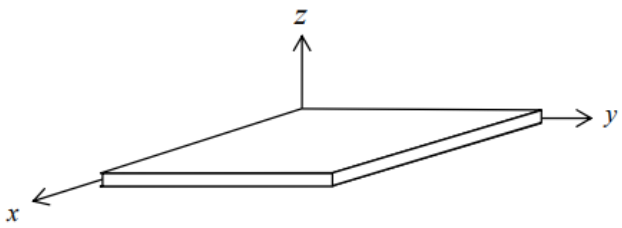

Figure 3.3: Cartesian axes

The stress components applied to a representative element of the plate are illustrated in Figure 3.4.
The following assumptions are made:

(i) **The mid-plane is a "neutral plane"**

- The middle plane of the plate remains free of in-plane stress/strain.
- Bending of the plate will cause material above and below this mid-plane to deform in-plane.

(ii) **Vertical strain is ignored**

- Line elements lying perpendicular to the mid-surface do not change length during deformation, so that $\varepsilon_{zz} = 0$ throughout the plate.

(iii) **Line elements remain normal to the mid-plane**

- Line elements lying perpendicular to the middle surface of the plate remain perpendicular to the middle surface during deformation.

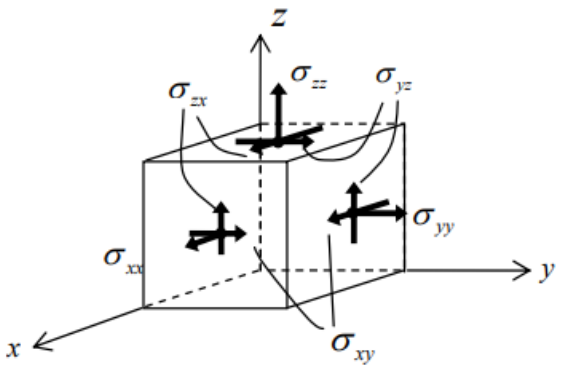

Figure 3.4: Stresses acting on a element

In terms of the mid-surface, displacements can be expressed as:

$$u = u_0 - z\frac{\partial w_0}{\partial x} \tag{3.1}$$

$$v = v_0 - z\frac{\partial w_0}{\partial y} \tag{3.2}$$

$$w = w_0 \tag{3.3}$$

When the mid-surface strains are neglected, according to the final assumption of the classical plate theory, one has:

$$\varepsilon_{xx} = -z\frac{\partial^2 w}{\partial x^2} \tag{3.4}$$

$$\varepsilon_{yy} = -z\frac{\partial^2 w}{\partial y^2} \tag{3.5}$$

$$\gamma_{xy} = -2z\frac{\partial^2 w}{\partial x \partial y} \tag{3.6}$$

From Hooke's law, taking $\sigma_{zz} = 0$, these relations are obtain:

$$\varepsilon_{xx} = \frac{1}{E}\sigma_{xx} - \frac{\nu}{E}\sigma_{yy}, \quad \varepsilon_{yy} = \frac{1}{E}\sigma_{yy} - \frac{\nu}{E}\sigma_{xx}, \quad \gamma_{xy} = \frac{2(1+\nu)}{E}\tau_{xy} \tag{3.7}$$

With these equations and in conjunction with 3.4, 3.5 and 3.6, normal stresses are deduced.

$$\begin{Bmatrix} \sigma_{xx} \\ \sigma_{yy} \\ \tau_{xy} \end{Bmatrix} = \frac{E}{1-\nu^2}\begin{bmatrix} 1 & \nu & 0 \\ \nu & 1 & 0 \\ 0 & 0 & \frac{1-\nu}{2} \end{bmatrix}\begin{Bmatrix} \varepsilon_{xx} \\ \varepsilon_{yy} \\ \gamma_{xy} \end{Bmatrix} \tag{3.8}$$

This matrix equation represents the plane stress relationship in linear elasticity, where E is the Young's modulus and ν is the Poisson's ratio.

3.1.2. Abaqus elements library

Abaqus provides an extensive element library, offering a versatile set of tools for solving diverse engineering problems. Each element in Abaqus is uniquely identified by its name, such as `T2D2`, `S4R`, `C3D8I`, or `C3D8R`, which encodes information about its properties.

Family

Element families are categorized by their geometry type, which is one of the primary distinctions among them. The first letter(s) of an element's name indicate the family to which it belongs. Commonly used element families in stress analysis are illustrated in Figure 3.5.

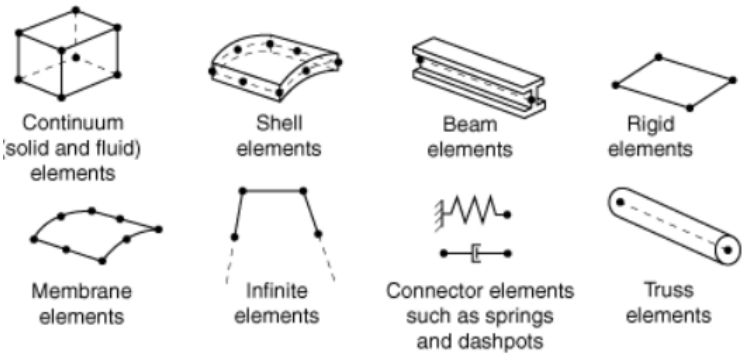

Figure 3.5: Commonly used element families

Degrees of Freedom

The degrees of freedom (DOF) represent the fundamental variables calculated during an analysis. In stress/displacement simulations, DOF include translations and, for shell and beam elements, rotations at each node. For heat transfer simulations, DOF correspond to temperatures at each node. In coupled thermal-stress analyses, temperature DOF are included in addition to displacement DOF at each node. Since the DOF differ, heat transfer and coupled thermal-stress analyses require different element types than stress analyses.

Number of Nodes and Interpolation Order

Displacements or other DOF are calculated at the nodes of an element. Displacements at other points within the element are obtained by interpolating from the nodal values. The interpolation order depends on the number of nodes in the element:

- **Linear elements (first-order):** These elements have nodes only at their corners and use linear interpolation in each direction.
- **Quadratic elements (second-order):** These elements include midside nodes and use quadratic interpolation.
- **Modified second-order elements:** Triangular or tetrahedral elements with midside nodes employ modified second-order interpolation.

The number of nodes in an element is typically indicated in its name.

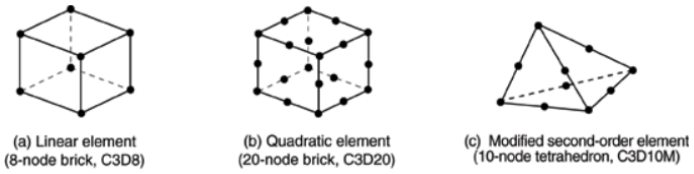

Figure 3.6: Interpolation nodes

Formulation

The formulation of an element defines the mathematical framework governing its behavior. Abaqus offers two primary formulations:

- **Lagrangian formulation:** In this approach, elements deform along with the material. Most stress/displacement elements in Abaqus use this formulation.
- **Eulerian formulation:** In this method, elements remain fixed in space while the material flows through them. This is commonly used in fluid mechanics simulations. For example:
  - **Abaqus/Standard** employs Eulerian elements to model convective heat transfer.
  - **Abaqus/Explicit** offers multimaterial Eulerian elements for stress/displacement analyses and adaptive meshing. Adaptive meshing combines Lagrangian and Eulerian characteristics, allowing elements to move independently of the material.

In Abaqus/Explicit, Eulerian elements can interact with Lagrangian elements using general contact definitions.To accommodate various behaviors, some Abaqus element families include multiple formulations. The conventional shell element family comprises:

- General-purpose shell elements.
- Thin shell elements.
- Thick shell elements.

Abaqus also offers continuum shell elements, which are similar to continuum elements but designed to simulate shell behavior with minimal elements through the thickness.

Some Abaqus/Standard element families include alternative formulations, indicated by additional characters in their names. For example hybrid elements, designed to address incompressible or inextensible behaviors, are marked with an H at the end of their names (e.g., `C3D8H`, `B31H`).

Mass Formulation and Dynamic Analyses

Abaqus employs different mass formulations depending on the solver:

- **Abaqus/Standard** uses the lumped mass formulation for low-order elements.
- **Abaqus/Explicit** applies the lumped mass formulation across all elements. However, this may lead to deviations in the second mass moments of inertia, particularly for coarse meshes.

For steady-state dynamic and frequency extraction analyses, Abaqus/Standard uses a specialized projected mass matrix algorithm for certain shell elements (e.g., `S3`, `S3R`, `S4`, `S4R`, `SC6R`, `SC8R`, and `S4R5`). This approach may result in slight variations when comparing these results with those obtained from implicit dynamic analyses.

In Abaqus/CFD, hybrid elements are employed to address common stability issues in incompressible flow simulations. Additionally, Abaqus/CFD allows extra degrees of freedom to be added based on the procedure settings, such as turbulence models or optional energy equations.

Integration

Abaqus uses numerical methods to integrate quantities over the volume of each element, enabling flexibility for diverse material behaviors. Gaussian quadrature is the primary technique, with material responses evaluated at integration points within each element. For continuum elements, both full and reduced integration options are available, significantly impacting accuracy. Reduced integration elements are identified by the letter R in their names.

For shell, pipe, and beam elements, properties can either be defined as general section behaviors or integrated numerically to track nonlinear material responses. Additionally, composite layered sections can be specified, allowing for different materials in each layer. This capability is available for shells and, in Abaqus/Standard, for three-dimensional brick elements.

3.1.3. S4R element

The S4R element is a popular shell element in Abaqus, belonging to the conventional shell element family. It is specifically designed for modeling structures where one dimension, the thickness, is significantly smaller than the other dimensions, that is why it has been used to model the plates of the model.

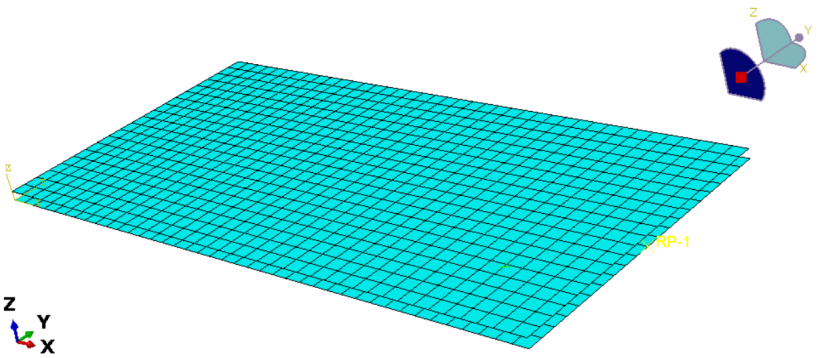

Figure 3.7: Plates mesh

Conventional shell elements, such as the S4R, discretize the structure by defining a reference surface and determining the thickness through section properties. These elements include both displacement and rotational degrees of freedom, which makes them particularly suitable for analyzing bending and deformation.

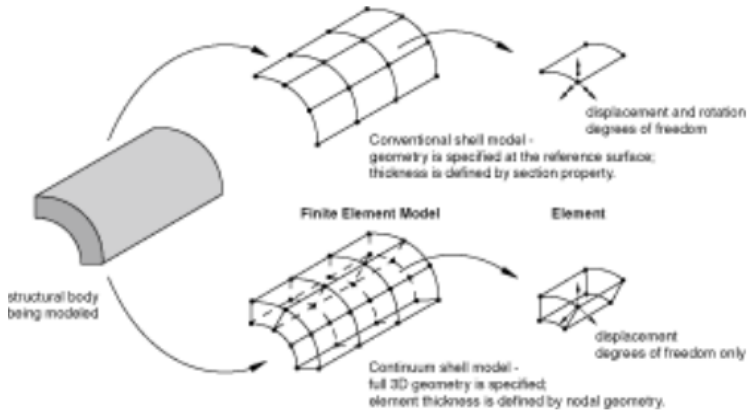

Figure 3.8: Conventional versus continuum shell element

The S4R element uses a set of conventions to define its behavior and orientation. Local directions on the shell surface are used for defining anisotropic material properties and reporting stress and strain components. These directions are typically output in the current configuration during large-deformation analyses, except in thin shell elements where the reference configuration is used.

The positive normal direction of the S4R element is determined using the right-hand rule and plays a critical role in defining the top and bottom surfaces for contact interactions and pressure load applications. The "top" surface corresponds to the positive normal direction (referred to as the SPOS face), while the "bottom" surface corresponds to the negative normal direction (SNEG face).

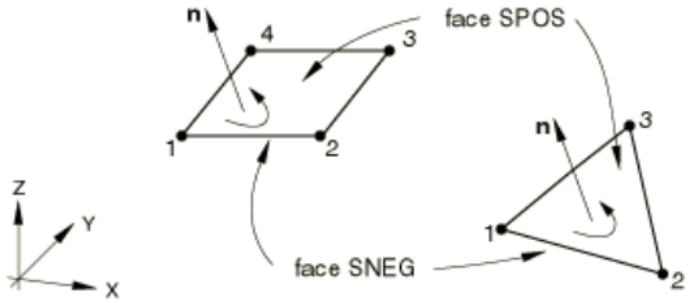

Figure 3.9: Conventional versus continuum shell element

The S4R element includes several advanced features that make it highly effective for shell modeling. It employs reduced integration to enhance computational efficiency while mitigating shear locking issues, which can arise in first-order elements. Each node of the element has six degrees of freedom, including three translational and three rotational, allowing for detailed modeling of structural behaviors. The S4R is a four-node quadrilateral element, making it a general-purpose choice for shell analysis in a variety of applications, such as thin to moderately thick structures and complex geometries.

Integration through the shell thickness can be customized for the S4R element. Users can define the number of integration points, with default settings determined by Simpson's rule (five points) or Gauss quadrature (three points). For composite sections, the integration points per layer can also be specified, allowing detailed modeling of laminate behavior. In Abaqus/Standard, the default output includes values at the top and bottom surfaces of the shell, while in Abaqus/Explicit, all section points through the thickness are included in the output by default.

3.1.4. *FASTENER

This element defines mesh-independent fasteners. The mesh-independent fastener capability provides a convenient method for defining point-to-point connections between two or more surfaces such as spot welds or rivet connections. It uses spatial coordinates of fastener locations to establish connections independently of the underlying meshes it combines either connector elements or BEAM MPCs with distributing coupling constraints allowing connections to be placed anywhere between two or more surfaces regardless of mesh refinement or node locations on each surface it can connect both deformable and rigid element-based surfaces it can model rigid elastic or inelastic connections with failure by leveraging the generality of connector behavior definitions and it is available only in three dimensions.

The fastener can be positioned anywhere between the components to be joined, independent of the mesh configuration. In other words, the fastener's placement does not depend on the location of the nodes on the connecting surfaces. Instead, the connection to each part is distributed among multiple nodes on the surfaces near the fastening points.

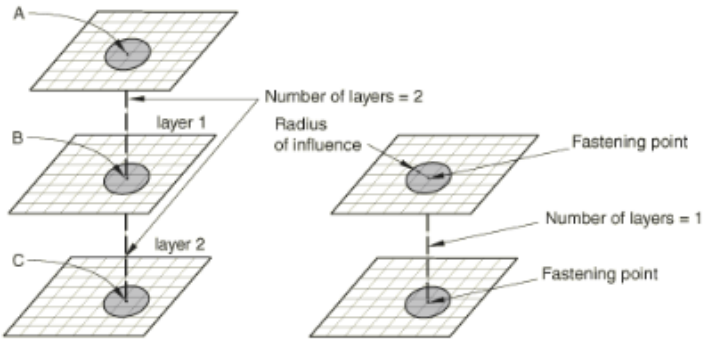

Figure 3.10: One-layer and two-layer fastener configuration

Connector elements

Using connector elements as the foundation for a point-to-point connection enables the modeling of highly complex behavior in fasteners. Similar to other applications of connector elements, the connection can either be fully rigid or allow for unrestricted relative motion in local connector components. Additionally, deformable behavior can be defined through a connector behavior specification, which may incorporate the effects of elasticity, damping, plasticity, damage, and friction. There are two approaches to defining fasteners that utilize connector elements to represent the interaction between fastening points. In both cases, the fastener interaction is associated with an element set containing the connector elements, and a connector section definition referencing this element set must be specified.

When connector elements are genearted by Abaqus, there is no need to explicitly define the connector elements that link the fastening points of the fastener. Instead, the fastener interaction refers to an empty element set. You must specify a connector section definition that references this element set. Additionally, a reference node set containing a list of user-defined nodes is assigned to the fastener interaction. The nodes in this reference set serve as positioning points for locating the fasteners.

For single-layer fasteners, Abaqus generates individual connector elements, with each node in the reference node set becoming the first node of a connector element. The second node of each connector element is generated internally by Abaqus.

For multi-layer fasteners, Abaqus creates linked sets of connector elements. Each node in the reference node set becomes the first node of the first connector element in each linked set, while subsequent nodes within the set are generated internally. The number of connector elements in each linked set corresponds to the

number of layers in the fastener. These connector elements are assigned internally generated element numbers and grouped into a named, user-specified element set. This element set can be used to request output for the connector elements, but it should not be included in another element set definition.

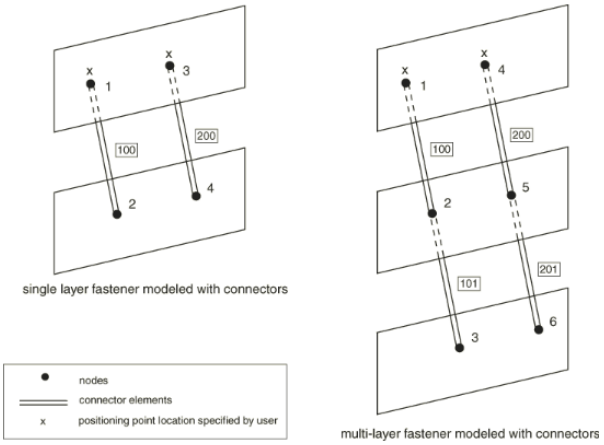

Figure 3.11: Single layer fastener modeled with connectors

Attachment method: face-to-face

Each interaction defines one or more fasteners, with the total number of fasteners corresponding to the number of positioning points used to place them. Positioning points are nodes specified at the fastener locations and assigned as a reference node set for the interaction.

In general, a positioning point should be placed as close as possible to the surfaces being joined. The reference node defining the positioning point can either be one of the nodes on the connected surfaces or a separately defined node. Abaqus determines the exact locations where the fastener layers attach to the connected surfaces by first projecting the positioning point onto the nearest surface.

The face-to-face projection method is the most appropriate when the surfaces to be fastened together are nearly parallel to each other. In this method, Abaqus projects each positioning point onto the nearest surface along a directed line segment that is normal to the surface. Alternatively, you can define the projection direction manually. This option can be particularly useful when two-dimensional drawings are used to determine the positioning point locations, as these locations may be precisely known in two dimensions but not in the third. In such cases, the specified direction is typically perpendicular to the plane of the drawing.

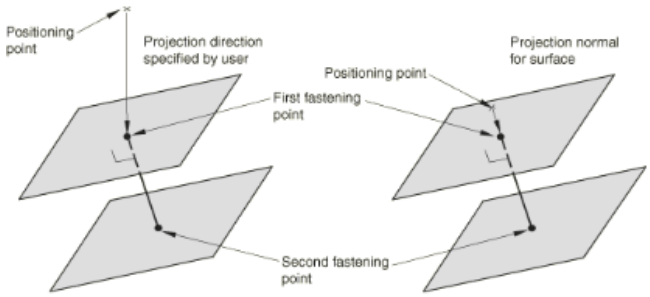

Figure 3.12: Directed and normal projection to locate the fastening points for the face-to-face projection method

Once the fastening point on the closest surface is identified, Abaqus determines the corresponding points on the other surface(s) by projecting the initial fastening point onto them along the fastener's normal direction,

which is generally perpendicular to the nearest surface. Figure 3.12 illustrates the two methods for locating projection points. When the surfaces to be fastened are not perfectly parallel, Abaqus may sometimes position attachment points at the nearest facet edges or corners of the surface instead of following the fastener's normal direction.

The positioning point (a node in the reference node set) may not align exactly with the fastening points determined by Abaqus. As a result, the coordinates of the node at the positioning point may deviate from the user-specified values when it is relocated to a fastening point. If this node is part of the connectivity of a user-defined element, its displacement can lead to unacceptable initial distortions in the element that includes it. In such cases, it is advisable to define the node at the positioning point separately. Generally, this node should not be one of the nodes belonging to the connected surfaces.

Fastener orientation

Each fastener is defined within a local coordinate system that moves along with the fastener. By default, Abaqus determines this local system by projecting the global coordinate system onto the fastened surfaces, following the standard convention for surfaces in space. In this approach, the local z-axis of each fastener is oriented perpendicular to the surface closest to the fastener's reference node.

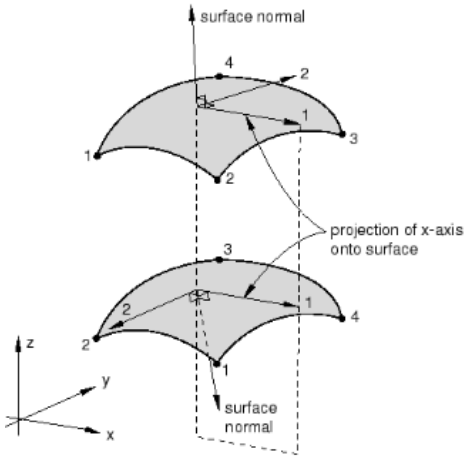

Figure 3.13: Default local surface directions

Radius of influence

Each fastening point is linked to a group of nodes on the surface within its immediate vicinity, referred to as the region of influence. The movement of the fastening point is then connected to the motion of the nodes in this region through a weighted distributed coupling constraint.

To determine the region of influence, Abaqus calculates an internal radius of influence based on the fastener's geometric properties, the characteristic length of the connected facets, and the selected weighting function. By default, the radius of influence is set as the largest value among the internally computed radius, the physical fastener radius, and the distance from the projection point to the nearest node. Users can define a specific radius of influence, but Abaqus will override any user-defined value that is smaller than the computed default. Regardless of the calculation method, each region of influence will always include at least three nodes.

Weighting method

Abaqus calculates a larger default radius of influence for higher-order weighting methods because nodes farther from the fastening point contribute minimally to its motion. To ensure an adequate "smearing" effect, the number of nodes within the region of influence must be increased by expanding the default radius. In contrast, a uniform weighting scheme assigns significant influence to surface nodes farther from the fastening point. As a result, a smaller default radius of influence is sufficient, as the smearing effect remains strong even with fewer nodes. If fewer than three cloud nodes are detected, increasing the radius of influence can help form the fastener by incorporating more nodes into the coupling node cloud. By default, Abaqus uses the uniform weighting method.

Surface coupling: continuum method

The default continuum coupling method links the translation and rotation of each fastening point to the average translation of the group of coupling nodes on each fastened surface. This constraint distributes forces and moments at the fastening point solely as a coupling node-force distribution. When the weight factors are interpreted as bolt cross-section areas, the force distribution corresponds to the classic bolt pattern force distribution. For each fastening point and its associated group of coupling nodes, the constraint enforces a rigid beam connection between the fastening point and a point located at the weighted center of the coupling nodes' positions.

Fastener properties

Each fastener interaction definition must reference a property that defines the geometric section properties of the fastener. Fasteners are assumed to have a circular projection onto the connected surfaces, requiring the user to specify the fastener's radius. For fasteners modeled using connector elements, both translational and rotational degrees of freedom can be released by selecting connector section types that allow unconstrained degrees of freedom.

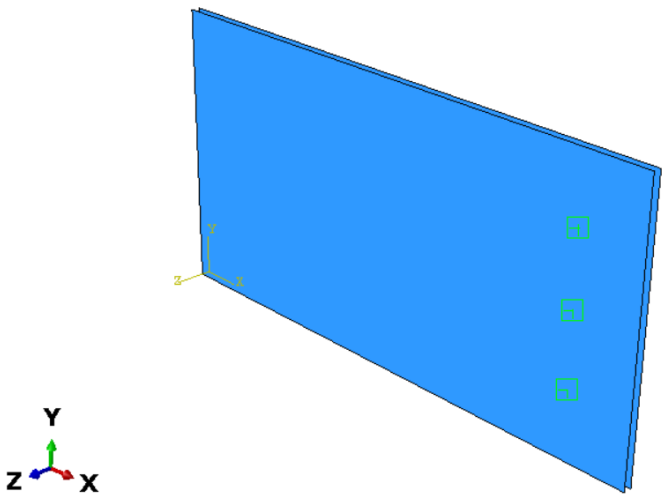

Figure 3.14: Model with fasteners

3.2. FEM validation

To validate the results from the model, the distribution for each fastener is analytically calculated. This calculation is performed according to the method outlined in the book *"Airframe Stress Analysis and Sizing"* [10] for eccentric joints.

Concentric riveted connections that do not carry moments are assumed to have an even load distribution, meaning the load is shared equally among the rivets. This holds true approximately, even when the rivets are aligned in a single row, as the end or first fasteners are not excessively loaded as one might expect.

Shear load on fastener 1, due to the concentrated load:

$$P_{s,1} = P\left(\frac{A_1}{\sum A}\right) \tag{3.9}$$

where A is the fastener area and the load goes through the centroid of fastener clusters.

This force corresponds to the shear force in the direction of the applied force (x-axis). The shear force in the y-direction is considered to be zero.

Using this equation, these assumptions are made:

- Fastener materials are the same
- Fastener bearing on the same material and thickness
- Fastener shear load assumes straight line distribution

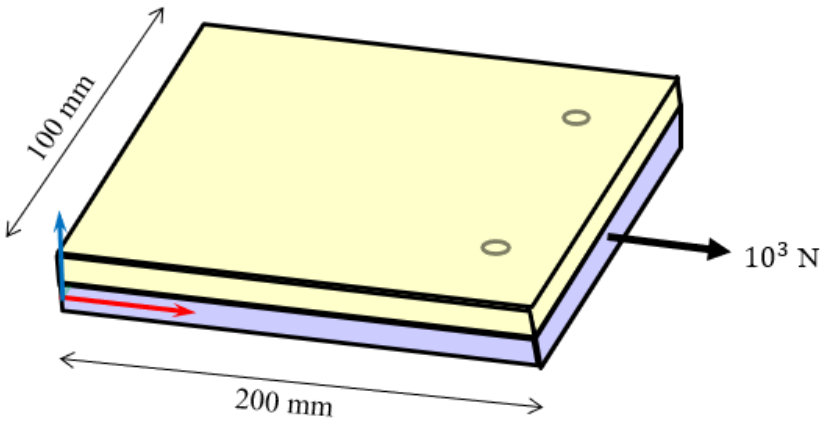

Figure 3.15: Model configuration

According to [10], for the model configuration shown in Figure 3.15 the shear load is the following on each fastener:

$$P_{s1,s2} = 5000N \tag{3.10}$$

As there is an eccentricity between the point of application of the axial force and the midplane of the joint, a moment is generated which gives place to the axial force. It is calculated analytically with the following formula, where N is the number of joints.

$$P_{a1,a2} = \frac{M}{LN} = 85.23N \tag{3.11}$$

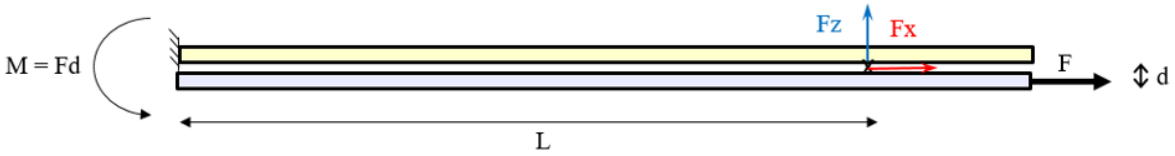

Figure 3.16: Load scheme

Table 3.1 shows the forces at each joint obtained by Abaqus. It can be seen that the value of the shear force at x differs very little from the calculated one. The value of the axial force is higher when calculated analytically. Once these values are obtained, it can be said that the model is verified.

Joint	Shear X (N)	Axial (N)
1	4999.47	73.17
2	4999.47	73.17

Table 3.1: Joint forces by Abaqus

4

Methodology

4.1. Objective of the work

The main objective of this work is to develop an automated model for analyzing failure criteria in plate joints using Abaqus. This involves building a comprehensive simulation framework that can evaluate the structural integrity of joints under various loading conditions, identifying points of potential failure. By automating this process, it becomes possible to efficiently simulate a range of configurations and conditions, allowing for more robust and accurate analysis in structural engineering applications.

To achieve this main objective, several specific goals have been established. First, the creation of scripts in Python will enable parameterization of the model, providing flexibility in adjusting key variables such as plate dimensions, load magnitudes, and the number and arrangement of fasteners. This parametrization is crucial for conducting sensitivity analyses and optimizing joint configurations based on structural demands.

Furthermore, automation of the post-processing stage is an essential component of this work. This includes extracting and analyzing key data points such as stress, strain, and failure criteria values from the simulation results. Automating post-processing allows for a streamlined evaluation of results, enabling comparisons across different simulation runs without manual intervention.

Through this automated approach, the project aims to provide a reliable and efficient method for structural engineers to assess and optimize plate joints in various industrial contexts. This methodology could have broad applicability in sectors where joint integrity is critical, such as aerospace, automotive, and civil engineering, ultimately contributing to safer and more cost-effective design solutions.

4.2. Procedure

4.2.1. Base model creation with Python

A Python code is developed to establish the foundational structure of a single-shear joint in Abaqus. This serves as the starting point for further modifications and parameterizations.

In the script the model will be generated, where the sketches and the parts of the plates are created. Then the plates are assembled and placed in the desired position. To create the joint between them it is necessary to define the connector section and the surfaces to be joined. The surface to surface contact is also defined.

Once this is done, the mesh of the plates is generated using S4R elements. Then the boundary conditions are determined by fixing the edge of one of the plates. The applied load is applied at the center of the edge of the unfixed plate.

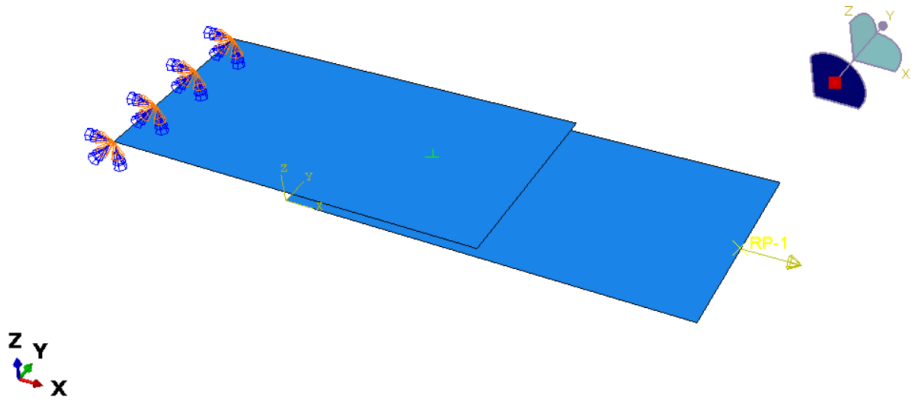

Figure 4.1: Simple shear model

4.2.2. Model parameterization

The model is parameterized to allow flexibility in adjusting key variables such as plate dimensions, load magnitudes, and the number and arrangement of fasteners. This parameterization is essential for conducting sensitivity analyses and optimizing joint configurations according to structural demands.

The code of our model is adapted to parameterize the variables shown in Figure 4.2 and Figure 4.3.
The correspondence between the numbers and the variables is as follows:

1. Plate 1 length
2. Plate 1 width
3. Thickness plate 1
4. Plate 2 length
5. Plate 2 width
6. Thickness plate 2
7. Displacement plate 2
8. Load magnitude
9. Mesh size
10. Number of joints along x axis
11. Number of joints along y axis
12. Fastener radius

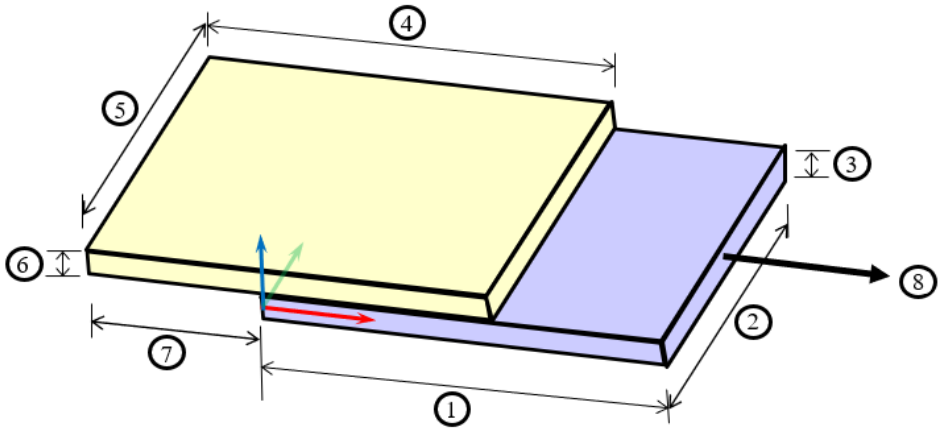

Figure 4.2: Model parameters I

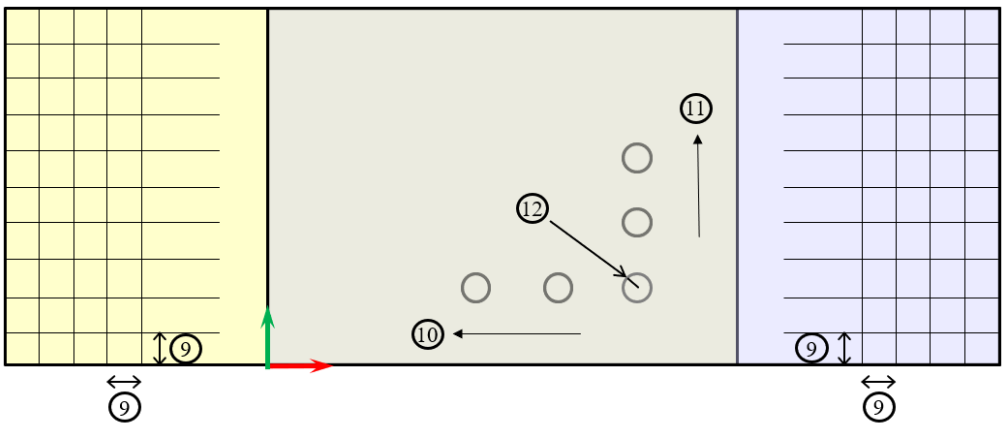

Figure 4.3: Model parameters II

The different parameter values are stored in an excel file in the format shown in Table 4.1, where the first line is the name of the parameter, and the following lines contain the values for each model, with the first line containing the values for the first model, the second line for the second, and so on.

plate1_length	**plate1_width**	**plate2_length**	**plate2_width**	**thickness1**	**thickness2**	**...**
200	100	200	100	3	5	...
200	100	200	100	3	5	...

Table 4.1: Model parameters in Excel format

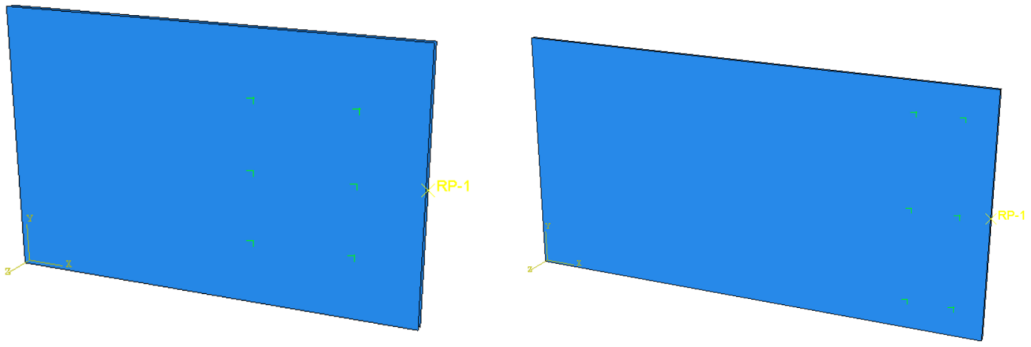

Figure 4.4: Variation of plate length parameter

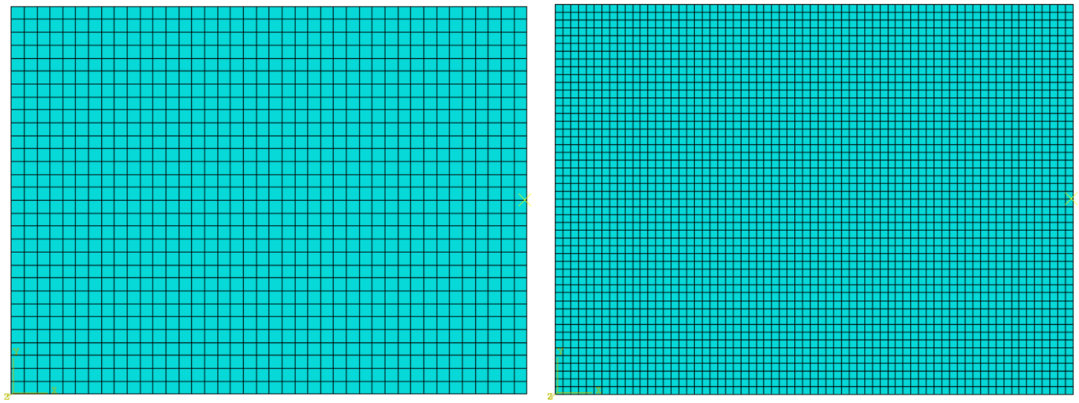

Figure 4.5: Variation of mesh parameter

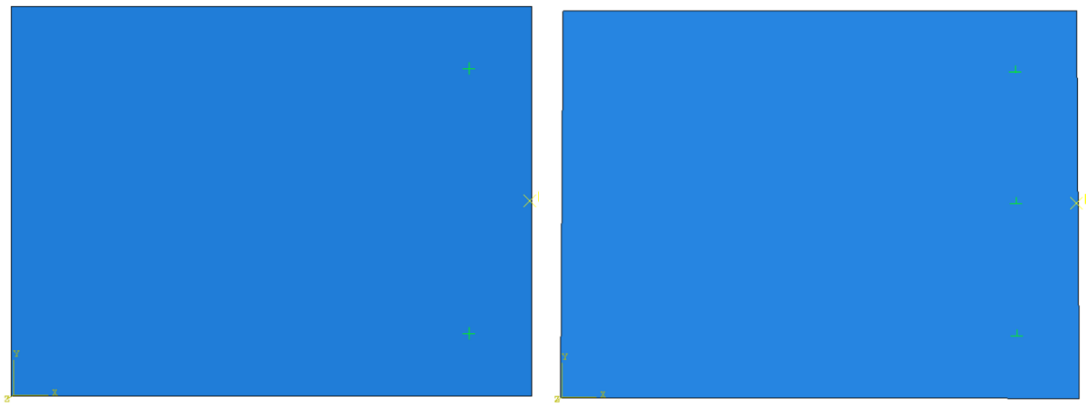

Figure 4.6: Variation of joints along Y axis

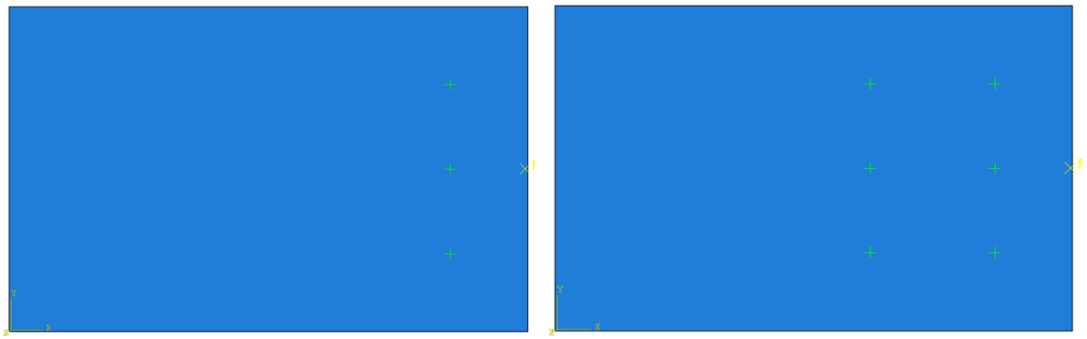

Figure 4.7: Variation of joints along X axis

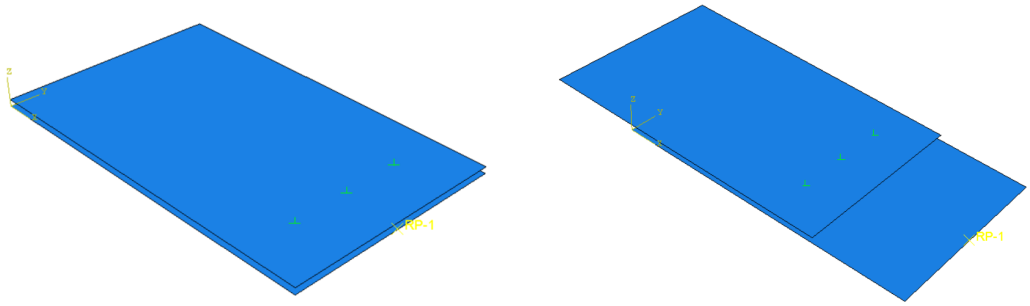

Figure 4.8: Variation of displacement plate 2

The script reads all these parameters, and stores them in a dictionary. Based on this, it creates the sketch by assigning the correct dimensions for each model, assigns a mesh size, etc.

```
def read_parameters_from_excel(file_path):
    df = pd.read_excel(file_path)
    param_sets = []

    for _, row in df.iterrows():
        parameters = {}
        for param_name in df.columns:
            param_value = row[param_name]
            try:
                param_value = eval(param_value) if isinstance(param_value, str) and param_value.startswith('(') else param_value
            except:
                pass
            parameters[param_name] = param_value
        param_sets.append(parameters)
    return param_sets
```

Figure 4.9: Read paratemers function

```
# Model creation
myModel = mdb.Model(name=model_name)

# Parameterise dimensions of plate 1
length1, width1 = plate1_dims

# Sketch plate 1
s1 = myModel.ConstrainedSketch(name='Plate1Sketch', sheetSize=300.0)
s1.rectangle(point1=(0.0, 0.0), point2=(length1, width1))

# Part plate 1
plate1 = myModel.Part(name='Plate1', dimensionality=THREE_D, type=DEFORMABLE_BODY)
plate1.BaseShell(sketch=s1)
```

Figure 4.10: Plate 1 definition

```
myFastenerSection = myModel.ConnectorSection(name='BoltSection', assembledType=BEAM)

targetSurfaces = [plate1Surface, plate2Surface]

myAssembly.engineeringFeatures.PointFastener(
    name='BoltConnection',
    region=AttPointSet,
    physicalRadius=fastener_radius,
    sectionName='BoltSection',
    attachmentMethod=FACETOFACE,
    targetSurfaces=targetSurfaces)
```

Figure 4.11: Fastener point-based definition

```
myModel.ContactProperty('ContactProp')
myModel.interactionProperties['ContactProp'].TangentialBehavior(formulation=FRICTIONLESS)
myModel.interactionProperties['ContactProp'].NormalBehavior(
    pressureOverclosure=HARD, allowSeparation=OFF, constraintEnforcementMethod=DEFAULT)

myModel.SurfaceToSurfaceContactStd(
    name='Int-1',
    createStepName='Initial',
    main=plate1Surface,
    secondary=plate2Surface,
    sliding=FINITE,
    thickness=ON,
    interactionProperty='ContactProp',
    adjustMethod=OVERCLOSED,
    initialClearance=OMIT,
    datumAxis=None,
    clearanceRegion=None)
```

Figure 4.12: Contact definition

4.2.3. Batch execution

The model stack is launched in batch mode to enable the simultaneous execution of multiple simulations in Abaqus. This approach improves efficiency by allowing large numbers of configurations to be processed without manual intervention, making it ideal for projects that require extensive parametric studies.

```
def main():
    for inputFile in glob.glob(os.path.join(input_folder, "SimpleShearJointJob_*.inp")):
        print(f"Processing file: {inputFile}")

        job_name = os.path.splitext(os.path.basename(inputFile))[0]
        command = f"{abaqusVersion} job={job_name} input={inputFile} cpus={nCores} scratch={scratch_folder} int"

        original_dir = os.getcwd()
        os.chdir(input_folder)

        startTime = time.time()
        subprocess.call(command, shell=True)
        jobTime = time.time() - startTime

        os.chdir(original_dir)

        for ext in ['.odb', '.dat', '.msg', '.sta', '.com', '.prt']:
            output_file = os.path.join(input_folder, f"{job_name}{ext}")
            if os.path.exists(output_file):
                try:
                    shutil.move(output_file, os.path.join(output_folder, f"{job_name}{ext}"))
                    print(f"Moved {output_file} to {output_folder}")
                except Exception as e:
                    print(f"Error moving {output_file} to {output_folder}: {e}")
            else:
                print(f"File {output_file} not found in {input_folder}")

        log_file = os.path.join(base_folder, "log.txt")
        with open(log_file, "a") as fout:
            fout.write("[%s] %s finished in %f seconds\n" % (socket.gethostname(), inputFile, jobTime))

    return True
```

Figure 4.13: Script for batch execution

4.2.4. Postprocess

Once the models are run and the output files are obtained, it is time to postprocess them to be able to analyze and visualize the results. The post-processing phase is crucial for interpreting the simulation data and extracting meaningful insights about the model's behavior.

In the script where the model are created, there is also a part where the results of interest are requested.

```
output_request_name = f'FieldOutputs_{step_name}'
myModel.fieldOutputRequests.changeKey(fromName='F-Output-1', toName=output_request_name)
myModel.fieldOutputRequests[output_request_name].setValues(variables=('U', 'S', 'CTF', 'NFORC', 'CSTRESS'))
```

Figure 4.14: Output request code

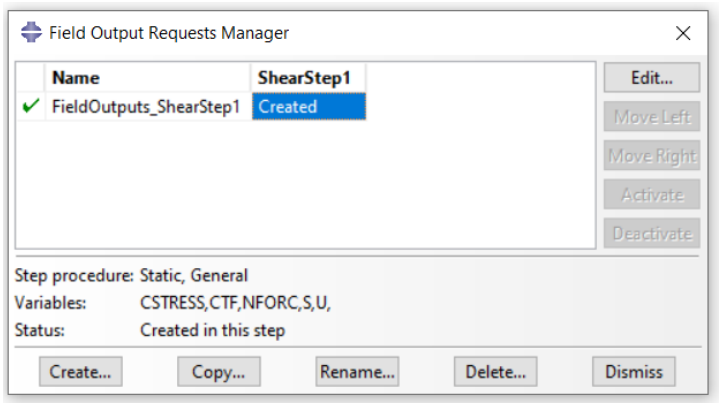

Figure 4.15: Output request Abaqus CAE

The following results were obtained:

- **U (Displacements)**: It is a noval variable output. Represents all physical displacement components, including rotations at nodes with rotational degrees of freedom. Allows evaluation of how the structure deforms under different loading conditions. It is crucial to verify that displacements are within acceptable design limits.

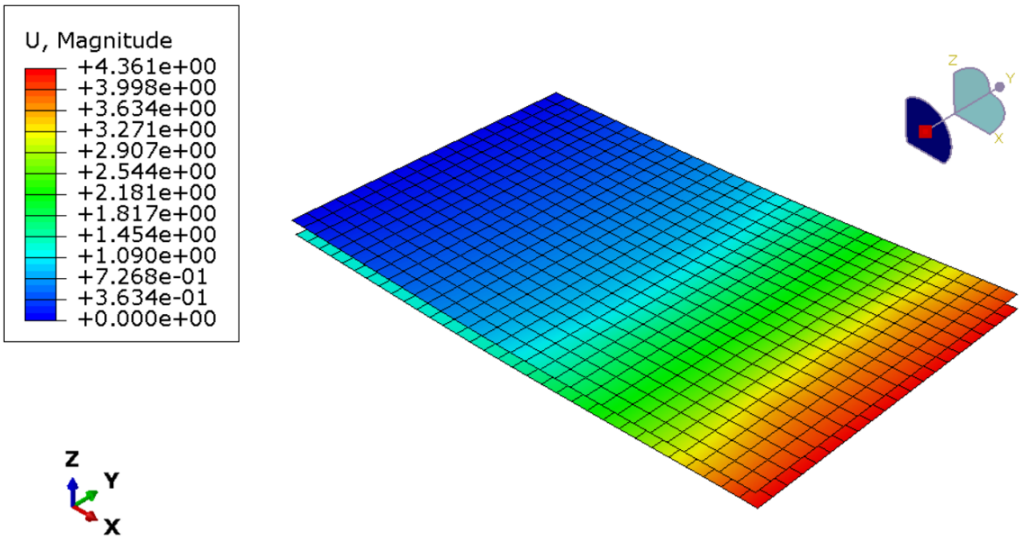

Figure 4.16: Output U

- **S (Stresses)**: Represents the Cauchy stress tensor in the model elements, which includes normal and shear stresses. Helps identify high-stress areas that could be prone to failure. It is essential for the analysis of material strength and durability.

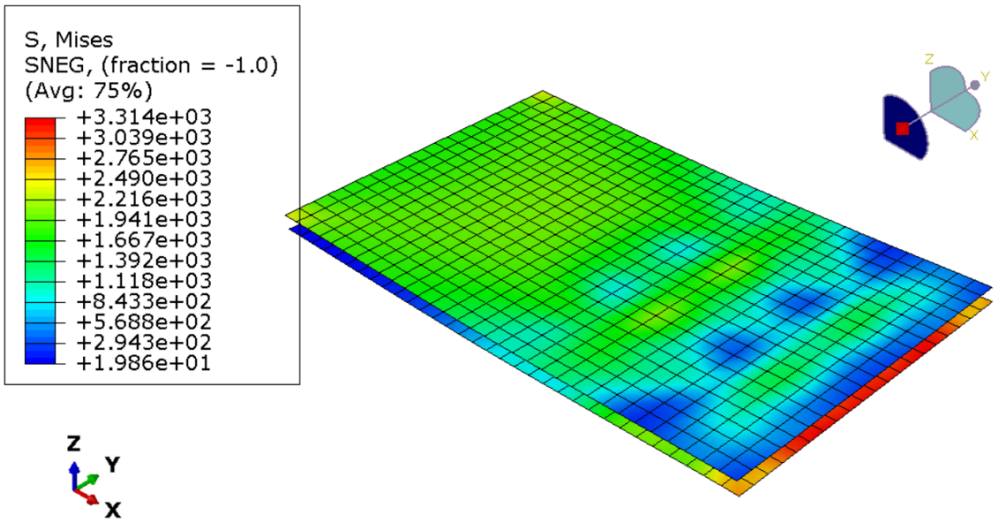

Figure 4.17: Output S

- **CTF (Connector Forces)**: All components of connector total forces and moments. Fundamental for analyzing the effectiveness and safety of the joints. It allows verification that the connectors are operating within their design capacities.

- **NFORC (Nodal Forces)** Forces at the nodes of the element caused by the stress in the element (internal forces in the global coordinate system). Helps understand how loads are distributed throughout the structure, which is vital to ensure the model is in equilibrium and loads are transferred appropriately.

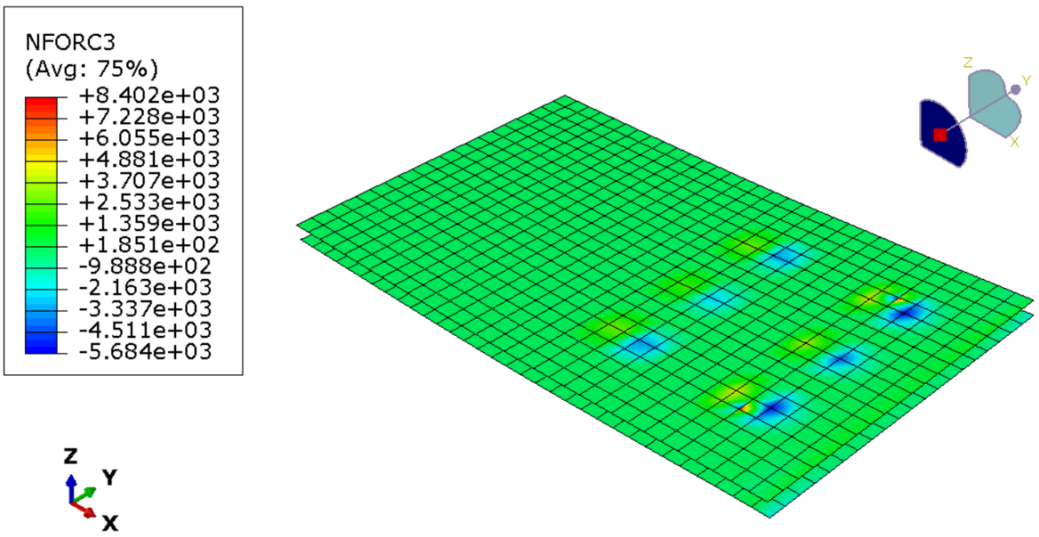

Figure 4.18: Output NFORC3

- **CSTRESS (Connector Stresses)** Contact pressure (CPRESS) and frictional shear stresses (CSHEAR). Allows evaluation of connector performance under load. It is crucial to ensure that connectors do not fail due to excessive stresses.

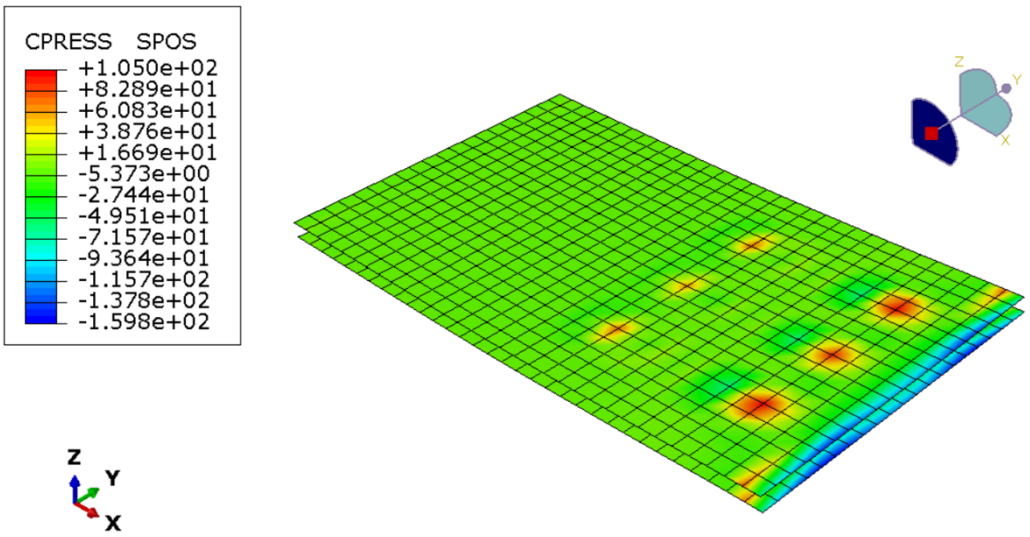

Figure 4.19: Output CPRESS

CTF and CPRESS simulation results are extracted using Python scripts that access the output database (ODB) files generated by Abaqus. These data are collected in a csv file, that can then be imported into Excel for easier data manipulation and analysis.

```
Type,ID,Force X (N) / Cpress (Pa),Force Y (N),Force Z (N)
Connector Force,1,162405.7,-14307.301,6802.2363
Connector Force,2,200523.81,26406.113,10984.173
Connector Force,3,120216.03,2.5567186e-09,4448.341
Connector Force,4,153237.5,4.461983e-09,7526.539
Connector Force,5,162405.7,14307.301,6802.2363
Connector Force,6,200523.81,-26406.113,10984.173
Contact Pressure,1,-62.21822738647461,,
Contact Pressure,2,79.54209899902344,,
Contact Pressure,3,-13.645059585571289,,
Contact Pressure,4,-3.789114236831665,,
Contact Pressure,5,0.48875176906585693,,
Contact Pressure,6,1.1547534465789795,,
Contact Pressure,7,2.7691707611083984,,
Contact Pressure,8,2.730609893798828,,
Contact Pressure,9,1.9463316202163696,,
Contact Pressure,10,1.0212428569793701,,
Contact Pressure,11,0.4667682945728302,,
Contact Pressure,12,0.29057493805885315,,
Contact Pressure,13,0.31116122007369995,,
Contact Pressure,14,0.3582833409309387,,
Contact Pressure,15,0.24867944419384003,,
Contact Pressure,16,0.10382415354251862,,
Contact Pressure,17,-0.010196221061050892,,
Contact Pressure,18,-0.12314503639936447,,
Contact Pressure,19,-0.22293798625469208,,
Contact Pressure,20,-0.2839338779449463,,
```

Figure 4.20: Output data in csv file

5

Analysis

5.1. Parametric study

In this section, a comprehensive parametric study is conducted to evaluate the impact of various parameters on the performance of the joints. The objective is to understand how each parameter influences joint behavior and identify potential areas for optimization. By systematically varying parameters such as plate thickness, fastener configuration, and load application, the study aims to uncover insights that can guide the design and enhancement of joint structures.

The model configuration shown in Figure 5.1 serves as the baseline for all cases of study. This configuration provides a consistent starting point, ensuring that the effects of each parameter variation are isolated and accurately assessed.

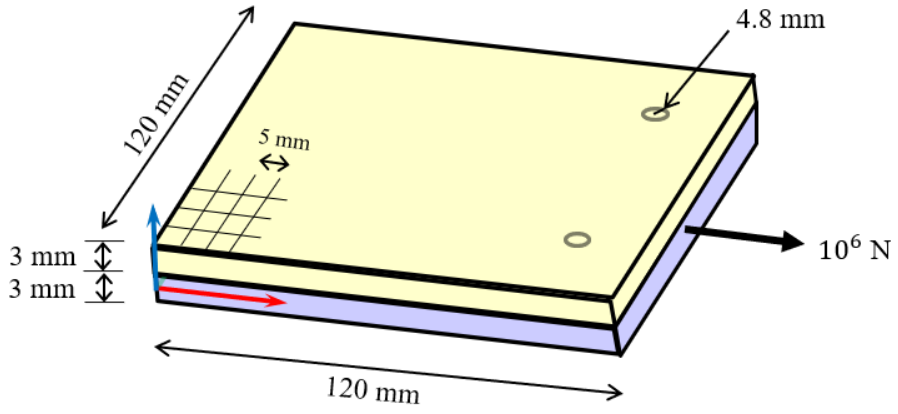

Figure 5.1: Initial model configuration

Through detailed analysis and comparison, this parametric study seeks to optimize joint design. The findings will contribute to the development of more robust and reliable joint configurations, enhancing the structural performance of the system under various loading conditions.

To carry out the parametric study, a parameter is taken, for example the plate length, and the other parameters are maintained with the values shown in Figure 5.1. For the next model the length increases by 20 mm, so that in the second model the length is 140 mm, in the third model it is 160 mm, and so on, until it reaches 400 mm. For each model, the forces at the joints are obtained to compare how they evolve as the length varies. This process is repeated with all the parameters, in order to isolate the effect of each one.

Table 5.10 lists the studied parameters and the range in which they vary. For a better understanding of the parameters go to section 4.2.2.

PARAMETER	**STUDY RANGE**	**VARIATION BETWEEN MODELS**
Plate length (mm)	120 - 400	20
Plate width (mm)	120 - 400	20
Plate thickness (mm)	1 - 9	0.5
Mesh size (mm)	1 - 8	0.5
Fastener radius (mm)	1 - 8	0.5
Nº joints along x-axis	1 - 4	1
Nº joints along y-axis	1 - 5	1
Load (N)	10^5 - 15 $\times 10^5$	10^5

Table 5.1: Studied parameters

5.1.1. Plate length

In order to study the influence of length on the behavior of the model, several cases are analyzed. The length of plate 1 is varied up to 40 cm, keeping the length of plate 2 constant.

Joint	Length (mm)	Fx (N)	Fy (N)	Fz (N)
1	120	498630.7	-23815.5	72585.1
	400	498455.6	-2193.4	73709.4
2	120	498630.7	23815.5	72585.1
	400	498455.6	2193.4	73709.4

Table 5.2: Comparison of forces for 120mm and 400mm lengths

Figure 5.2 shows the evolution of the forces for a range of lengths between 120 and 400 mm. As the forces are equal in absolute value in both connections, there is no difference between joints in the curves.

As one of the plate is elongated, the point of load application also becomes more distant and the structure is subjected to more buckling. The moment generated causes the value of the axial load to increase. This effect is greater when the plates go from having the same length to one of them protruding. This increase in axial force is compensated by the decrease in both shear forces. By contrast, increasing the length of both plates results in a constant behavior of the forces on the rivets.

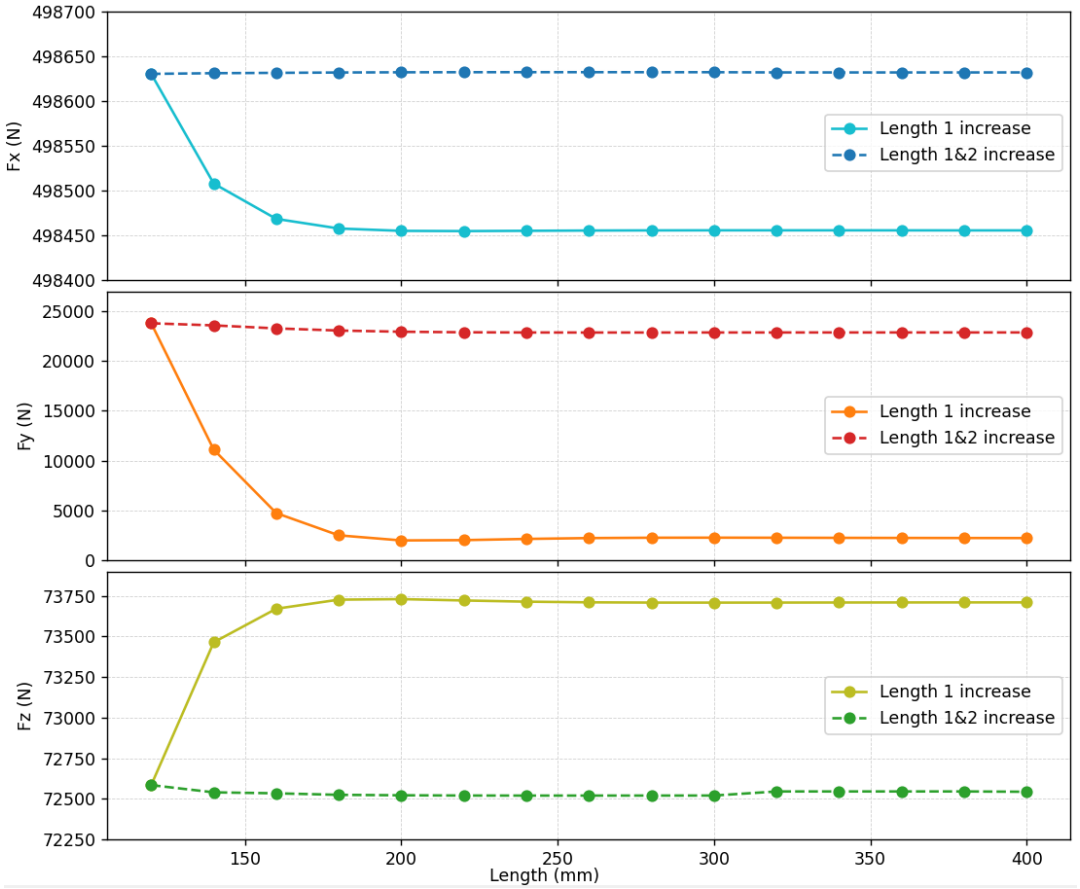

Figure 5.2: Evolution of forces

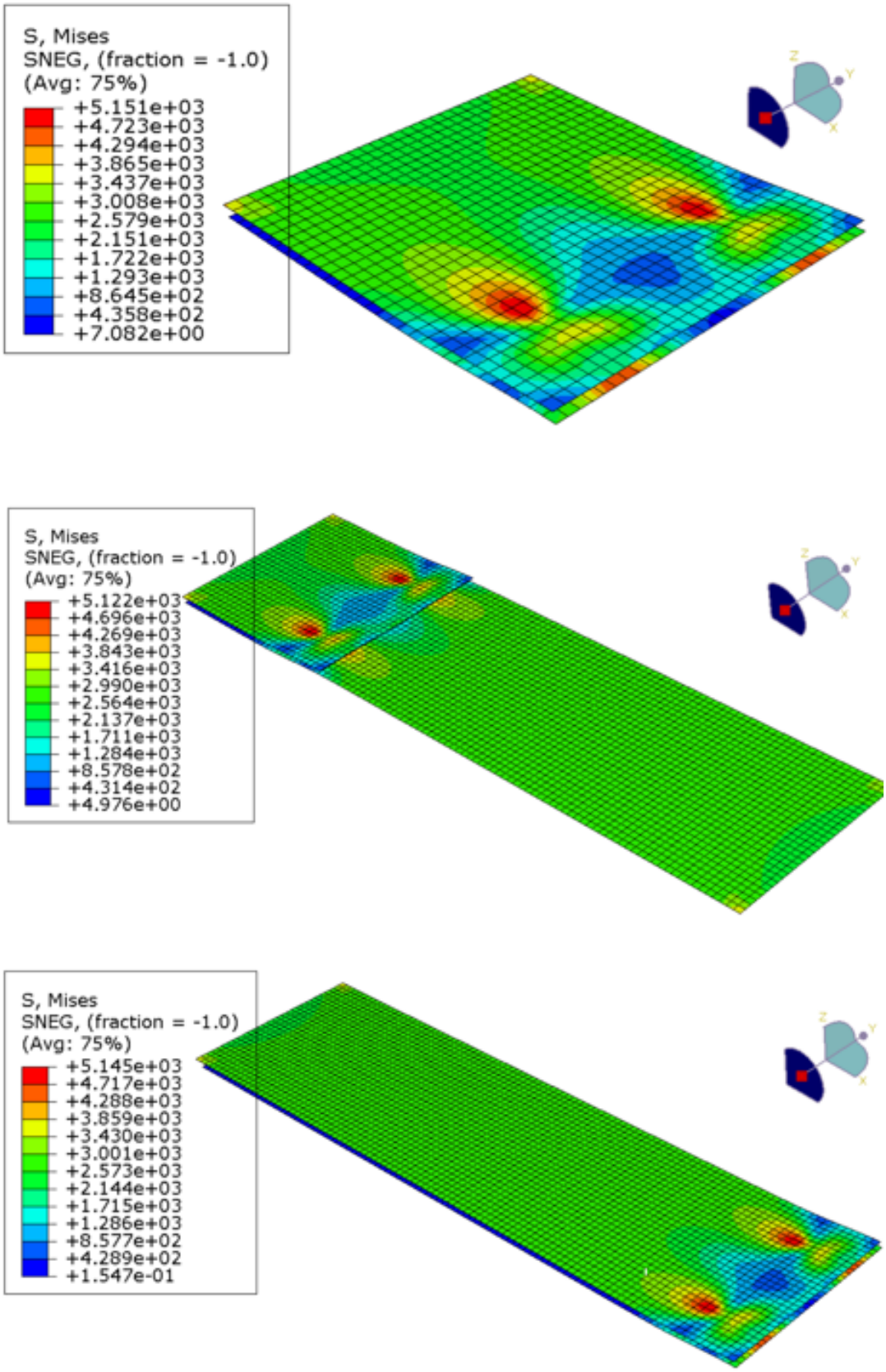

Figure 5.3: Stress for initial conf. (up), plate 1 elongated (middle) and both plates elongated (down)

5.1.2. Plate width

This section examines how increasing the width of the plates affects the structural behavior of the joint. By modifying the width, the aim is to understand its impact on the distribution of loads.

Joint	Length (mm)	Fx (N)	Fy (N)	Fz (N)
1	120	498630.7	-23815.6	72585.1
	400	498655.4	-26949.1	69186.1
2	120	498630.7	23815.6	72585.1
	400	498655.4	26949.1	69186.1

Table 5.3: Comparison of forces for 120mm and 400mm widths

The oscillating pattern in Fx suggests that as the width changes, there are fluctuations in how the load is distributed along the plate. This could be due to variations in stiffness and load path as the width increases, causing periodic changes in force distribution. Fy shows a general increasing trend, indicating that a wider plate provides better lateral support, allowing it to bear more load in the Y direction. This increase suggests improved stability and load distribution as the width expands. The oscillations in Fz are indicating that changes in width affect the load distribution in the Z direction as well. These fluctuations may result from changes in how the plate interacts with the applied load and the resulting stress distribution.

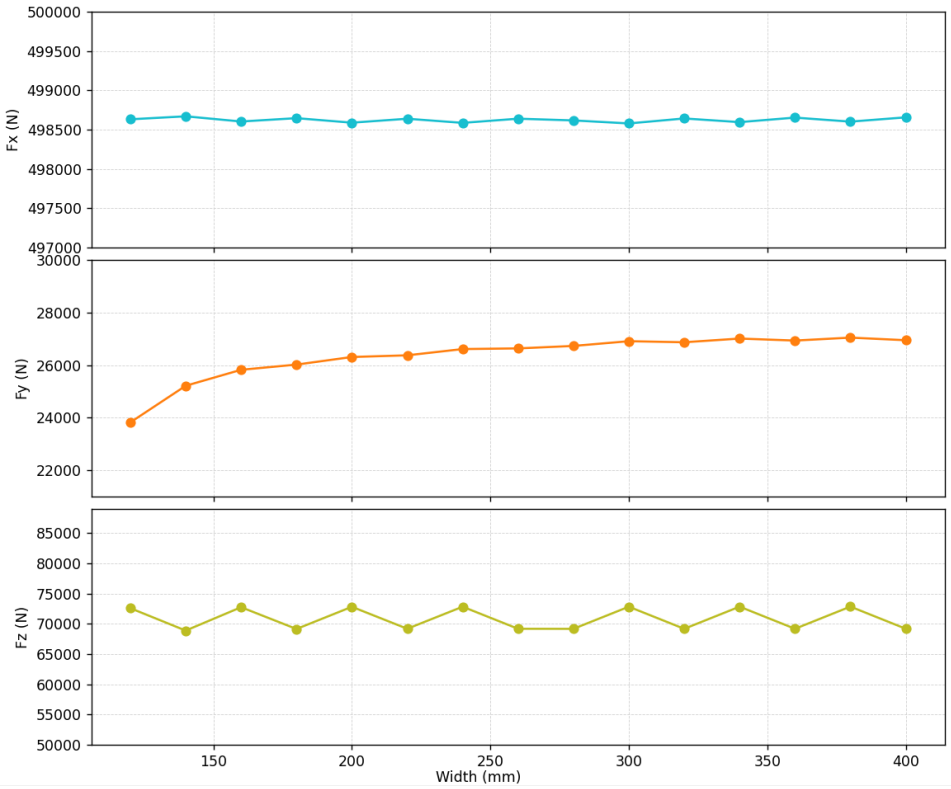

Figure 5.4: Evolution of forces

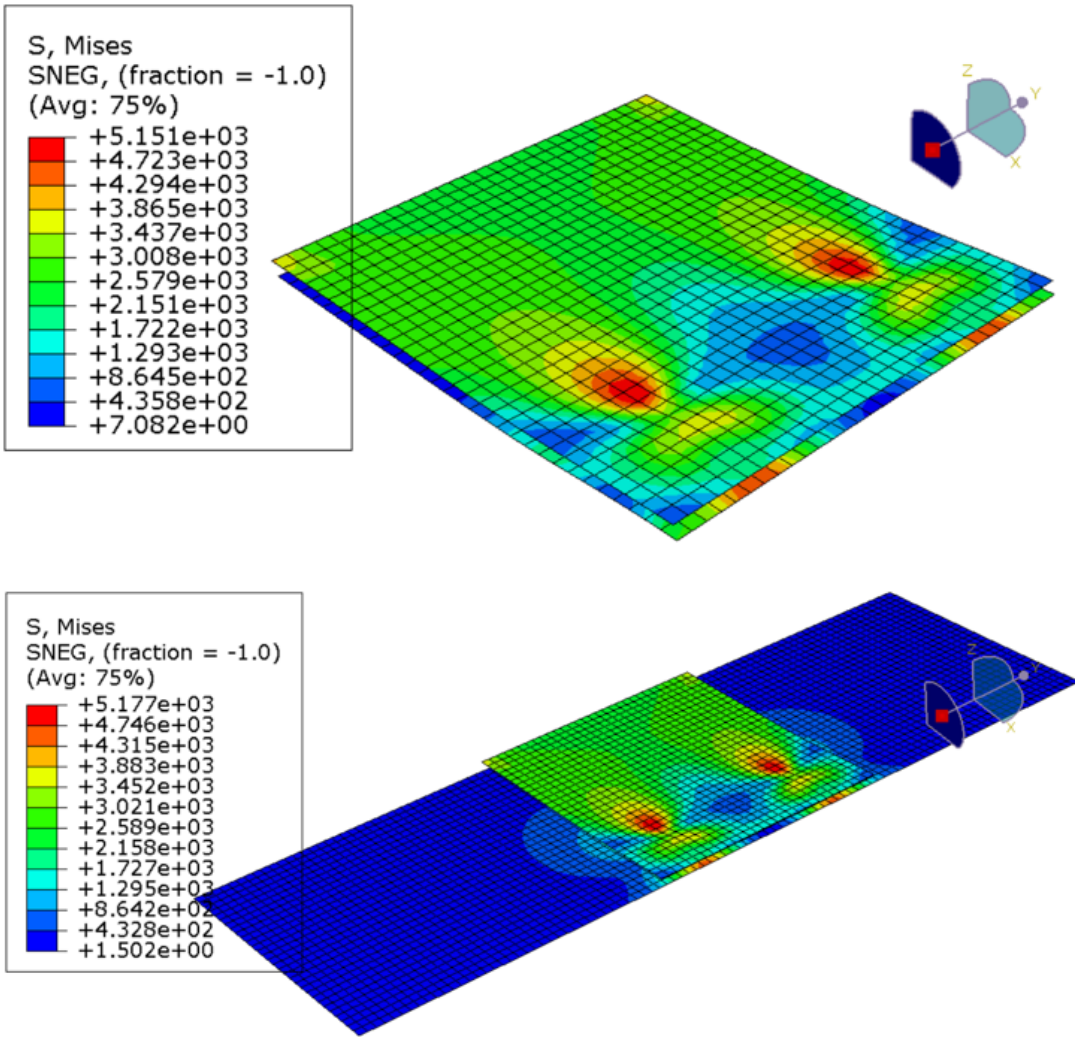

Figure 5.5: Stress for width 120 mm (up) and 400 mm (down)

5.1.3. Plate thickness

This section examines how the thickness of the plate 1 affects the structural behavior of the joint. Thicknesses ranging from 1 mm to 6 mm have been considered for plate 1, while plate 2 remains at a constant thickness of 3 mm.

Joint	Thickness (mm)	Fx (N)	Fy (N)	Fz (N)
1	1	475538.9	-48816.9	154341.6
	3	498319.0	-57544.1	74073.3
	6	499107.5	-72325.3	45625.7
	9	499475.0	-78974.3	30922.8
2	1	475538.9	48816.9	154341.6
	3	498319.0	57544.1	74073.3
	6	499107.5	72325.4	45625.7
	9	499475.0	78974.3	30922.8

Table 5.4: Comparison of forces for different thickness

Increasing the thickness of plates increases their stiffness. This is because the bending stiffness of a plate is proportional to the cube of the thickness (according to Kirchhoff's plate theory for small deformations). As the thickness of plate 1 increases, Fx rises. If the plates are stiffer, the joints must be able to support higher loads since the structure itself absorbs less energy through deformation. The bending moments at the joints are reduced as the stiffness of the plates increases (when the thickness increases), since the plate deforms less under load. The reduction of moments is reflected in the axial force, which also decreases.

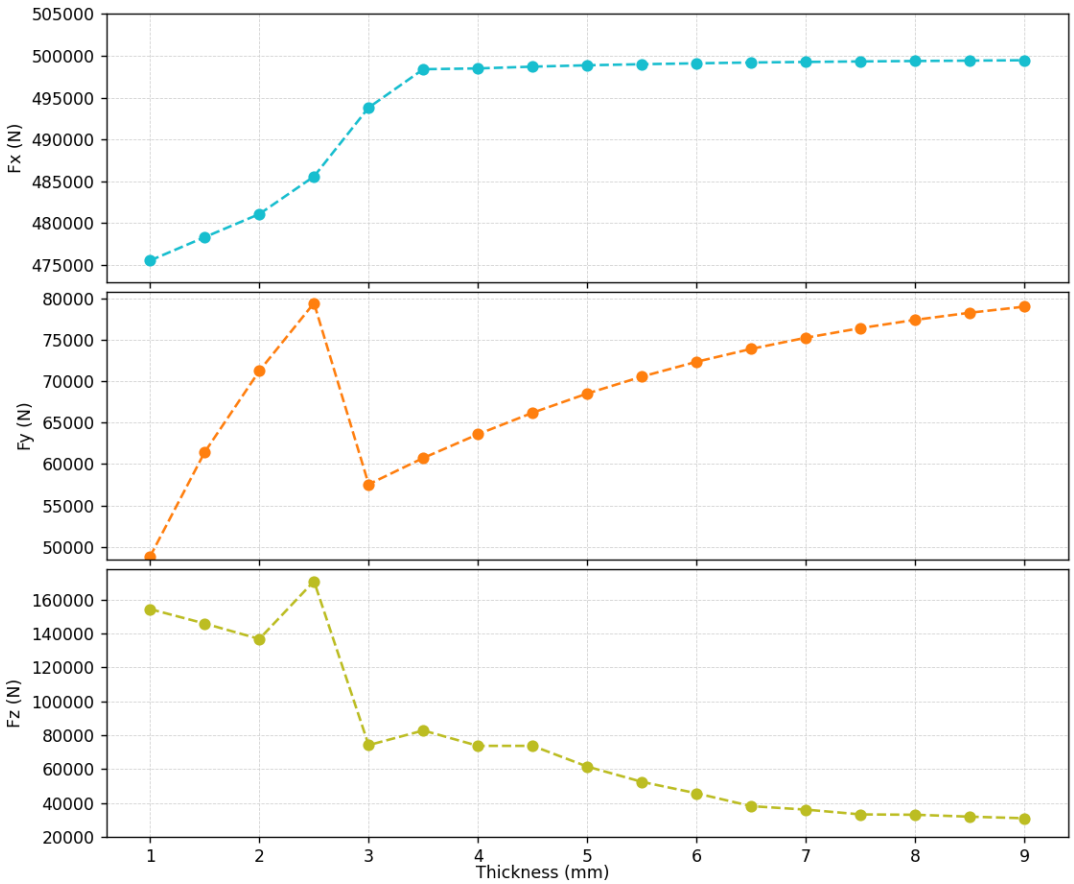

Figure 5.6: Evolution of the forces

Fy shows peaks before reaching the thickness of plate 2 (3 mm), suggesting that differences in stiffness and deformation compatibility between the plates generate temporary stress concentrations.

A thinner plate may lead to higher stress concentrations and greater deformation, whereas a thicker plate could enhance the plate's ability to withstand the applied load.

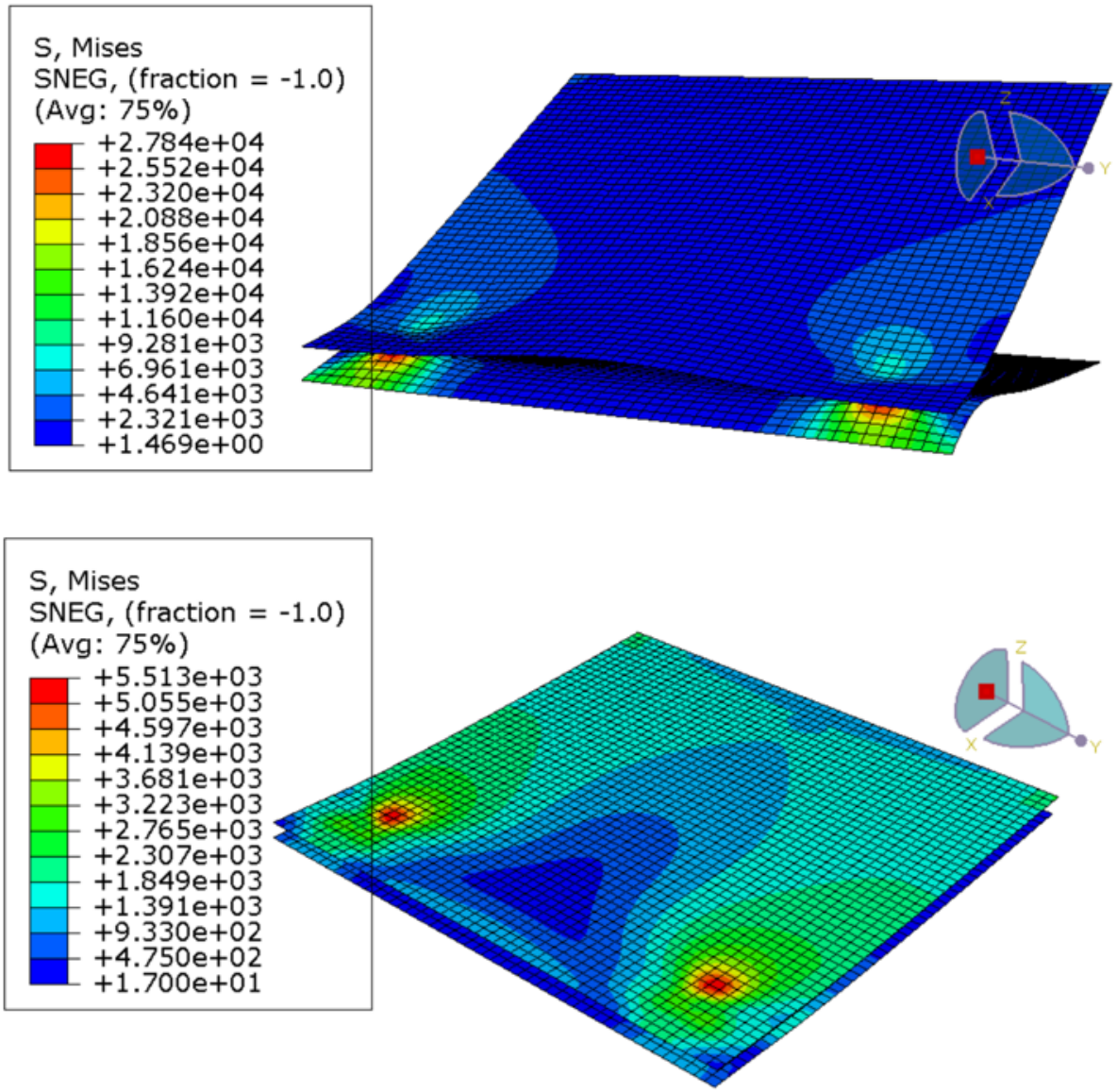

Figure 5.7: Stress for thickness 1 mm (up) and 9 mm (down)

5.1.4. Mesh size

The element size varies from 1 to 8 mm to see the effect of the mesh on the results.

When a finer mesh size is used, the simulation can better capture the structural behavior due to the increased number of nodes and elements, as shown in Figure 5.8. This allows for a more precise discretization of the geometry and loading conditions.

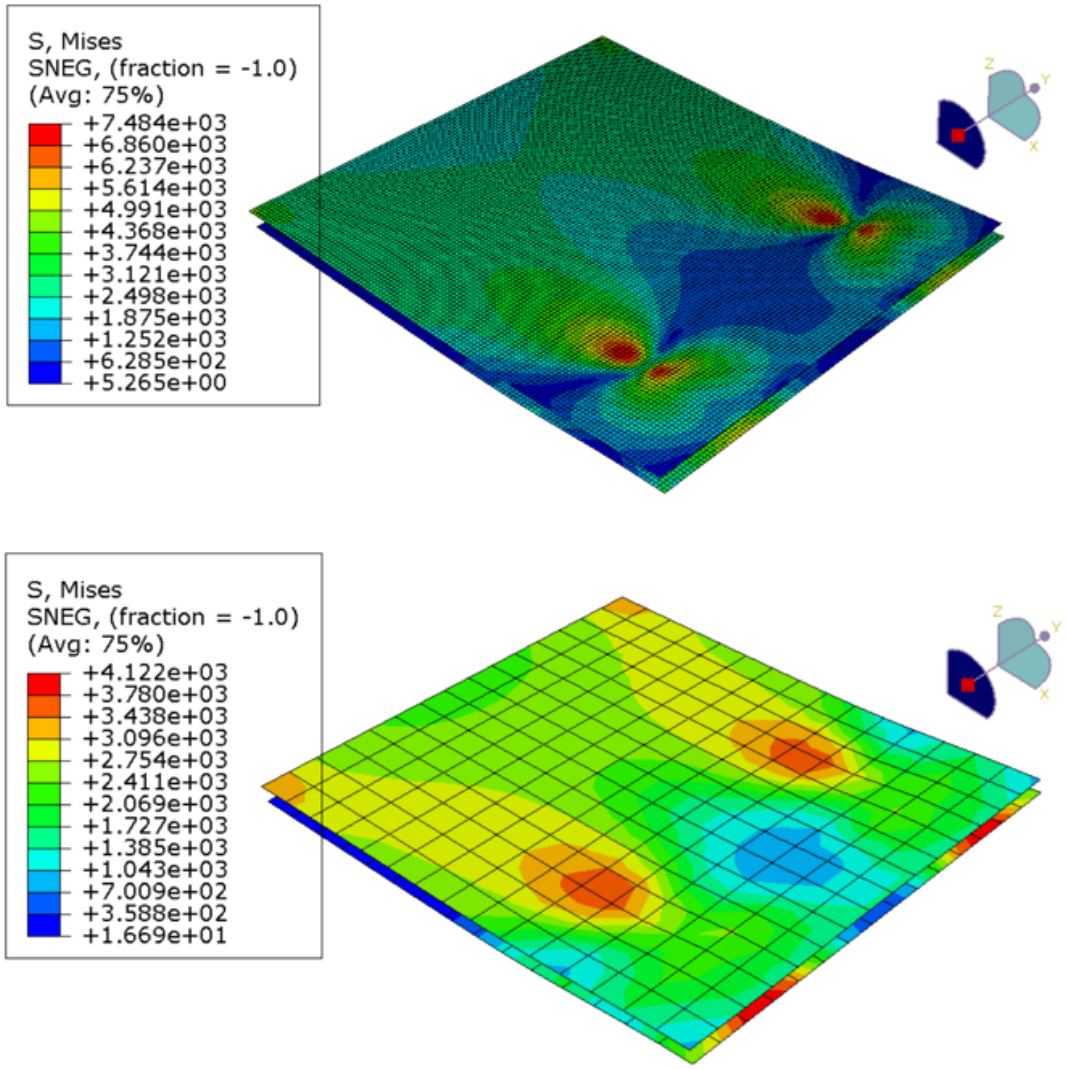

Figure 5.8: Stress for 1mm mesh (up) and 8mm mesh (down)

Joint	Mesh (mm)	Fx (N)	Fy (N)	Fz (N)
1	1	499436.6	-29797.7	22842.4
	4	498897.3	-23389.0	44516.2
	8	495303.0	-20468.9	170179.9
2	1	499436.6	29797.7	22842.4
	4	498897.3	23389.0	44516.2
	8	495303.0	20468.9	170179.9

Table 5.5: Comparison of forces for different mesh sizes

Figure 5.9 shows the evolution of the forces for a range of mesh sizes. As the forces are equal in absolute value in both connections, only the values of a joint are shown. With a finer mesh, higher shear forces may be observed because the simulation can identify stress concentrations and local variations in the structure that a coarser mesh might overlook. For axial force, a finer mesh may reveal that the load is distributed more evenly, reducing load concentrations in certain areas.

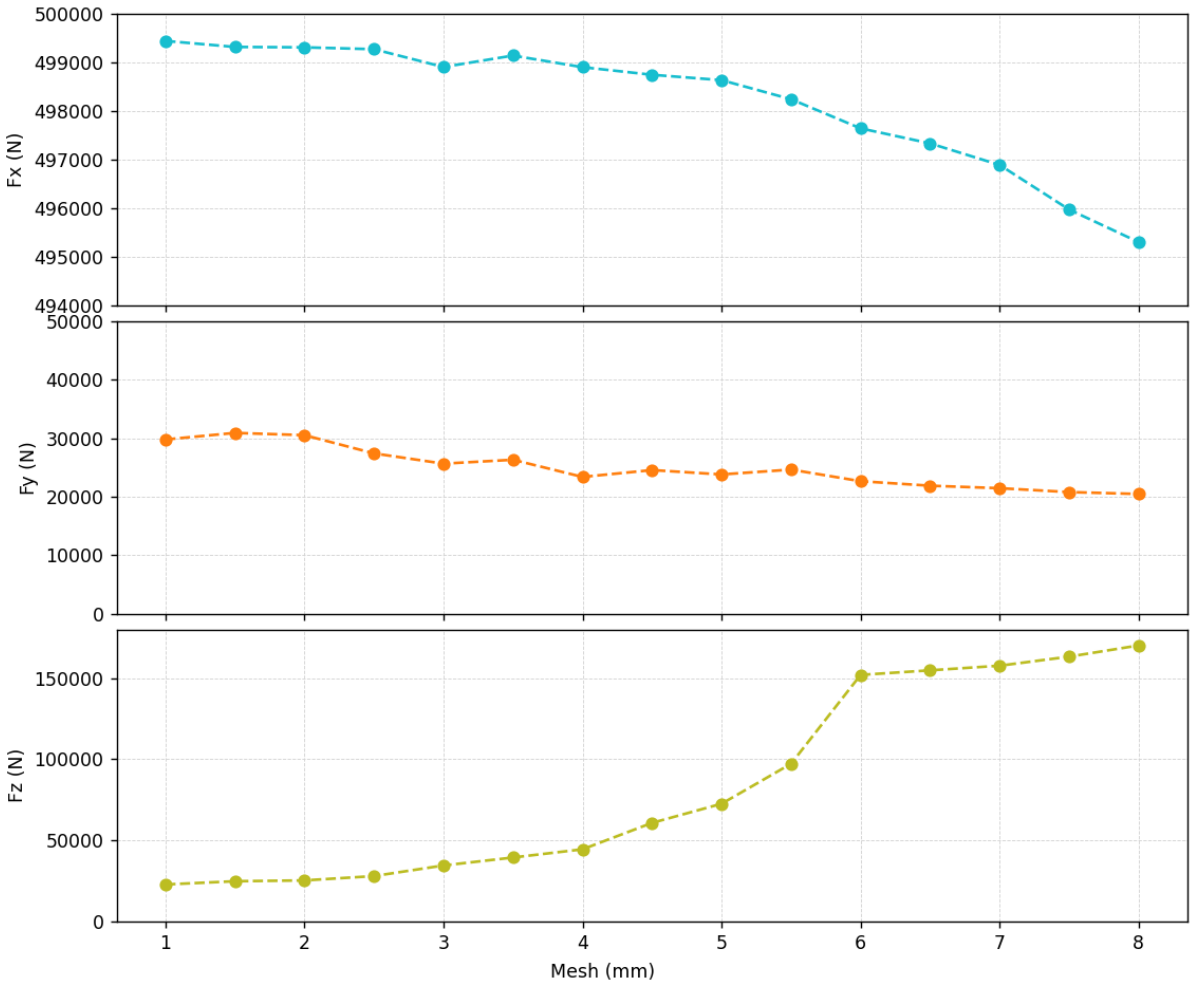

Figure 5.9: Evolution of the forces

Larger element sizes may lead to inaccurate representation of stress concentrations in the joints. These concentrations may be overestimated because the mesh is not fine enough to smooth these transitions, resulting in higher values.

Also, with larger elements, the application and distribution of loads may not be as accurate as with a fine mesh. This may result in incorrect application of loads on the elements, which in turn may cause the coarser mesh to predict higher load values due to inappropriate load concentration on fewer elements.

Axial loads are extremely sensitive to the location of stresses and strains, and a coarse mesh may not adequately capture these details. In contrast, the distribution of shear stresses is often more uniform and less prone to sharp stress concentrations compared to normal stresses induced by axial loads. Therefore, shear loads tend to be less sensitive to variations in mesh quality.

5.1.5. Fastener radius

The fastener radius varies from 4.4 to 10 mm to see the effect on the results.

Joint	Radius (mm)	Fx (N)	Fy (N)	Fz (N)
1	1	498080.3	-65365.1	73830.1
	8	498297.8	-10764.1	138977.9
2	1	498080.3	65365.1	73830.1
	8	498297.8	10764.1	138977.9

Table 5.6: Comparison of forces for different mesh sizes

The results indicate that the shear force in the direction of the applied load remains relatively constant as the fastener radius increases. This suggests that changes in the radius do not significantly affect the joint's ability to directly support the applied load. On the other hand, the shear force perpendicular to the load decreases with a larger fastener radius. Increasing the radius at joints typically helps reduce stress concentrations. With a larger radius, the load is more evenly distributed across the joint, decreasing peak stresses. Additionally, the axial force increases with the fastener radius. A larger cross-sectional area directly increases the ability of the joint to support axial loads, reflected in an increase in measured axial forces. In addition, a larger cross-section may increase the local stiffness of the joint. Higher local stiffness may allow the joint to transmit a higher axial load without significant deformation.

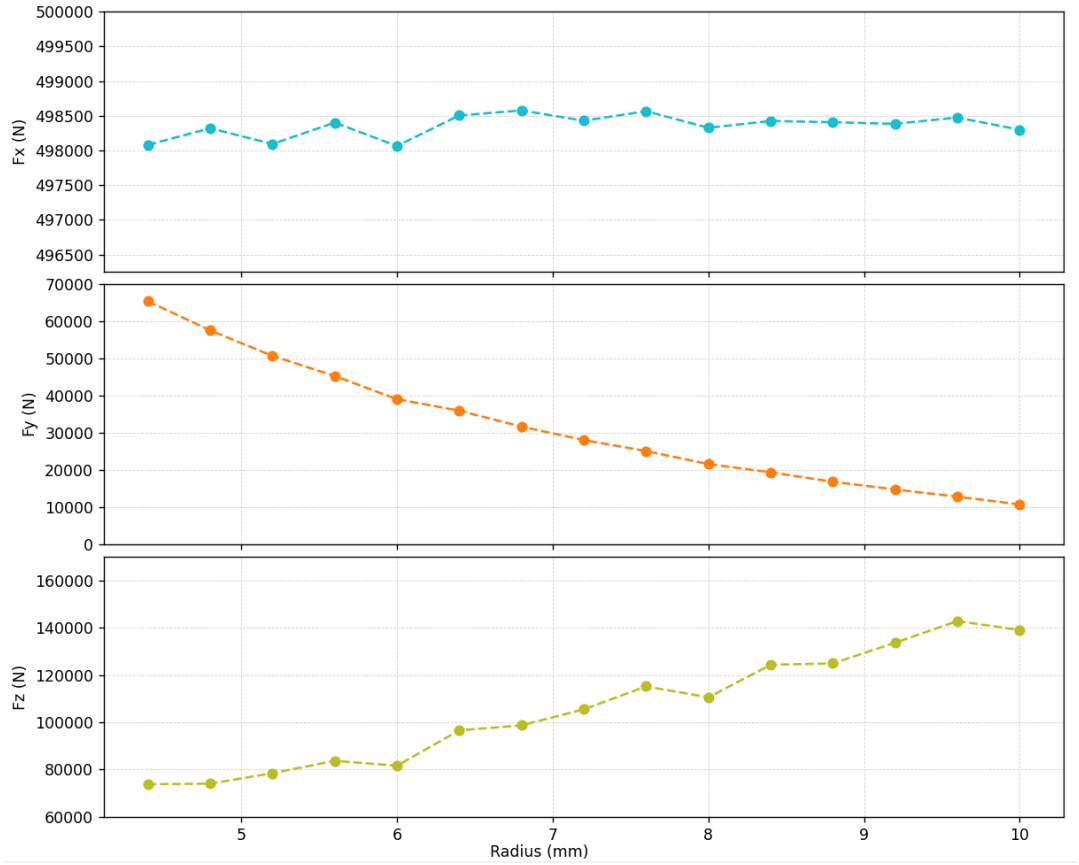

Figure 5.10: Evolution of the forces

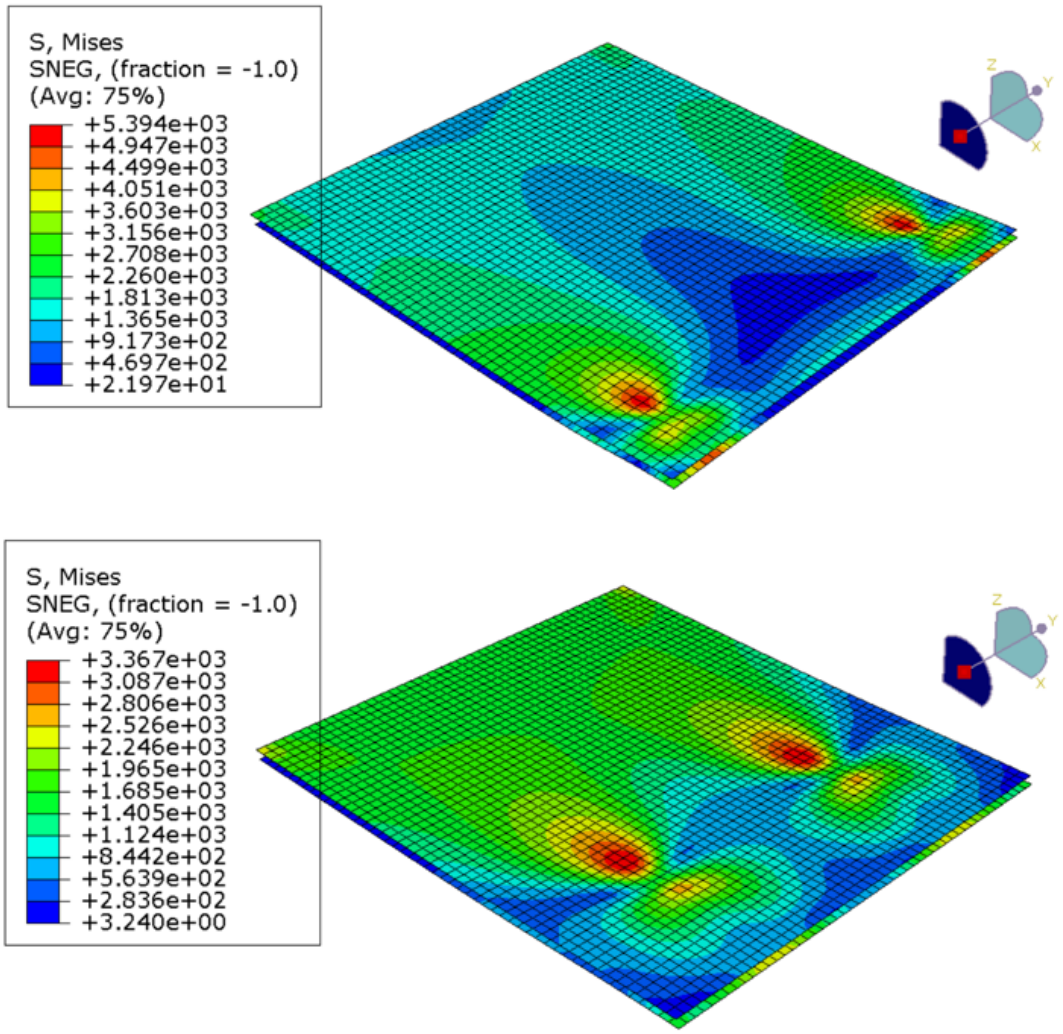

Figure 5.11: Stress for radius 4.4 mm (up) and 10 mm (down)

5.1.6. Nº joints along x-axis

Rows of joints are added along x-axis until there are eight joints to evaluate how the forces are distributed. Increasing the number of fasteners along the improves the load distribution across the joint.

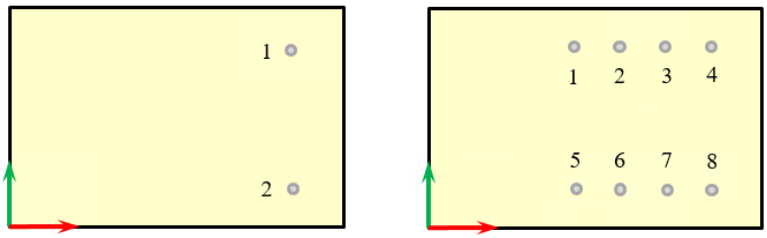

Figure 5.12: Joints configuration: A (left), B (right)

This distribution reduces stress concentrations on individual fasteners and decrease the risk of overloading. The additional fasteners increase the stiffness and stability of the structure, allowing it to absorb and redistribute loads more efficiently.

Observing the forces, it makes sense that the most loaded joints are those farthest from and closest to the point of force application. The joints farthest from the point experience greater moments due to the lever effect, increasing the forces they must bear to balance the moment generated by the applied load. Similarly, the joints closest to the point of application bear significant loads as they are directly in the path of the applied force.

Configuration	Joint	Fx (N)	Fy (N)	Fz (N)
A	1	498319.0	-57544.133	74073.32
	2	498319.0	57544.133	74073.32
B	1	155879.3	-7532.6	7683.2
	2	94287.3	-746.6	2856.4
	3	92565.7	-515.7	2791.3
	4	157124.8	-21491.8	8078.5
	5	155879.3	7532.6	7683.2
	6	94287.3	746.6	2856.4
	7	92565.7	515.7	2791.3
	8	157124.8	21491.8	8078.5

Table 5.7: Comparison of forces for different joint configurations

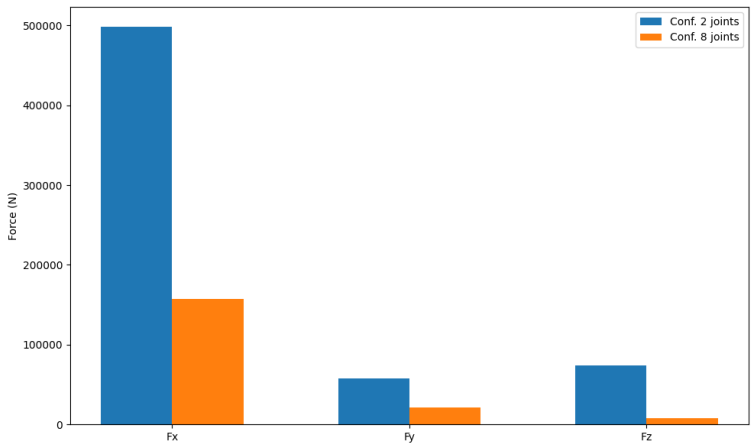

Figure 5.13: Comparison of maximum forces

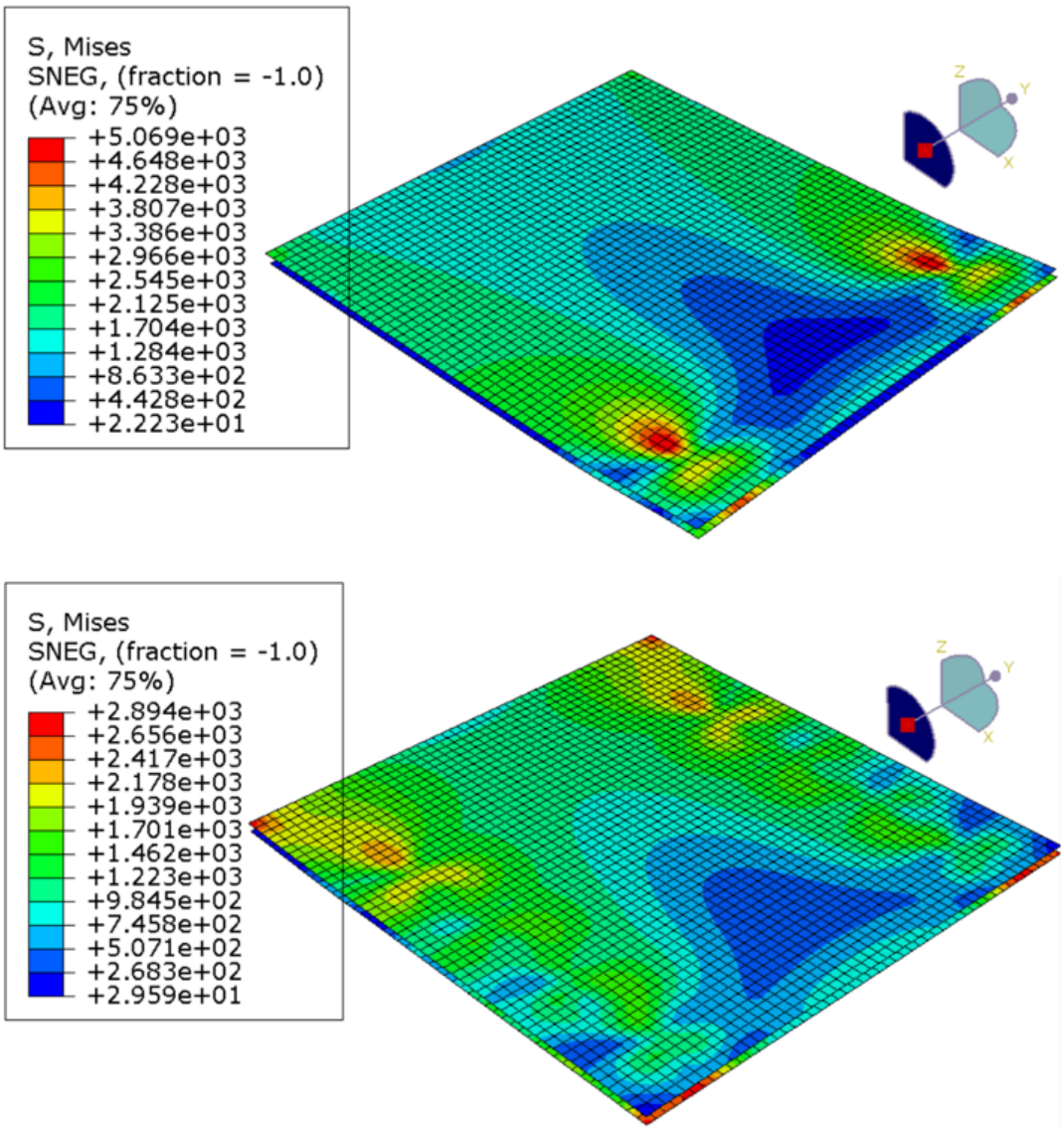

Figure 5.14: Stress for 2 joints (up) and 5 joints (down) along y-axis

5.1.7. Nº joints along y-axis

The number of joints along y-axis is varied from 2 to 5 to evaluate how the forces are distributed. Increasing the number of fasteners along the y-axis improves the load distribution across the joint.

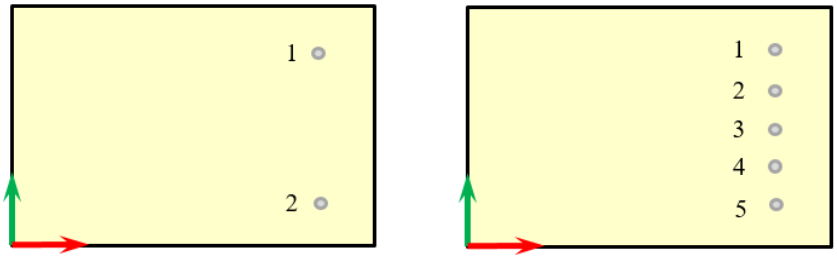

Figure 5.15: Joints configurations

More fasteners provide additional points of contact and support, allowing the load to be distributed more evenly throughout the joint. This reduces load concentrations on individual fasteners, thereby decreasing the shear and axial forces on each one. Additionally, having more fasteners increases the stiffness of the joint, which can help absorb and redistribute loads more efficiently.

It is also possible to observe that the position of the fasteners plays a crucial role. Fasteners located at the edges of the joint tend to bear more load due to their position relative to the applied force.

Joint	Fx (N)	Fy (N)	Fz (N)
1	498319.0	-57544.1	74073.3
2	498319.0	57544.1	74073.3
1	214789.7	-12432.5	15008.1
2	189910.6	-9366.1	11314.2
3	189831.8	5.8×10^{-9}	11820.4
4	189910.6	9366.1	11314.2
5	214789.7	12432.5	15008.1

Table 5.8: Comparison of forces for different joint configurations

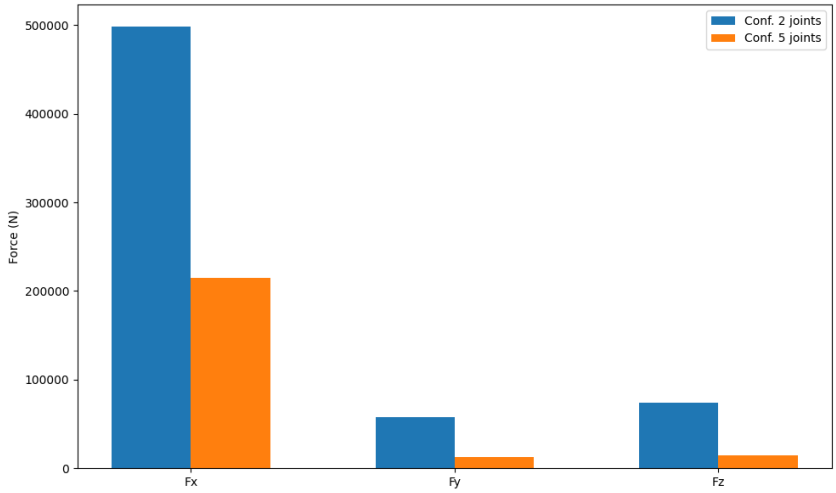

Figure 5.16: Comparison of maximum forces

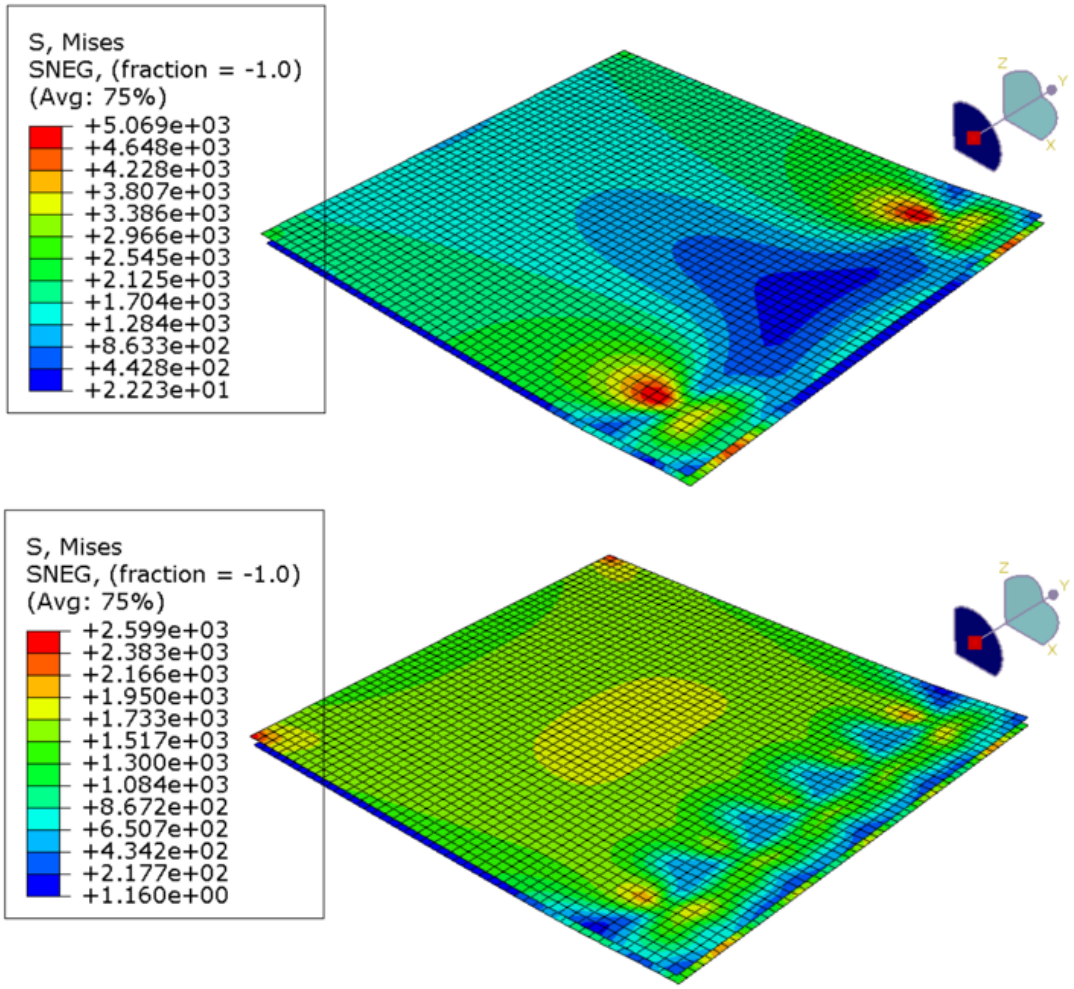

Figure 5.17: Stress for 2 joints (up) and 5 joints (down) along y-axis

5.1.8. Load magnitude

To study the influence of the force on the behavior of the model, the applied force is increased from 10^4 to 14×10^5.

Joint	Load (N)	Fx (N)	Fy (N)	Fz (N)
1	10^4	5000.2	-456.1	11.7
	14×10^5	696846.3	-32710.8	130579.6
2	10^6	5000.2	456.1	11.7
	14×10^5	696846.3	32710.8	130579.6

Table 5.9: Comparison of forces

When the applied shear force on a joint is increased, both the shear and axial forces are observed to rise. The load is applied to one of the plates, creating a moment due to the eccentricity relative to the center of the joint. As a result, the generated moment can cause a tensile or compressive effect on the joint elements, increasing the axial force. This occurs because the moment induces internal stresses along the axis of the joint, increasing the axial load that the components must bear. Additionally, the extra load and resulting moment redistribute the forces across the joint, increasing the shear force in certain areas.

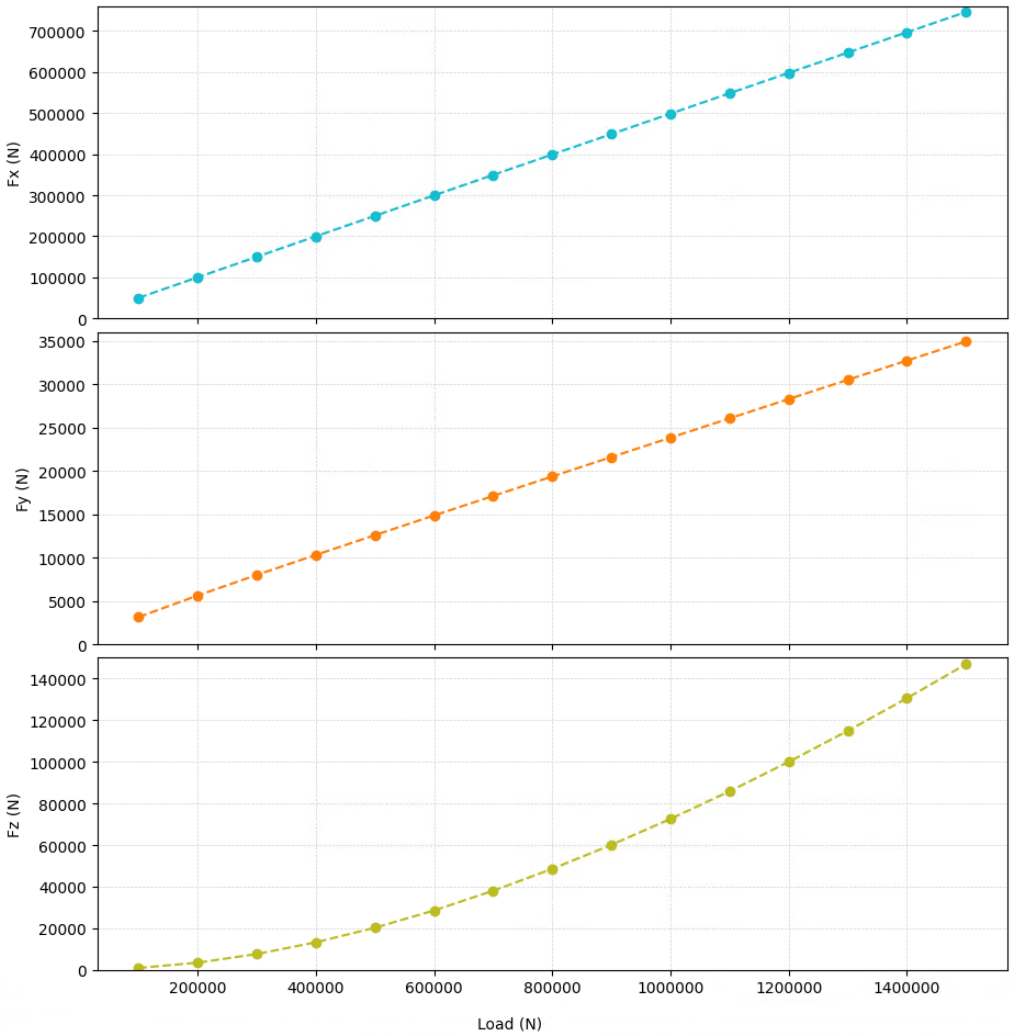

Figure 5.18: Evolution of the forces

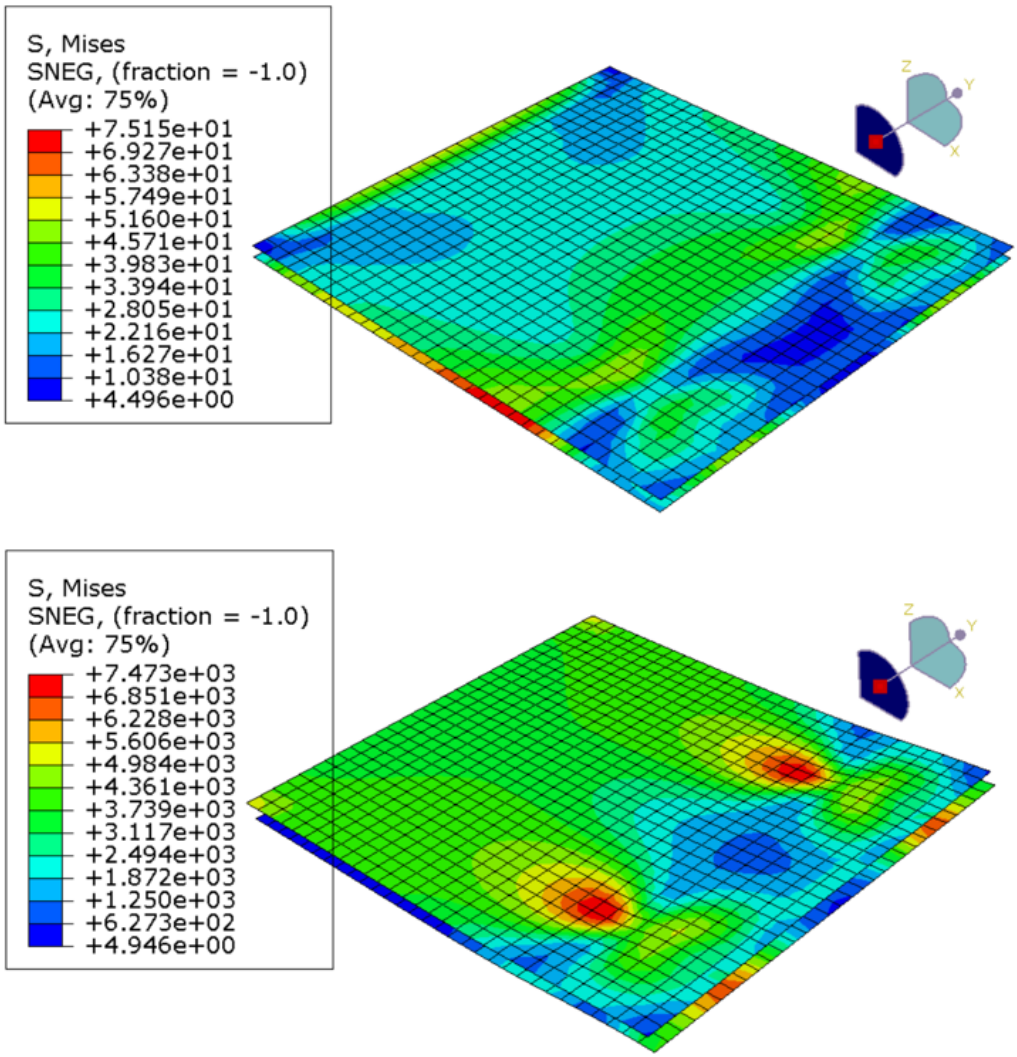

Figure 5.19: Stress for minimum (up) and maximum (down) load

5.1.9. Summary

This table shows the joint forces obtained for the minimum and maximum value of each parameter. It is possible to observe the evolution of the forces when varying each parameter individually.

PARAMETER	**RANGE**			$\mathbf{F}_{shear,max}$	$\mathbf{F}_{axial,max}$	**VARIATION**
Plate length (mm)	120 – 400	120	→	498630.7	72585.1	F_{shear}: −0.04%
		400	→	498455.6	73709.4	F_{axial}: 1.55%
Plate width (mm)	120 – 400	120	→	498630.7	72585.1	F_{shear}: 0.00%
		400	→	498655.4	69186.1	F_{axial}: −4.68%
Plate thickness (mm)	1 – 9	1	→	475538.9	154341.6	F_{shear}: 5.03%
		9	→	499475.0	30922.8	F_{axial}: −79.96%
Mesh size (mm)	1 – 8	1	→	499436.6	22842.4	F_{shear}: −0.83%
		8	→	495303.0	170179.9	F_{axial}: 645.02%
Fastener radius (mm)	1 – 8	1	→	498080.3	73830.1	F_{shear}: 0.04%
		8	→	498297.8	138977.9	F_{axial}: 88.24%
Nº joints (x-axis)	1 – 4	1	→	498319.0	74073.3	F_{shear}: −68.47%
		4	→	157124.8	8078.5	F_{axial}: −89.09%
Nº joints (y-axis)	1 – 5	1	→	498319.0	74073.3	F_{shear}: −56.90%
		5	→	214789.7	15008.1	F_{axial}: −79.74%
Load (N)	$10^5 – 15 \times 10^5$	10^5	→	5000.2	11.7	F_{shear}: 1.4×10^4%
		15×10^5	→	696846.3	130579.6	F_{axial}: 1.1×10^6%

Table 5.10: Results summary

The following conclusions can be drawn from the results shown in the table:

- The dimensions of the plate (length or width) have no impact on the shear force supported by the joints. The axial force varies somewhat more than the shear force, about 2% for the length and 5% for the width, but without reaching significant values.
- The increase in thickness significantly affects the axial force of the joints. As the thickness increases, the stiffness of the plate increases, thus reducing the bending moment, and therefore the axial force. If

we look at the table, when the thickness is 9mm, the axial force is 80% lower than when the thickness is 1mm.

- Shear loads remain stable, while axial loads are very sensitive to element size. As the mesh becomes finer, these forces decrease, stabilizing their value for an element size of about 4 mm.
- The fastener radius does not affect the shear force, but has a direct impact on the axial force. Increasing the radius results in a larger cross section and the stiffness of the fastener increases, which allows the fastener to transmit a greater axial load without significant deformation.
- The greater the number of fasteners, the better the load distribution, reducing the concentration of each fastener and therefore reducing the axial and shear load.
- As the applied shear load is increased, the shear force rises with it. The axial load also climbs, since the moment also rises due to the eccentricity relative to the center of the joint.

It is observed that the parameters that significantly affect the shear force are the number of joints and the applied force. In addition, the axial force is also influenced by the thickness, the mesh size and the fastener radius. With this it can be concluded that the length and width of the plates have no significant effect.

5.2. Huth Stiffness

The application of the Finite Element Method (FEM) in determining fastener stiffness provides highly accurate results. However, when dealing with numerous joints of varying thicknesses, the preparation and computation of a comprehensive FEM model can be time-consuming. In industrial practice, various analytical and semi-empirical formulas are available for estimating bolt stiffness. These formulas typically rely on basic mechanical principles, supplemented by numerical factors derived from independent experimental validation.

The use of these formulas can greatly accelerate the calculation process; however, the reliability of the results may be uncertain. This variability often arises from the omission of geometric and physical features typically present in fasteners, such as pre-tension, bolt spacing, surface roughness, and the application of primer or sealant. In some cases, secondary bending—relevant for single-shear fasteners—is considered through empirical factors, while in others it is disregarded. Nevertheless, accounting for such effects can be critical to achieving accurate results in subsequent analyses.

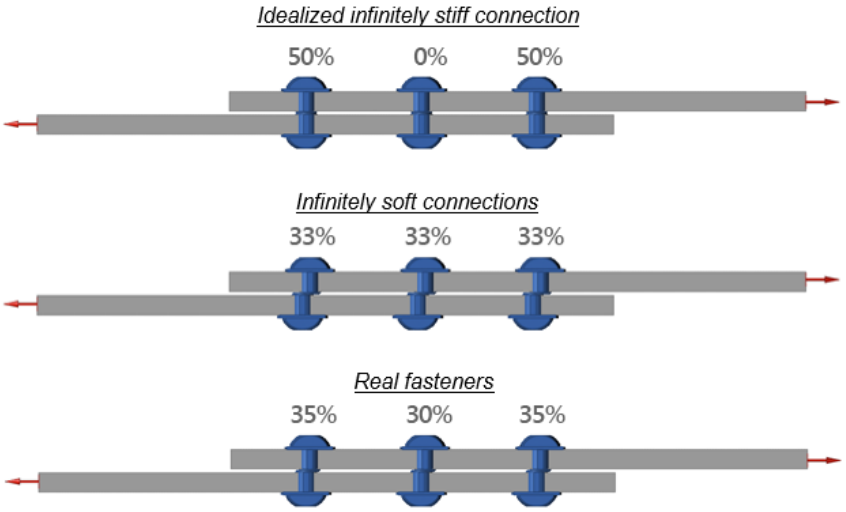

Figure 5.20: Load transferred to each rivet

For connections to and between plates, as are often found in the aircraft industry, a popular way to approximate the fastener stiffness is by using the Huth-Schwarmann method. This stiffness is calculated using the following formula for flexibility:

$$C = \left(\frac{t_1 + t_2}{2d}\right)^a \times \frac{b}{n}\left(\frac{1}{t_1 E_1} + \frac{1}{n t_2 E_2} + \frac{1}{2 t_1 E_f} + \frac{1}{2 n t_1 E_f}\right), \tag{5.1}$$

where E_1 – upper membrane modulus of elasticity, t – shell thickness, E_2 – lower membrane modulus, E_f – fastener modulus of elasticity, d – hole diameter, a, b, n – joint-related coefficients.

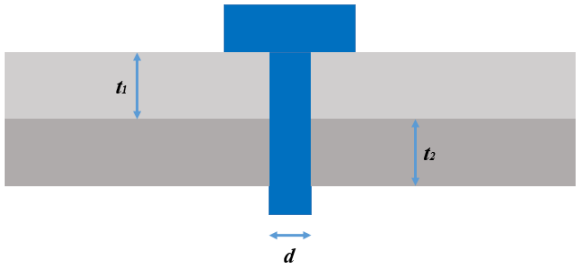

For single shear $n = 1$, and a and b depend on the type of joint as per the following table:

Type of joint	Coefficient value
Metal bolted joint	a=2/3, b=3
Metal joint with rivets	a=2/5, b=2.2
Composite bolted joint	a=2/3, b=4.2

Table 5.11: Coefficient values for different types of joints

5.2.1. Implementation in the model

To correctly implement the Huth formula in the Abaqus model, several changes have been made to the code to accurately reflect the axial and shear stiffness of the rivets in the joint. In particular, the configuration of the connectors has been modified, transitioning from a beam-based model (*BEAM*) to one with translational constraints (*CARTESIAN*), which allows for a more precise representation of the load transfer in this type of joint.

5.2.2. Modifications in the code

The Huth formula has been implemented to determine the shear stiffness of the rivets. This stiffness is dynamically calculated based on the model parameters (plate thicknesses, material elastic modulus, and fastener dimensions), extracting these values from an Excel parameter file.

```python
def calculate_shear_stiffness(d, t1, t2, E1, E2, Ef):
    """
    Calculate the shear stiffness of the rivet using Huth's formula.

    :param d: hole diameter
    :param t1: thickness of plate1
    :param t2: Thickness of plate2
    :param E1: Young's modulus plate1
    :param E2: Young's modulus plate2
    :param Ef: Young's modulus rivet
    :return: rivet shear stiffness
    """
    # "riveted_metallic"
    a = 2 / 5
    b = 2.2
    n = 1

    term1 = ((t1 + t2) / (2 * d)) ** a
    term2 = b / n
    term3 = (1 / (t1 * E1)) + (1 / (n * t2 * E2)) + (1 / (2 * t1 * Ef)) + (1 / (2 * n * t2 * Ef))

    shear_stiffness = 1/(term1 * term2 * term3)

    return shear_stiffness
```

Figure 5.21: Shear stiffness function

The *assembledType=BEAM* configuration, which modeled the fastener as a beam capable of bending, has been replaced with *translationalType=CARTESIAN*, which only allows displacements without moment transmission. The choice of *CARTESIAN* is based on the need to represent the axial and shear stiffness of the fastener without adding undesired bending effects.

The connector section has been defined using *ConnectorElasticity*, where the values of axial and shear stiffness are set in the corresponding directions.

```
myFastenerSection = myModel.ConnectorSection(name='BoltSection', translationalType=CARTESIAN)

myFastenerSection.setValues(behaviorOptions = (connectorBehavior.ConnectorElasticity(
    components=(1, 2, 3),
    table=((float(axial_stiffness), float(shear_stiffness), float(shear_stiffness)),)
    ), ))
myFastenerSection.behaviorOptions[0].ConnectorOptions()
```

Figure 5.22: Connector section definition

5.2.3. Implications

The transition from BEAM to CARTESIAN in the connector configuration has several implications for the simulation. It provides greater accuracy in representing the actual stiffness of the fastener, as this type of joint primarily works under axial and shear stress without generating significant moments. Additionally, it eliminates moment transmission in the connectors, preventing overestimation of the global stiffness of the joint. The change also optimizes computation time, as CARTESIAN connectors have fewer degrees of freedom compared to BEAM.

Aspect	BEAM	CARTESIAN
Modeled stiffness	Includes bending, torsion, axial force, and shear	Only considers axial force and shear
DOF	3 translations + 3 rotations.	3 translations
Moment transmission	The fastener can generate moments	The fastener does not transmit moments
Accuracy in load transfer	May overestimate axial stiffness in short fasteners	More precise for modeling load transfer in riveted joint

Table 5.12: Comparison between BEAM and CARTESIAN connectors

Both in BEAM and CARTESIAN, the axial stiffness K_a is calculated as

$$K_a = \frac{A_f \cdot E}{L_f} \tag{5.2}$$

```
def calculate_axial_stiffness(d, t1, t2, Ef):
    """
    Calcula la rigidez axial del remache

    :param d: Diámetro del agujero.
    :param t1: Espesor de la primera placa.
    :param t2: Espesor de la segunda placa.
    :param Ef: Módulo de Young del remache.
    :return: Rigidez axial del remache.
    """
    Lf = t1 + t2
    Af = (math.pi * (d**2)) / 4
    print(Af, Ef, Lf)
    axial_stiffness = (Af * Ef) / Lf if Lf != 0 else float('inf')

    return axial_stiffness
```

Figure 5.23: Axial stiffnes function

For one model shown in Figure 5.24, the forces in the joints have been extracted with both methods. The axial force has a significant lower value when using CARTESIAN as it does not transmit moments. Shear forces have a lower value using Huth's formula. This is due to the fact that with BEAM, the rivet was almost infinitely rigid and now it has become more flexible.

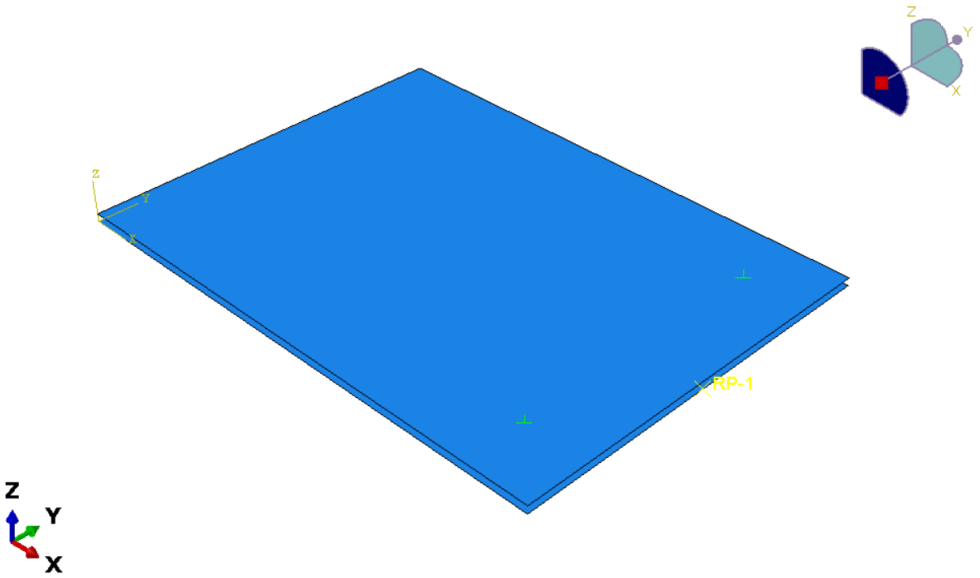

Figure 5.24: Simple shear model

Connector	Fx Huth	Fx BEAM	Fy Huth	Fy BEAM	Fz Huth	Fz BEAM
1	4999.67	4999.86	-224.36	-634.57	-4.98×10^{-3}	9.545715
2	4999.67	4999.86	-224.36	-634.57	-4.98×10^{-3}	9.545715

Table 5.13: Comparison of Forces for Connectors: Huth vs BEAM

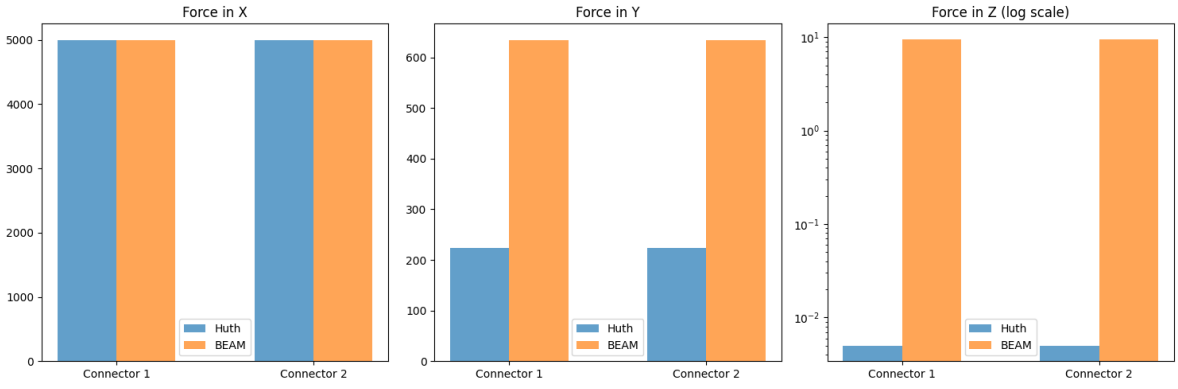

Figure 5.25: Results comparison

5.3. Clearance

This study focuses on how clearance affects joint behavior. To simulate the effect of clearance in Abaqus, a very low stiffness is introduced in the perpendicular direction to the applied shear force. This approach allows for observing how the load path varies through the joint.

By reducing stiffness in the perpendicular direction, the presence of gaps or misalignments in the joint is simulated, which can lead to load redistribution and potentially undesirable stress concentrations. This approach provides a more realistic view of how joints may behave under typical manufacturing and assembly conditions.

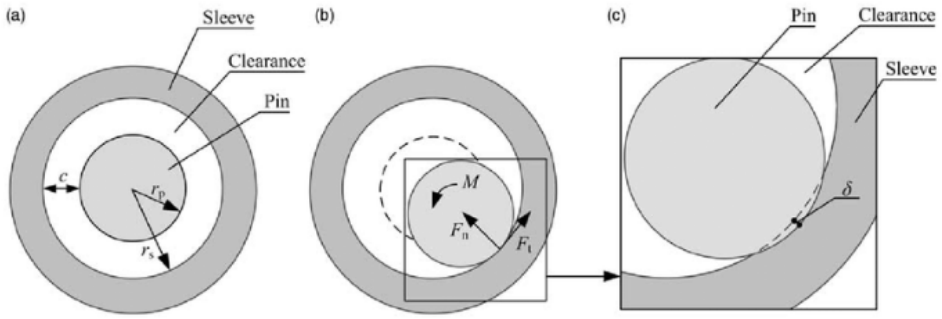

Figure 5.26: Model of clearance joint: (a) free movement; (b) contact deformation; and (c) detail of contact area

5.3.1. Clearance results

The stiffnesses obtained by Huth's method are used for this model. With these stiffnesses the forces shown in Table 5.14 are obtained. To simulate the clearance, a value of order one hundred is entered in the shear stiffness perpendicular to the applied load.

Joint	Clearance	Fx (N)	Fy (N)	Fz (N)
1	✓	499618.3	-8.0	1139.8
	✗	499616.3	-8570.8	1139.7
2	✓	499618.3	8.0	1139.8
	✗	499616.3	8570.8	1139.7

Table 5.14: Comparison of forces

The Fx, which is the primary shear direction, remains practically constant across both configurations, regardless of the presence of clearance. The stiffness in x is high, deformations are minimal, and the load distribution in this direction remains constant. This consistency suggests that the applied load is well-aligned with the x-direction and that the joint interaction is predominantly governed by stiffness in this direction, which is not altered.

In the y-direction, significant variations in force are observed, indicating that the clearance allows for some lateral movement of the plates, changing how forces are distributed across the joints. This movement can lead to a redistribution of transmitted loads. A joint with greater clearance typically exhibits lower stiffness and strength. This is because the bolt can move within the hole before it fully engages with the material, which delays the development of full joint stiffness and reduces the overall load-bearing capacity.

The minimal variation in Fz across all cases aligns with the fact that this is the axial direction, where significant effects from the clearance are not expected.

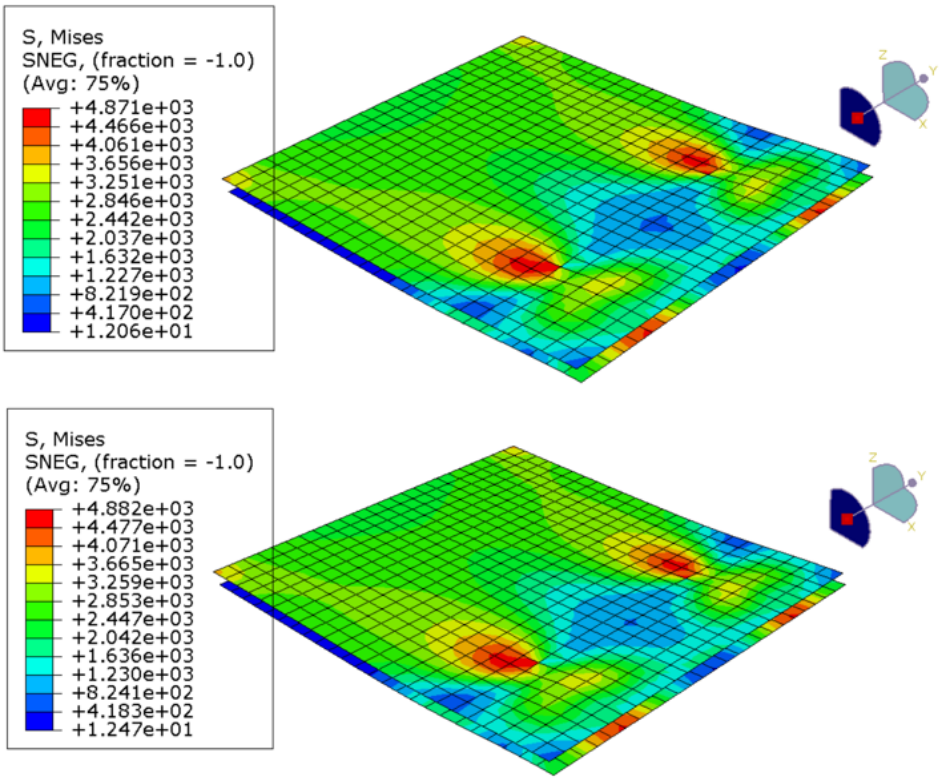

Figure 5.27: Stress without (up) and with (down) clearance

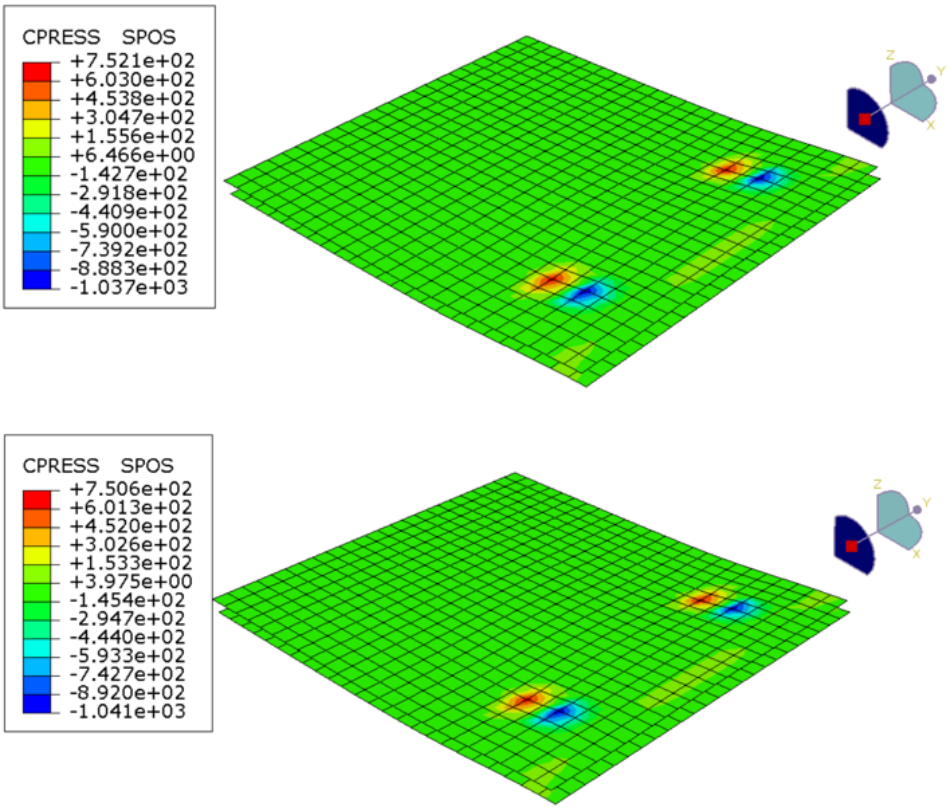

Figure 5.28: CPRESS without (up) and with (down) clearance

Clearance affects the stress distribution around the hole and the load path through the structure. Ideally, loads are evenly distributed across the bolt and the material surrounding the hole. However, excessive clearance can lead to non-uniform load distribution, causing some areas to experience higher stresses.

Increased clearance can lead to more significant bolt bending or tipping, altering the stress states within the connected plates. This can increase the risk of premature failure modes such as wear, fatigue, or even fracturing due to uneven load distributions.

The presence of clearance affects the contact area between the bolt and the hole. Reduced contact area can lead to higher local stresses and strain concentrations. Friction plays a significant role in maintaining the integrity of the joint. In joints with clearance, the frictional forces can be less predictable and may not be sufficient to prevent relative motion between the bolt and the structure under loading conditions, leading to slippage and further stress concentrations.

5.4. Further work

Building on the findings of this study, several avenues for future research can be explored to enhance the understanding and application of joint performance.

One potential direction is to conduct analyses using 3D models. This approach would capture the geometric complexity and interactions within the joints more accurately, providing deeper insights into their behavior under various conditions.

Another area of interest is examining the model's performance under double shear conditions. By comparing the differences in load distribution and stress between single and double shear, a more comprehensive understanding of joint mechanics can be achieved.

Exploring the implications of using composite materials is also a promising avenue. This could lead to improvements in strength and weight reduction, offering significant benefits in structural applications.

Further investigation into the different failure modes of connectors is essential. Understanding the conditions that lead to failure and developing strategies to prevent them will enhance joint reliability and safety.

Finally, validating the simulation results with experimental tests is crucial. By comparing the outcomes with physical experiments, the model can be refined and parameters adjusted to ensure accuracy and reliability.

A

Model creation in Abaqus CAE

This appendix shows a step-by-step process to create the single-lap shear model using the Abaqus CAE interface.

Part

In Abaqus, a *Part* is a geometric object representing a physical component of the model. It serves as the foundation for modeling and can be defined with different geometry types. It is created in the *Part module* of Abaqus/CAE and is the starting point for defining the model. First, the parts for the two plates are created, selecting the shell type and deformable body option.

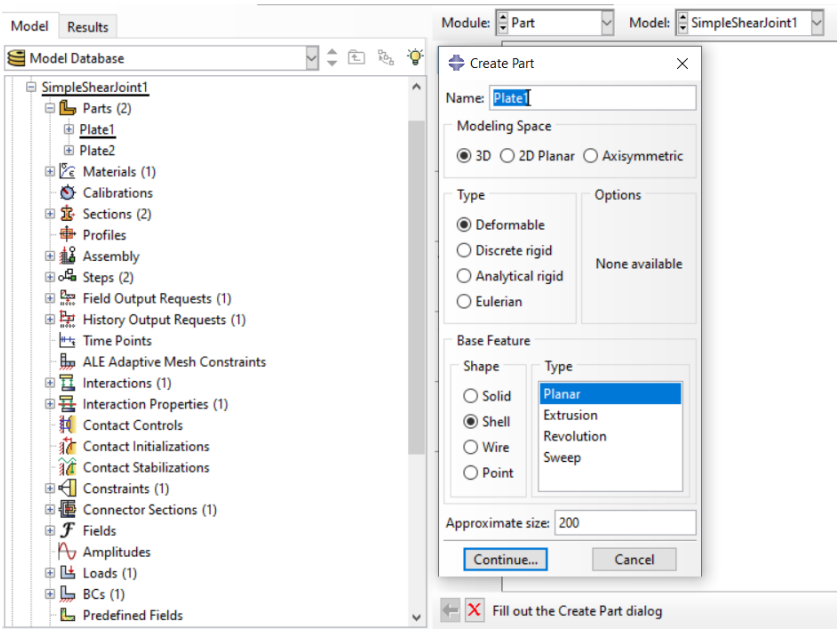

Figure A.1: Part definition

A *Sketch* is a 2D geometric profile used to create the shape of a *Part*. It serves as the foundation for defining the geometry of each plate.

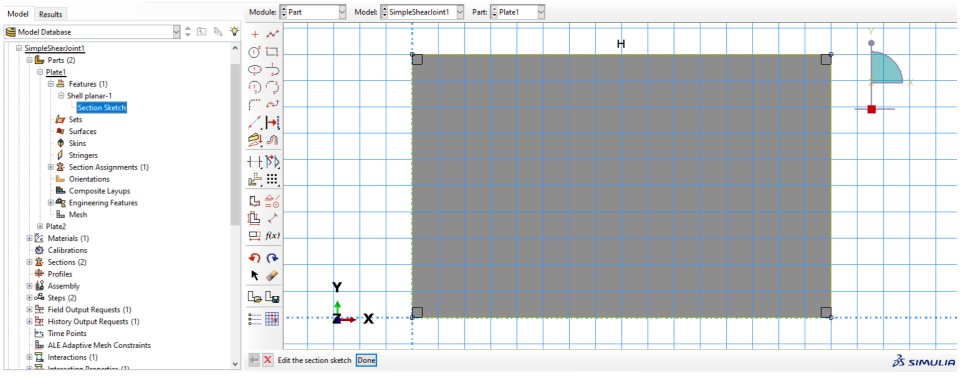

Figure A.2: Material definition

Material

A material defines the physical and mechanical properties assigned to a *Part* or *Section* to simulate realistic behavior under applied loads and boundary conditions.

To define the elastic behavior of steel in Abaqus, an elastic property must be created by assigning the Young's Modulus and Poisson's Ratio. This is done in the *Property module* within Abaqus/CAE.

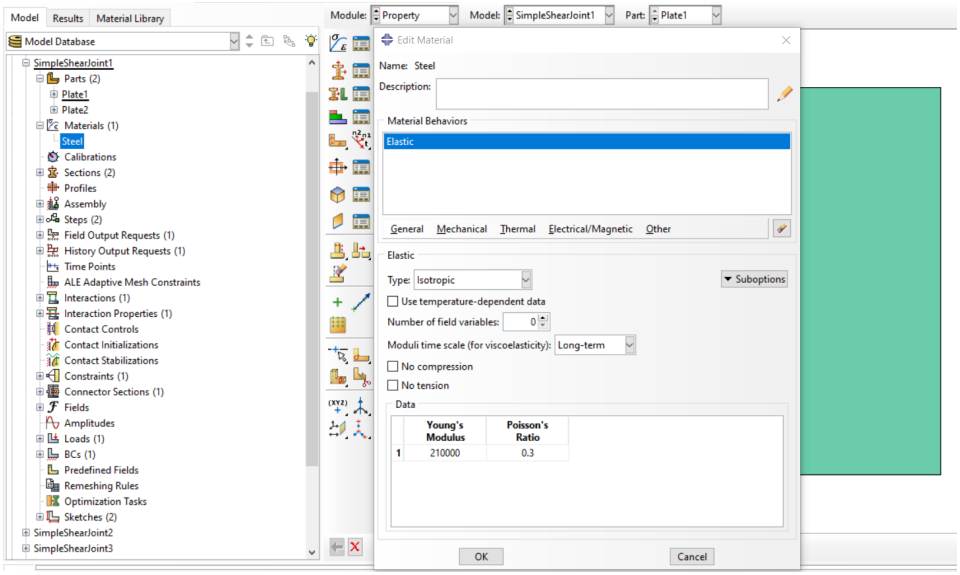

Figure A.3: Plate sketch

Section

A *Section* in Abaqus defines the material properties and thickness of a *Part* or a region of the model. It is independent of geometry and is assigned to one or more parts to specify their structural behavior. For the plates, a *Shell Section* is selected, which defines the thickness and material for shell elements.

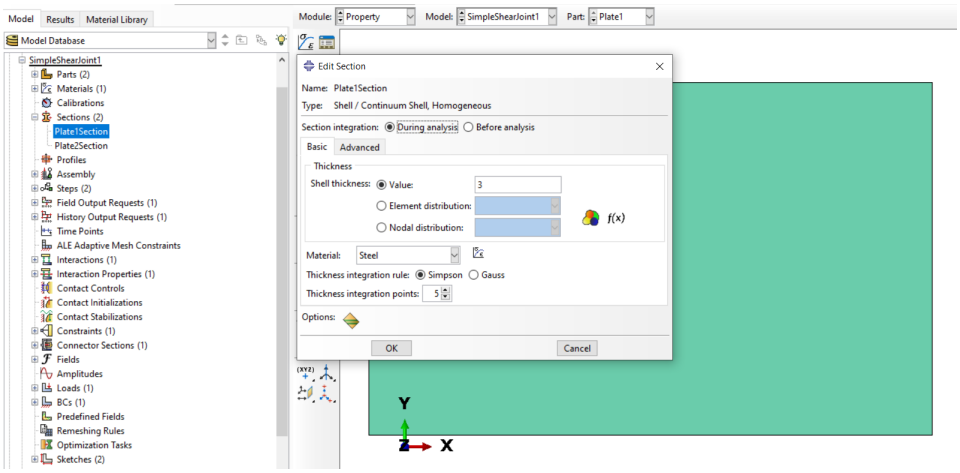

Figure A.4: Section definition

Once a *Section* has been created, it must be assigned to the plate to ensure that the material properties and other parameters (such as thickness for shell elements) are applied correctly. This process is done in *Assign Section* in the *Property module toolbar*.

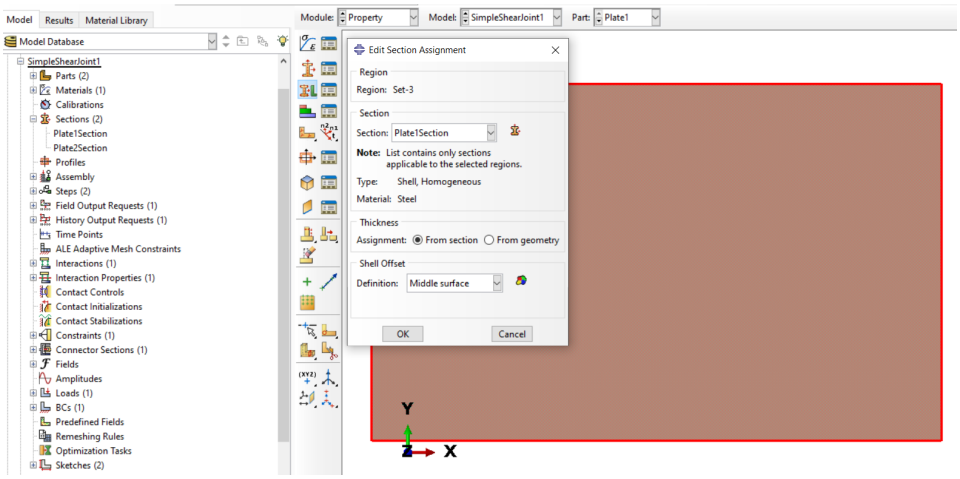

Figure A.5: Section assignment

Instance

An *Instance* is a copy of a *Part* placed in the *Assembly module*. The instancing system allows multiple copies of the same *Part* to be used in the model without modifying the original *Part* definition. This approach improves efficiency and consistency in simulations. Instances are created in the *Assembly module* from the main menu.

For the plates, dependent instances have been chosen, meaning that the meshing is defined at the *Part* level and cannot be modified at the *Instance* level. Mesh and properties remain consistent across all instances.

With independent instances the mesh is defined at the Instance level, allowing modifications per instance. It is useful when applying different mesh refinements to the same geometric *Part*.

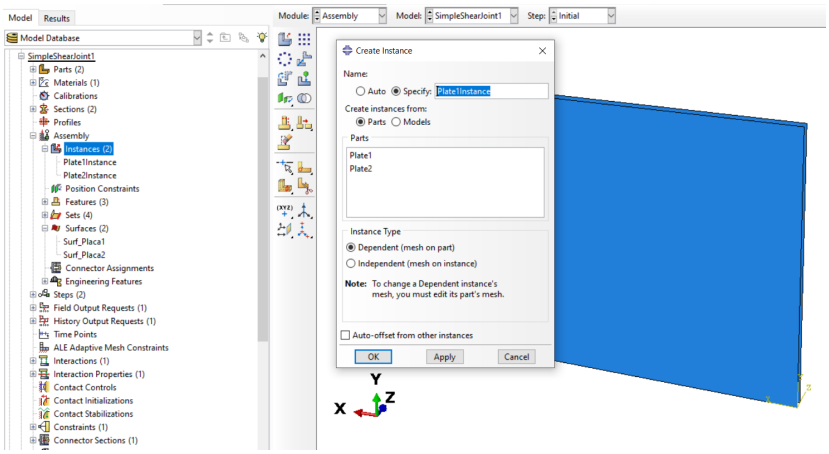

Figure A.6: Instance definition

Attachment points

Attachment Points are reference points used to define connections, constraints, or interactions between different parts of a model. They are used in the assembly to define fastener locations.

They are created from the *Interaction module*, and a reference edge must be selected from which the offsets are measured, as well as the face where the attachment points are placed. For the distance to the edge, a value of 2.5 times the bolt diameter is defined, and for the distance between them, a value of 4 times the diameter is applied. The number of rivets will correspond to the number of attachment points generated.

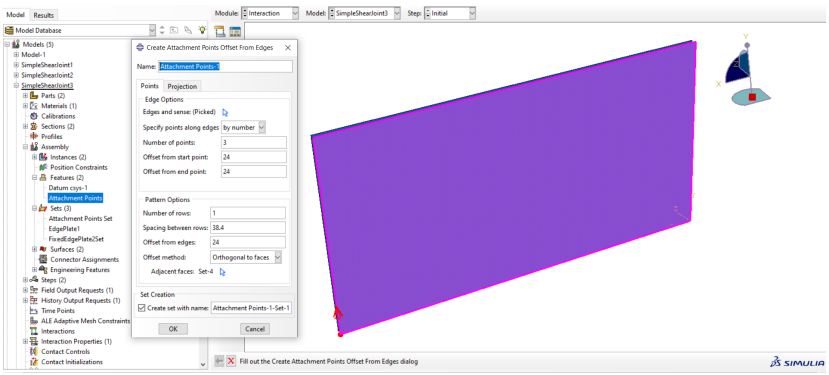

Figure A.7: Attachment points definition

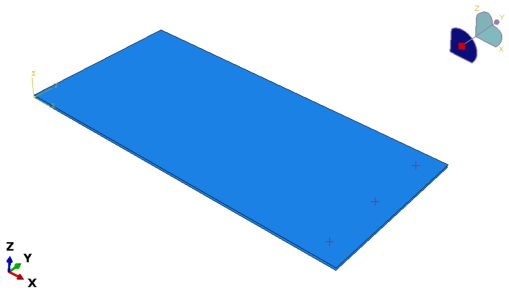

Figure A.8: Attachment points

Connector Section

A *Connector Section* is used to define the mechanical behavior of connections between parts. When working with fasteners, the *Connector Section* specifies how these elements transfer forces and moments between the connected components.

Beam connector type automatically constrains all degrees of freedom (U1, U2, U3, UR1, UR2, UR3) and behaves like a rigid link.

A *Connector Section* defines the interaction properties of a fastener, including axial and shear stiffness, rotational stiffness (if applicable), failure criteria or connector behavior.

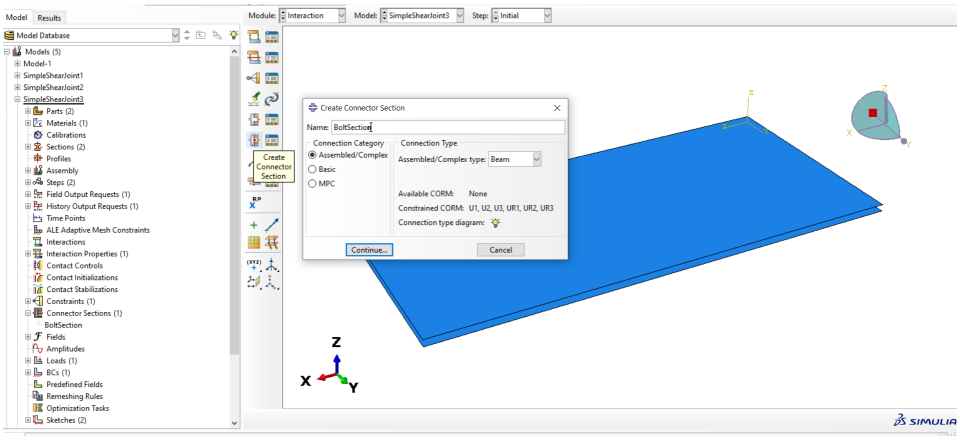

Figure A.9: Connector Section definition

Fastener

Point-based fasteners are a method to define fastening elements (bolts, rivets, spot welds, etc.) at specific points rather than defining individual connector elements. This is useful when modeling connections between plates without explicitly meshing the fastener geometry.

Before defining the fastener, the surfaces of the plates to be joined must be created.

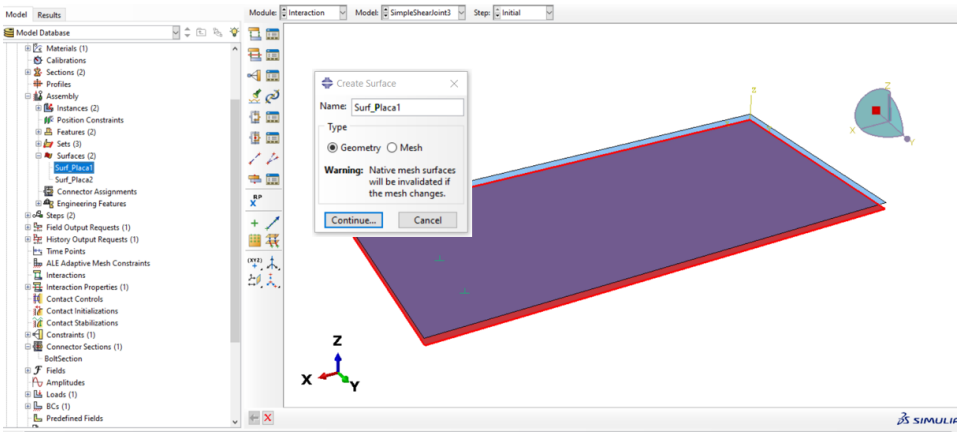

Figure A.10: Surface definition

The fastener element connects two or more surfaces at a discrete location and allows for force transfer in axial and shear directions. To create them, go to *Create fasteners* in the *Interaction module* toolbox, select *Point-based fasteners*, the attachment points defined before and the surfaces to be joined.

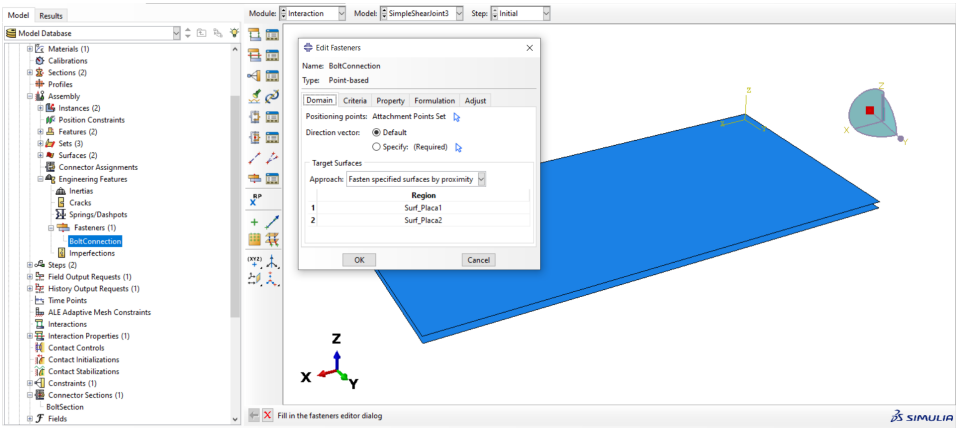

Figure A.11: Fastener definition

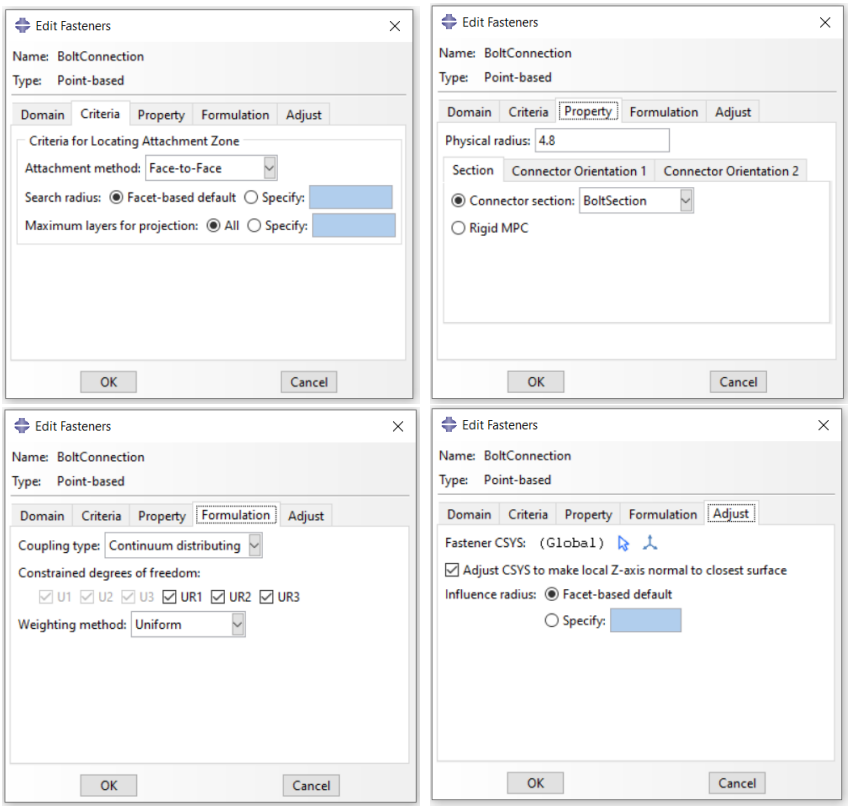

Figure A.12: Fastener parameters

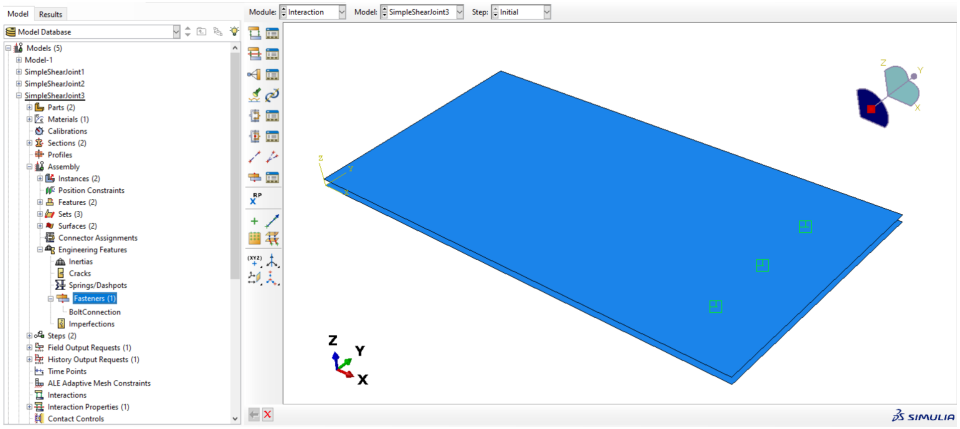

Figure A.13: Fasteners

Contact property

A *Contact Property* defines the interaction behavior between surfaces, including friction or normal contact behavior. When modeling fasteners, defining an appropriate *Contact Property* ensures realistic force transfer between connected plates. It is created from the *Interaction module*.

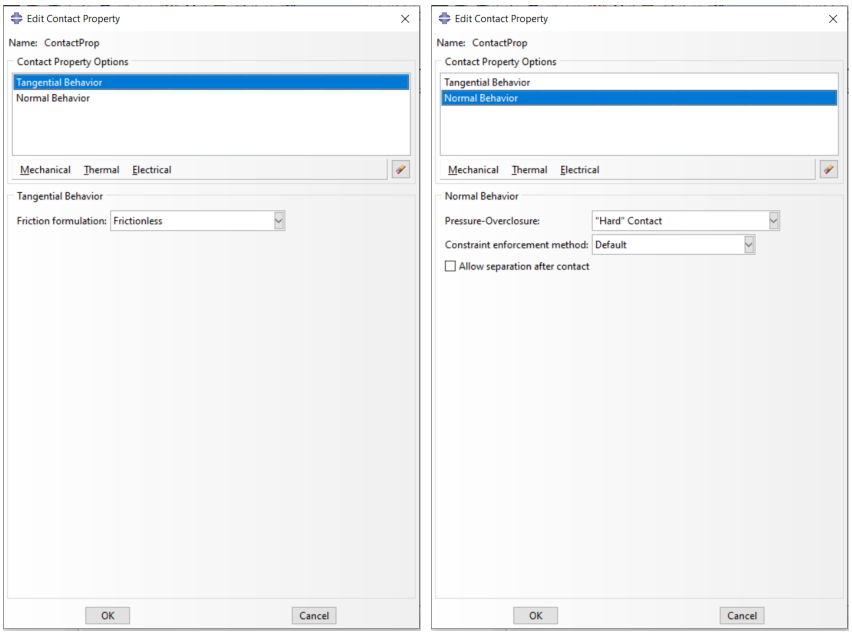

Figure A.14: Fastener parameters

Tangential behavior defines how surfaces resist relative motion (sliding). Selecting *Frictionless*, ABAQUS assume that surfaces in contact slide freely without friction.

Normal behavior defines how surfaces interact in normal direction. Default method is used to enforce contact constraints by using a contact pressure-overclosure relationship. Select a “Hard” Contact to use the classical Lagrange multiplier method of constraint enforcement. Toggle off Allow separation after contact if you want to prevent surfaces from separating once they have come into contact.

Contact

Defining contact in Abaqus/Standard can be done in terms of two surfaces that may interact with each other as a *"contact pair"*. Abaqus enforces contact conditions by forming equations involving groups of nearby nodes from the respective surfaces.

To define a contact pair, you must indicate which pairs of surfaces may interact with one another or which surfaces may interact with themselves. Contact surfaces should extend far enough to include all regions that may come into contact during an analysis.

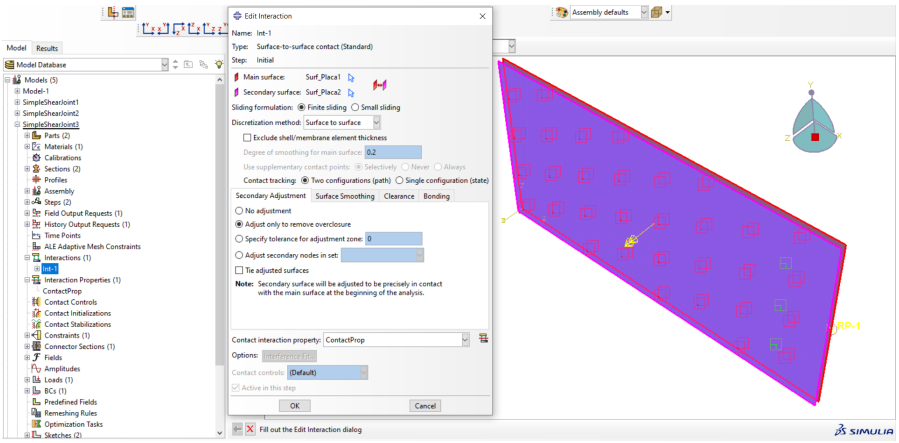

Figure A.15: Fasteners

In Abaqus/CAE, go to the *Interaction Module* and create a new interaction by selecting *Create Interaction*. Choose the master surface and the slave surface. In the *Interaction Editor*, set the *Finite Sliding*, to use the finite-sliding formulation, which is the most general and allows any arbitrary motion of the surfaces. As discretization method choose the *Surface-to-Surface*, and assign the *Contact Interaction Property*.

Mesh

The mesh definition is a crucial step in finite element analysis (FEA). The mesh determines how the model is discretized into elements, which affects the accuracy, stability, and computational cost of the simulation.

To define the mesh go to the Mesh Module and select the Seed Part to determine element density.

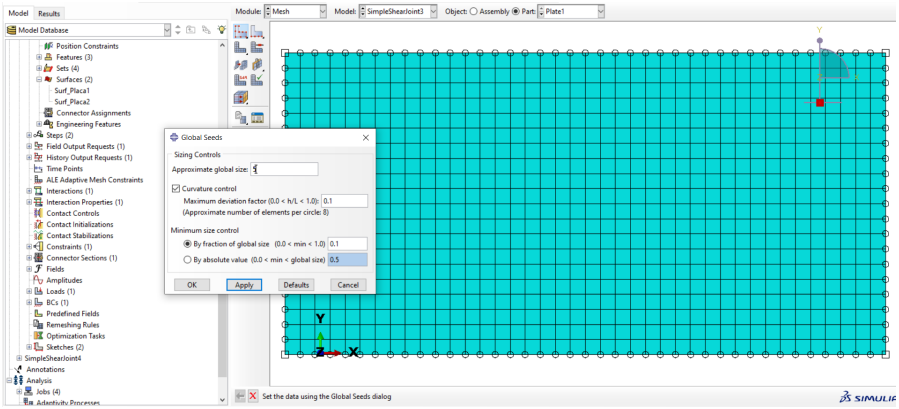

Figure A.16: Fasteners

Boundary conditions

Boundary Conditions (BCs) are essential for defining how a model interacts with its environment. They restrict degrees of freedom (DOF) in translation and rotation, ensuring that the simulation behaves correctly.

In this model, boundary conditions are applied in one of the plates, which has one of its sides fixed ($U_x = U_y = U_z = 0, R_x = R_y = R_z = 0$).

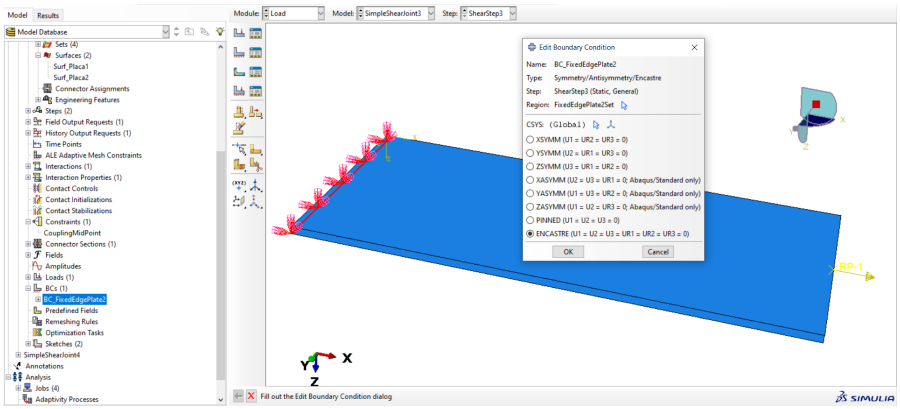

Figure A.17: Fasteners

To define the boundary conditions go to the Load Module, click Create Boundary Condition, select the type of BC and assign the BC to a region.

Load

In the model, a concentrated force is applied in the middle of the edge of one of the plates. To apply the force, a reference point is created in the desired position.

Abaqus does not distribute the force automatically to the surrounding nodes when the force is applied to a referenced point. To ensure the load is correctly transferred to the edge or the full structure, a coupling constraint.

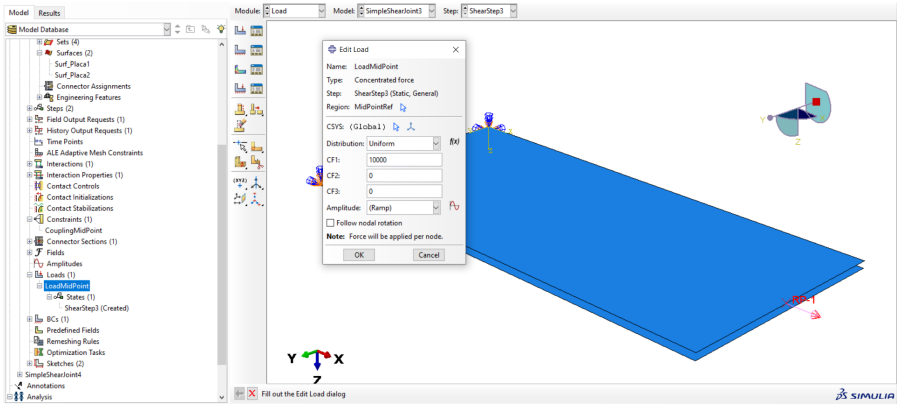

Figure A.18: Load definition

Bibliography

[1] Yasin ÇAPAR. *Implicit vs Explicit Approach in FEM*. URL: https://yasincapar.com/implicit-vs-explicit-approach-in-fem/.

[2] Dassault Systèmes. *Overview of Simulation with Abaqus*. 2024. URL: https://help.3ds.com/2024/english/dssimulia_established/SIMACAEKERRefMap/simaker-c-ov.htm?contextscope=all&id=cf96ae2ef8834b8ca091f914821ddbd3.

[3] Carlos Isaías Quijano Dzul. "Análisis numérico del comportamiento estático y dinámico de una unión remachada incluyendo la rigidez de los elementos". MA thesis. Centro Nacional de Investigación y Desarrollo Tecnológico (CENIDET), 2014.

[4] W. X. Fan and C.T. Qiu. "Load Distribution of Multi-Fastener Laminated Composite Joints". In: *International Journal of Solids and Structures* 30.21 (1993), pp. 3013–3023.

[5] GMN Bearing USA. *Understanding Bearing Loads*. https://www.gmnbt.com/resources/guides/ball-bearing/understanding-bearing-loads/.

[6] M. W. Hyer and E. C. Klang. "Contact Stresses Pin-Loaded Orthotropic Plates". In: *Journal of Composite Materials* (1987).

[7] Alexandra Korolija. "FE-modeling of bolted joints in structures". MA thesis. Linköping University, 2012.

[8] M. A. Mohammed, A. A. Al-Dulaimi, and W. A. Al-Azzawi. "Analysis of Adhesively Bonded Riveted Joints". In: *Alexandria Engineering Journal* 58.1 (2019), pp. 1–8. DOI: 10.1016/j.aej.2018.11.006.

[9] R.A. Naik and J.H. Crews. "Stress Analysis Method for Clearance-Fit Joints with Bearing-Bypass Loads". In: *NASA Technical Memorandum 89153* (May 1987).

[10] Michael C.Y. Niu. *Airframe Stress Analysis and Sizing*. Adaso/Adastra Engineering Center, 1999.

[11] Kelly P. *Solid Mechanics Part II: Plate Theory*. Chapter 6 of Solid Mechanics Part II. 2011. URL: https://pkel015.connect.amazon.auckland.ac.nz/SolidMechanicsBooks/Part_II/06_PlateTheory/06_PlateTheory_Complete.pdf.

[12] Ramadas Chennamsetti. *Theory of Plates*. URL: https://imechanica.org/files/theory%5C%20of%5C%20plates.pdf.

[13] ResearchGate. *Elastic connectors in Abaqus CAE*. URL: https://www.researchgate.net/post/Elastic_connectors_in_Abaqus_CAE.

[14] Niclas Strömberg and Anders Klarbring. "Minimization of Compliance of a Linear Elastic Structure with Contact Constraints by using Sequentially Linear Programming and Newton's method". In: *Proceedings of the 7th ASMO UK Conference on Engineering Design Optimization*. 2008.

[15] A. Bolshikh V. Eremin. "Methods for flexibility determination of bolted joints: empirical formula review". In: *Journal of Physics: Conference Series* 1925.1 (2021), p. 012058. DOI: 10.1088/1742-6596/1925/1/012058.